IMPERIAL COLLEGE LONDON

DOCTORAL THESIS

Static spherically symmetric solutions in higher derivative gravity

Author:
Alun Perkins

Supervisor:
Kellogg Stelle

A thesis submitted in part fulfilment of the requirements for the degree of PhD

in the

Theoretical Physics Group
Department of Physics

December 31, 2016

Declaration of Authorship

I hereby declare that the work presented in this thesis is my own except where explicitly referenced as the work of others or as work undertaken by me in collaboration with others. In particular section 1.3, part 2 and sections 3.1 and 3.2 and appendix A are based on research published in [1] and [2] and undertaken in collaboration with Kelly Stelle, Chris Pope and Hong Lu.

IMPERIAL COLLEGE LONDON

Abstract

Faculty of Natural Sciences
Department of Physics

PhD

Static spherically symmetric solutions in higher derivative gravity

by Alun Perkins

We consider the four-derivative modification to the Einstein-Hilbert action of general relativity, without a cosmological constant. Higher derivative terms are interesting because they make the theory renormalisable (but non-unitary) and because they appear generically in quantum gravity theories.

We consider the classical, static, spherically symmetric solutions, and try to enumerate all solution families. We find three families in expansions around the origin: one corresponding to the vacuum, another which contains the Schwarzschild family, and another which does not appear in generic theories with other number of derivatives but seems to be the correct description of solutions coupled to positive matter in the four-derivative theory. We find three special families in expansions around a non-zero radius, corresponding to normal horizons, wormholes and exotic horizons. We study many examples of matter-coupled solutions to the theory linearised around flat space, which corroborate our arguments.

We are assisted by use of a "no-hair" theorem that certain conditions imply that $R = 0$, which is applicable in many cases including asymptotically flat space-times with horizons.

The Schwarzschild black hole still exists in the theory, but a second branch of black hole solutions is found that can have both positive and negative mass, and that coincide with the Schwarzschild black holes at a single mass.

The space of asymptotically flat solutions is probed numerically by shooting inwards from a weak-field solution at large radius, and the behaviour at small radius is classified into the families of series solutions (most of which make an appearance). The results are inconclusive but show several interesting features for further study.

Acknowledgements

I would like to thank my supervisor Kelly Stelle for all of his insightful guidance and advice over the past four years, and for many stimulating discussions which were full of enthusiasm for investigation and without which my research would not have been possible. I would also like to thank my collaborators Chris Pope, Hong Lu and Alfio Bonanno for taking the time to correspond with me as their collaborator and for all of the discussions we had which were responsible for much of the progress that was made.

I would like to thank my fellow PhD students for all of their help understanding difficult topics and for all their advice for getting through my PhD, especially Andrew Hickling, Andrej Stepanchuk, Ben Crampton, Oli Gould, Silva Nagy and Alexandros Anastasiou.

I would like to thank my wonderful fiancée Veronica McCormick for all her kind support and patience which made all the stresses of a PhD bearable.

I would like to thank the theoretical physics group for all their hospitality and the Science and Technologies Facilities Council (STFC) for their financial support.

Contents

List of Figures

List of Tables

Chapter 1

Introduction

1.1 Introduction to higher derivative gravity theories

General relativity is one of the most successful physical theories to exist. It provides the most accurate predictions of the movements of planets and stars and it predicted experimentally testable phenomena that did not appear in Newtonian gravity, including light bending, gravitational redshift, the precession of the perihelion of Mercury and gravitational waves. General relativity also provides us with the only example of an exact description of macroscopic objects: black holes. A stationary, isolated black hole in general relativity is highly constrained by powerful uniqueness theorems and is described exactly by known solutions expressible in terms of standard functions, and in fact a good deal is understood about how this idealised situation (isolated and stationary) relates to the more realistic setting of the final state after gravitational collapse of stellar objects. Stationary, isolated black holes in general relativity are described by just three parameters: their mass, angular momentum and electric charge. Unlike all other macroscopic objects, black holes are not interpreted as approximations or aggregates of smaller objects, but are exact. General relativity has been a very great success, but physicists are still led to seek a superseding theory because general relativity turns out to be fundamentally incompatible with quantum mechanics.

We now give a heuristic explanation of the incompatibility using power counting, following [3]. The Einstein-Hilbert action for general relativity is

$$S\left[g_{\mu\nu}\right] = \frac{1}{16\pi G}\int \sqrt{-g}\; R\; \mathrm{d}^4\mathrm{x}\,. \tag{1.1.1}$$

The path integral of the quantum field theory for gravity would be

$$\int \mathcal{D}\, g_{\mu\nu}\, \exp(iS[g_{\mu\nu}])\,. \tag{1.1.2}$$

We formulate the problem as the QFT of a graviton on a flat background, so let us write the expansion

$$\begin{aligned} g_{\mu\nu} =& \eta_{\mu\nu} + h_{\mu\nu} \\ g^{\mu\nu} =& \eta^{\mu\nu} - h^{\mu\nu} + h^{\mu}{}_{\rho}h^{\rho\nu} + \ldots \end{aligned}$$

so that the Lagrangian $\sqrt{-g}\,R$ has terms going as $(\partial h)^2$, $h(\partial h)^2$, $h^2(\partial h)^2$, $h^3(\partial h)^2$, etc. From this one can see that for momentum k the graviton propagator goes as k^{-2} and each vertex goes as either k^2, $k.p$, or p^2 where k is an internal momentum and p is the momentum of an external leg. The amplitude for a diagram goes as the integral $\int^{|k|<\Lambda}(\ldots)\mathrm{d}^4\mathrm{k}$ over each loop, and this goes as $\sim \Lambda^D$ with the momentum cutoff scale Λ, where D is called the degree of divergence. The maximal divergence of a graviton diagram therefore goes as $D = 4$(# of loops)$-$ 2(# of propagators)$+$2(# of vertices). Using the topological relation (# of vertices) $=$ (# of propagators)$-$

(# of loops) + 1, we see that $D = 2 + 2$(# of loops) which is always positive.

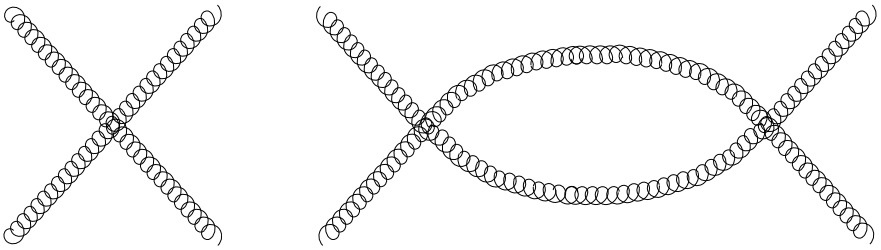

FIGURE 1.1: Example tree level and one-loop diagrams of graviton-graviton scattering

Consider the one-loop diagram in figure 1.1. If we consider the contribution to the one-loop diagram's amplitude from the k^2 contribution to the vertices, with the loop integral and the loop's two propagators, we get $\int^{\Lambda} k^0 p^0 \mathrm{d}^4\mathrm{k} \sim \Lambda^4\,\mathrm{p}^0$. If we add a cosmological term to the Lagrangian $\left(+(\text{const.}) \int \sqrt{g}\,\mathrm{d}^4\mathrm{x}\right)$, which has no derivatives of h, it modifies the amplitude of the (no-loop) four-point vertex by a factor $\sim p^0$ and can cancel the leading divergence of the one-loop diagram. If we next consider the contribution to the one-loop diagram's amplitude from the $k.p$ contribution to the vertices, with the loop integral and the loop's two propagators, we get $\int^{\Lambda} k^{-2} p^2 \mathrm{d}^4\mathrm{k} \sim \Lambda^2\,\mathrm{p}^2$. This can be cancelled out with the (no-loop) four-point vertex diagram, which also goes as p^2, so this can be absorbed with an adjustment to the coupling $G \to G(\Lambda)$. If we finally consider the contribution to the one-loop diagram's amplitude from the p^2 contribution to the vertices, with the loop integral and the loop's two propagators, we get $\int^{\Lambda} k^{-4} p^4 \mathrm{d}^4\mathrm{k} \sim \ln(\Lambda)\,\mathrm{p}^4$. For this to be cancelled out by the (no-loop) four-point vertex the Lagrangian must be modified to include a term with four-derivatives of the metric, schematically, a curvature squared term.

We then repeat the whole process for the two-loop diagram. At two loops the maximal divergence is $\sim \Lambda^6 p^0$, and the sub-leading divergences are $\sim \Lambda^4 p^2, \Lambda^2 p^4, \ln(\Lambda) p^6$, so we make another adjustment to the cosmological term and another adjustment to the coupling, and we adjust the coupling of the four-derivative term, but to cancel all the divergences we need a six-derivative term in the Lagrangian, schematically, curvature cubed. This continues, and to remove divergences at higher and higher loop orders we would need higher and higher derivative terms, and ultimately we would need an infinite number of counterterms.

The forms of the one-loop counterterms were found rigorously by 't Hooft and Veltman in [4] to be

$$R^2 \qquad \text{and} \qquad R^{\mu\nu}\,R_{\mu\nu}\,. \tag{1.1.3}$$

This relies on the four-dimensional Gauss-Bonnet identity that the integral

$$I_{\mathrm{GB}} = \int d^4x\sqrt{-g}(R_{\mu\nu\rho\sigma}R^{\mu\nu\rho\sigma} - 4R_{\mu\nu}R^{\mu\nu} + R^2) \tag{1.1.4}$$

is an integral of a total derivative, giving the Euler number of the space (a topological invariant), so that the quantity $R_{\mu\nu\rho\sigma}R^{\mu\nu\rho\sigma}$ is not independent of $R^{\mu\nu}R_{\mu\nu}$ and R^2. The counterterms for higher orders can also be found [5] but for the theory to be valid at all energy scales an infinite number of counterterms would be needed so the theory would not be predictive - this is the essence of the problem of non-renormalizability.

The form of the one-loop counterterms motivates the study of the quantum theory of the action

$$I = \int d^4x\sqrt{-g}\left(\gamma\left(R-2\Lambda\right) - 2\alpha\, R_{\mu\nu}R^{\mu\nu} + \left(\beta+\frac{2\alpha}{3}\right)R^2\right) \tag{1.1.5}$$

where α and β are dimensionless coupling constants. This Lagrangian has four derivatives of the metric, and is the most general four-derivative metric in four dimensions due to the Gauss-Bonnet identity. In [6] Stelle studied this theory, for $\Lambda = 0$ [1], and it was found to have linearised dynamical degrees of freedom corresponding to the massless graviton from general relativity and corresponding to two new massive particles, one with spin-two $\left(m_2^2 = \frac{\gamma}{2\alpha}\right)$ and one scalar $\left(m_0^2 = \frac{\gamma}{6\beta}\right)$. Unfortunately, the spin-two particle was found to be a ghost. In [7] Stelle showed that this theory is renormalizable, which can be seen from its graviton propagator which he showed to be

$$\begin{aligned} D_{\mu\nu\rho\sigma}(k) =& \frac{1}{(2\pi)^4 i}\left(\frac{2P^{(2)}_{\mu\nu\rho\sigma}(k)}{k^2(2\alpha k^2+\gamma)} - \frac{4P^{(0-s)}_{\mu\nu\rho\sigma}(k)}{k^2(6\beta k^2+\gamma)} + (\text{gauge fixing terms})\right) \\ =& \frac{1}{\gamma(2\pi)^4 i}\left(\frac{2P^{(2)}_{\mu\nu\rho\sigma} - 4P^{(0-s)}_{\mu\nu\rho\sigma}}{k^2} - \frac{2P^{(2)}_{\mu\nu\rho\sigma}}{k^2+m_2^2} + \frac{4P^{(0-s)}_{\mu\nu\rho\sigma}}{k^2+m_0^2} + (\text{gauge fixing terms})\right), \end{aligned}$$

where the $P_{\mu\nu\rho\sigma}(k)$ are the projectors for symmetric rank-two tensors. For $\alpha \neq 0, \beta \neq 0$ the large-k behaviour is modified from the k^{-2} of general relativity to k^{-4}, controlling the divergences. The second line shows the negative sign for the particle with mass m_2, and thus its ghost nature. The ghost causes the vacuum to be an unstable solution and the theory to be non-unitary, which are significant barriers to adopting the theory as a physical model. In fact all higher derivative theories, whether gravitational or any other theory with more than two time derivatives in the Lagrangian, generically suffer from Ostrogradsky's instability [8], of having energy unbounded from below. Though the higher derivative terms may appear to be perturbations of the lower-derivative theory, in fact they not only make the solutions unstable but also introduce additional degrees of freedom to the theory.

Various authors have discussed theories with ghosts, and not all are convinced that theories with ghosts are beyond saving. It was argued by Simon in [9] that a method of perturbative

[1] If reading [7] note that his couplings had the same names but were defined differently: (their β) = (our $\beta + \frac{2}{3}\alpha$) and (their α) = (our 2α). Our convention will prove more convenient for this study. They also use the opposite convention for the Riemann tensor, so that for the same ordering of indices their Riemann/Ricci tensor/scalar is minus our Riemann/Ricci tensor/scalar.

constraints should be applied at each stage of series of higher derivatives terms that are associated with a small expansion parameter, that exclude solutions that cannot be expressed as Taylor series in that small parameter. It has also been suggested by Smilga in [10] that certain theories can have ghosts of a sort that do not cause instabilities of the vacuum nor non-unitary scattering matrices, and further research in this direction may be applicable to higher derivative gravity. Another way to possibly save the theory of higher derivative gravity was presented by Hawking and Hertog in [11], where a toy model of a scalar field was used as an analogy for higher-derivative gravity and a prescription for calculating amplitudes was presented. The prescription removes the ghost's negative norm states, negative probabilities and instability, trading them for acausality and non-unitarity. An example of an electron showed that it responded to an interaction early but only by a time of order (its classical radius) $\frac{1}{c}$. The non-unitarity was shown to become measurable only at high energies and so its presence could be tolerated in the theory. The higher-derivative theory was then well-defined as a perturbation of the lower-derivative theory. Alternatively Salvio and Strumia [12] suggest casting the higher-derivative quantum theory as unitary but with negative norm states and building a useable theory of mixed-norm states, however they conclude by saying that a probabilistic interpretation of a theory with such states has yet to be found. Yet more ideas for naturally avoiding the problems caused by the ghost will appear below.

We shall use the Gauss-Bonnet theorem to write the action (1.1.5) in a form that shall prove more natural [2]. The theory we will study in this paper is defined by the action

$$I' = I - \alpha I_{\mathrm{GB}} = \int d^4x\sqrt{-g}\left(\gamma(R-2\Lambda) - \alpha C_{\mu\nu\rho\sigma}C^{\mu\nu\rho\sigma} + \beta R^2\right) , \tag{1.1.7}$$

where we shall always take $\Lambda = 0$ unless specified, and by correspondence with general relativity we use $\gamma = \frac{1}{16\pi G}$. In the research we present we do not deal with the problems of its corresponding quantum theory, but treat it as an effective theory appropriate over some range of energies and we shall seek to enumerate all or most of the classical solution families. The variation of the action (1.1.7) with respect to the metric, $\frac{\delta I}{\delta g^{\mu\nu}}$, is a symmetric, divergenceless tensor [6]. In more than four dimensions the Gauss-Bonnet term (1.1.4) is not a total derivative, so must be included in the action of a general four-derivative theory, where it is a Lovelock term [13], meaning that it also has the special property that its variation with respect to the metric is symmetric and divergenceless, and further that it features only two derivatives of the metric. The metric equations of motion of the term (1.1.4) would, however, not be solved by

[2] We use the identity

$$C^{\mu\nu\rho\sigma}C_{\mu\nu\rho\sigma} = \left(R^{\mu\nu\rho\sigma}R_{\mu\nu\rho\sigma} - 4R^{\mu\nu}R_{\mu\nu} + R^2\right) + 4\frac{d-3}{d-2}R^{\mu\nu}R_{\mu\nu} - \frac{d(d-3)}{(d-2)(d-1)}R^2 \tag{1.1.6}$$

in $d = 4$ dimensions

$R_{\mu\nu} = 0$, the well-understood solution to general relativity, so the theory would be more difficult to study. One can use Lovelock terms to construct gravity theories with higher curvature terms but entirely without ghosts, and in [14] Feng and Lu construct solutions to such gravity theories coupled to Maxwell fields and p-form field strengths, using non-minimal coupling schemes designed to avoid ghosts in the matter sector as well.

Quadratic curvature terms appear in a variety of contexts and there are a number of reasons to be interested in them. One appearance is in the low-energy effective theory of the 10 dimensional $E_8 \times E_8$ heterotic superstring, where a term $R_{\mu\nu\rho\sigma}R^{\mu\nu\rho\sigma}$ appears, multiplied by a function of the dilaton. The corresponding quantum theory has ghost modes, but one can add Ricci squared terms to the Riemann squared term to become the term (1.1.4) we have already mentioned. This removes the ghost modes from its quantum theory for $D > 4$ [15]. The Einstein-Gauss-Bonnet theory was also studied by Boulware and Deser in [16] where it was found that both flat space and anti-de-Sitter space are solutions. The AdS solution, however, has ghost excitations and thus the flat solution is naturally preferred for this theory. The cosmological Einstein-Gauss-Bonnet theory was also considered and it was found that it has an effective cosmological constant with two possible values, but only was ghost-free for the smaller value, which is interesting with regards to the cosmological constant problem.

The classical theory with Lagrangian $R - 2\Lambda + \alpha' R^2$ was found by Stelle [6] and Whitt [17] to be equivalent to a general relativity coupled to a massive scalar field and Whitt [17] and Starobinksy [18] found it to have solutions that describe Planck-era inflation. It was also shown to admit a limited no-hair theorem proving that stationary, axisymmetric, asymptotically flat solutions with a horizon, for $\Lambda = 0, \alpha > 0$, must have $R = 0$ [3]. In [19] Mignemi and Wiltshire pointed out that after using Whitt's results to show that $R = 0$ then the field equations become equivalent to those of GR with $R = 0$, and the uniqueness theorems of GR can be invoked to show that all static spherically symmetric asymptotically flat vacuum black hole solutions must be Schwarzschild. They further show that in all $f(R)$ theories of the form $f(R) = \sum_{n=1} a_n R^n, a_2 > 0$ it is still true that all static spherically symmetric black hole solutions are Schwarzschild. The matter coupling of the $R + R^2$ theory without a cosmological term was considered by Pechlaner and Sexl in [20] where they note that Schwarzschild is not the only asymptotically flat solution, and in fact it is not the exterior solution of a positive definite mass distribution with normal minimal coupling. Solutions of this theory coupled to a perfect fluid were considered by Michel in [21] and the total mass of the fluid matter was related to the pressure at its core ($r = 0$). It was found that the mass of a star has a maximum value, appearing at some finite central pressure. They also note that even for non-zero mass, there are non-trivial non-Schwarzschild non-singular solutions in this theory, and in all $f(R)$ theories [4]. The energy of the $R + \beta R^2$ theory was studied by Boulware, Deser and Stelle [23]

[3] we remark here that later on we shall present similar theorems for more general quadratic Lagrangians using the additional assumption of staticity

[4] comments on $f(R)$ theories are outside the scope of this work but for a review see for example [22]

[24] and they found that (assuming $\beta > 0$) if the quantity $1 + \beta R$ is non-negative on an initial spatial slice then the energy of the space-time is non-negative. This implies that such solutions near to flat space, which has zero energy, have greater energy, and thus that flat space is stable.

The scale-invariant theory with Lagrangian $R^2 + C^2$ has a "zero energy theorem", shown by Boulware, Horowitz and Strominger in [25], that all asymptotically flat vacuum solutions have zero ADM mass. The linearised solutions can have non-zero mass, however, so this implies that the linearised solutions are not limits of the exact solutions. This motivates the study of this theory because it may save it from the quantum instabilities caused by the ghost mode. On the other hand, non-asymptotically flat vacuum solutions include all Einstein spaces $R_{\mu\nu} = \lambda g_{\mu\nu}$, for λ the effective cosmological constant of the space (c.f. our presentation of the equations of motion for an Einstein space in eq (1.3.7) for $\gamma = 0$), and Deser and Tekin [26] [27] found an expression for the energy $E = m\lambda\frac{4}{3}(\alpha + 6\beta)$ where m is the mass parameter of the solution. Conformal gravity, with Lagrangian C^2, was found by Riegert [28] to have a Birkhoff theorem, that all spherically symmetric solutions are static and described by a 3-parameter solution family (including the charge of a Maxwell field). The ghost-free scale invariant theory, with only the R^2 term in the Lagrangian (the C^2 term being responsible for the ghost), has vacuum Einstein solutions, which are equivalent to solutions of general relativity with a cosmological term and coupled to a scalar field, and also a range of other solutions with $R = 0, R_{\mu\nu} \neq 0$ described by Kehagias et al. in [29]. Solutions of this theory coupled to matter cannot be asymptotically flat, and even small masses result in strong curvature [20]. Vacuum solutions can be asymptotically flat, and static spherically symmetric solutions include asymptotically Reissner-Nordstrom solutions with non-singular black holes and with traversable wormholes [30]. The issue of matter coupling in the general four-derivative Lagrangian will be one of our key interests and will be discussed in sections 2.3 and 3.1.

Our main consideration will be the theory of the most general four-derivative Lagrangian (1.1.7) without a cosmological constant, but including a cosmological constant leads to a number of differences. Deser and Tekin [26] [27] found that Schwarzschild-de-Sitter solutions in this theory have energy $E = m(1 + \frac{4}{3}\Lambda(\alpha + 6\beta))$. In [31] Lu and Pope considered the linearisation around the AdS background ($\Lambda < 0$) of the $\beta = 0$ case, i.e. with Lagrangian $R - 2\Lambda - \alpha C^2$. The equations of motion then show a massless graviton and a massive spin-2 mode that is stable for $0 < \alpha \leq -\frac{3}{4\Lambda}$. The theory where this is saturated ($\alpha = -\frac{3}{4\Lambda}$) they call critical gravity, because the mass of the spin-2 is reduced to zero. In critical gravity the energies of the now-massless spin-2 mode and the graviton are both zero, while new logarithmic modes appear, and the mass of the space-time (given by the formula above) vanishes. This was followed-up in [32] where instead an inequality for α is given so that theory's spin-2 modes can still be non-tachyonic, even while still having their usual problem of negative energy, but in fact they can then be truncated from the theory with a suitable boundary condition, leaving a unitary theory. Our consideration of the theory that includes a cosmological constant is limited to appendix A

where we present a limited "no-hair" theorem that static solutions of this theory, with a horizon and whose scalar curvature is asymptotically constant, must have $R = 4\Lambda$ throughout the space.

In the present work we consider four dimensions and $\Lambda = 0$, using the most general such four-derivative theory (1.1.7). The classical solutions were first studied in detail in [6], which focused on static spherically symmetric solutions. Such solutions will always have one free parameter due to the static symmetry allowing scaling of g_{tt}, but the radial coordinate is fixed. We shall give the number of free parameters in the form $n+1$ to avoid confusion over whether the time-scaling parameter is included or not. Linearised solutions around Minkowski space were found to have 5+1 free parameters, one of which is the ADM mass, two of which are coefficients of Yukawa potentials e^{-mr}/r (for r the radius, using Schwarzschild coordinates) for the two new massive particles, and the final two are coefficients of rising Yukawa potentials e^{mr}/r. Applying a boundary condition of asymptotic flatness removes the rising exponentials in the metric and also require that m_0 and m_2 are real, or equivalently that $\alpha > 0, \beta > 0$, or equivalently that the two massive modes are non-tachyonic. An asymptotically flat linearised solution coupled to a static, spherically symmetric perfect fluid existing for radius $r < l$ was found and it was apparent that the solution depended on the size and pressure of the source as well as its mass, in contrast to general relativity where Birkhoff's theorem finds spherically symmetric solutions to have 1+1 free parameters. Stelle recalled that the Schwarzschild solution is not the solution that couples to positive matter in the $R+R^2$ theory [20], and the Yukawa terms present in the matter-coupled linearised solutions in the general four-derivative theory imply that the Schwarzschild solution is not the exterior solution of positive matter in the more general theory either. We will review and develop the linearised solutions in section 2.3. A Frobenius analysis for asymptotic solutions around the origin, of the form $g_{rr} \sim r^s + O\left(r^{s+1}\right)$ and $g_{tt} \sim r^t + O\left(r^{t+1}\right)$, yielded three solution families $(s,t) = (0,0)_0$, $(1,-1)_0$ or $(2,2)_0$ (where we put the subscript to avoid confusion with other pairs of numbers with other meanings elsewhere in this work). The $(0,0)_0$ family is the only one of the three that does not have a curvature singularity at $r = 0$, the $(1,-1)_0$ family contains the 1+1 parameter Schwarzschild family, and the $(2,2)_0$ family was not well understood. At the time computer algebra was not available so further properties of these solution families were not very clear, but we shall review and considerably develop this approach in section 2.2.

Static spherically symmetric solutions were later also considered in detail by Holdom in [33]. Now using computer algebra, Holdom was able to find the $(0,0)_0$ family to many orders and determine that it has 2+1 free parameters. This family is interesting because it also appears in theories with 6, 8 and 10 derivatives (with the same number of free parameters), which makes it seem more physically relevant than the $(1,-1)_0$ and $(2,2)_0$ families which do not. In fact Holdom searched for solutions of the form $g_{rr} \sim r^s + O\left(r^{s+1}\right)$, $g_{tt} \sim r^t + O\left(r^{t+1}\right)$, assuming (unlike Stelle) that $s,t \in \mathbb{Z}$ and found that the $(0,0)_0$ family is the only such family present in

6, 8 and 10 derivative theories with generic couplings. This can be understood from the fact that the $(0,0)_0$ family does not have strong curvature at the origin, so is not very sensitive to the presence of higher-order curvature terms in the gravity Lagrangian being considered. In this family the metric component g_{rr} goes as $1 + O(r^2)$, which is positive at the origin, so asymptotically flat solutions in this family must have an even number of horizons and seem to lack singularities, in contrast to general relativity. The question of whether this family might replace Schwarzschild as the family that couples to matter was considered. It was observed that matter-coupled solutions of the $(0,0)$ form still had 2+1 free parameters, contrary to the expectation that they would be fixed by the properties of the source. We will observe later in section 2.3.6 that we believe the two non-trivial free parameters of this family (in vacuum and for the 4-derivative theory) both parameterise asymptotic non-flatness, which seems to correspond with this result.

Holdom found the $(2,2)_0$ family in the four-derivative theory to have 5+1 free parameters, the same number as the linearised solution, which suggested that it was the best candidate for constructing a solution that interpolates between weak gravity at large radius and a region of strong gravity near the origin. He found a numerical solution of an asymptotically flat $(2,2)_0$ solution for $\alpha = 3\beta = \frac{1}{32\pi} = \frac{1}{2}\gamma G$. It approximated the Schwarzschild solution outside the Schwarzschild radius, but instead of a horizon it had a region of strong curvature with radius of the same order as the Schwarzschild radius. This solution is classically physically reasonable, but the region of strong curvature suggests that including higher-derivative terms in the action might change the solution in the "interior", possibly making it non-singular.

Holdom also studied the matter coupling of the four-derivative theory. An incompressible source with density $\rho(r) = \rho_0 e^{-r^2/\mathcal{R}^2}$ (and a pressure $p(r)$ fixed relative to it) was coupled to an asymptotically flat horizonless non-vacuum $(0,0)$ solution, and a numerical solution found for a single value of $\mathcal{R}$ and a range of densities ρ_0. In general relativity the central pressure $p(0)$ increases with increasing mass ($M := \int \rho(r) 4\pi r^2 \mathrm{d}r$) and becomes infinite at a finite mass, causing gravitational collapse. In the higher derivative solution, in contrast, the integrated density is not the same as the ADM mass. The relation between mass and pressure $M(p(0))$ has a positive correlation for small pressures, but the mass reaches a maximum at finite pressure and then starts to decrease as the pressure increases (this picture is the same considering either kind of mass). It was argued that this is still true even with more realistic sources, and therefore that gravitational collapse may not occur. This is a rather strange picture of matter coupling, because only sources lighter than some maximum can exist. It may be that another solution family describes the more massive sources. The issue of matter coupling will be one of our key interests and in section 3.1 we shall argue that $(2,2)_0$ families are the correct description for positive minimally-coupled matter.

Nelson [34] considered static solutions (not requiring spherical symmetry) and proved that

the Ricci scalar must vanish in static asymptotically flat space-times with a horizon [5]. This contrasts with the various matter-coupled solutions that have been found by various authors, which do not generically have vanishing Ricci scalar. Roughly speaking, the implication is then that matter-coupled solutions must either be non-asymptotically-flat or must not have a horizon. To make a less rough, more solid argument of this point will require a lot more evidence and rigour, but still it is a striking statement that was a significant motivation for the current work. We review the proof and generalise it to space-times without horizons in section 2.1 and to theories with cosmological constants in appendix A. The theorem will enable us to make many comments connecting asymptotic solutions about finite radii with their behaviour at infinity, which was not possible before. Note that using this theorem, where applicable, to constrain solutions to have $R = 0$ reduces the theory's set of solutions to those of the $R + C^2$ theory.

This thesis primarily includes work presented in [1] and [2] and its structure is as follows: In section 1.2 we present some background material that will be useful for understanding some parts of the thesis. In section 1.3 we present the covariant and the static, spherically symmetric equations of motion which are this thesis's primary focus. In chapter 2 we try to find all the solution families of the theory and their basic properties, using expansions around the origin (section 2.2), around a non-zero radius (section 2.4), perturbative expansions around flat space (section 2.3), and inform the analysis with a theorem constraining the Ricci scalar (section 2.1). In chapter 3 we shift focus to firstly considering a physical property of a realistic solution, and then going from that property to see what solutions families can have it. In section 3.1 we use our knowledge of solution families to present arguments that coupling to positive matter is described by a solution family quite different to any in general relativity, and we present a sketch of some of the calculations that would be involved in constructing explicit solutions. In section 3.2 we discuss black hole solutions, and present a proof that the Schwarzschild solution above a certain mass is isolated, and then we find numerical examples of a second type of asymptotically flat black hole that coincides with the Schwarzschild solution below that mass. In section 3.3 we explore the space of asymptotically flat solutions numerically to see which finite-radius solution families connect to them. Most of the solutions families we found will appear but there will be some unexpected features and the results will be inconclusive.

1.1.1 Conventions and notation

We use the "mostly plus" convention for the metric, so its signature is

$$(-,+,+,+)$$

[5] Unfortunately the paper's further argument that certain conditions imply the entire Ricci tensor must vanish was found to contain errors.

We use the following convention for the Riemann tensor

$$[\nabla_\mu, \nabla_\nu] V^\rho = R_{\mu\nu}{}^\rho{}_\sigma V^\sigma \tag{1.1.8a}$$

and the following convention for the Ricci tensor and scalar

$$R_{\mu\nu} = R_\mu{}^\sigma{}_{\nu\sigma} \tag{1.1.8b}$$

$$R = R_\mu{}^\mu \, . \tag{1.1.8c}$$

By correspondence with general relativity our Lagriangian parameter γ has value

$$\gamma = \frac{1}{16\pi G} \, . \tag{1.1.9}$$

When doing numerical work we shall often set $\gamma = 1$ and leave it out of our equations, but when describing mass we shall still write GM instead of $\frac{M}{16\pi}$, for clarity.

We sometimes use the abbreviation "LO" for "leading-order" of a perturbative series, and "NLO" for the next-to-leading order.

1.2 Background material

1.2.1 Junction conditions

The problem of finding solutions of higher derivative gravity naturally has a lot in common with the problem of finding solutions of general relativity. Many of the same tools can be used, including all the differential geometry, but some important theorems cannot be used, in particular the uniqueness theorems. In this section we discuss the theory of coupling to a codimension 1 hypersurface using the formalism developed by Israel [35] and we shall follow the pedagogical discussion of it from [36]. The formalism for this is not covered in most undergraduate courses on general relativity but will be needed by us when we derive properties of solutions coupled to matter. We will wish to consider vacuum solutions, so we shall couple to concentrated matter sources. Matter sources with dimensions 0+1 or 1+1 are not well-defined [37] so we will consider only the examples of a thin or filled spherical shell with vacuum outside.

In four dimensions hypersurfaces with dimension 2+1 have codimension 1 and partition space-time into two regions. For example, we shall be particularly interested in static time-like hypersurfaces, which are extent in time and have normal vectors that are space-like, which partition space-time into interior and exterior regions. We shall consider examples where the hypersurface is a boundary surface, representing a jump discontinuity in the stress-energy density, or a surface layer where a stress-energy density is infinite and concentrated at the surface. In general relativity dealing with such surfaces is made difficult by the fact that not only may the line element be different on either side of the surface, the coordinates may also differ.

Let the time-like hypersurface Σ partition space into two regions, $\mathcal{M}^+$ and $\mathcal{M}^-$, with different metrics $g^+_{\alpha\beta}$ and $g^-_{\alpha'\beta'}$. Consider the $\mathcal{M}^+$ region, and describe the hypersurface with coordinates y_a. The induced metric on the surface Σ is $h^+_{ab} = g^+_{\alpha\beta}\frac{\partial X^\alpha}{\partial y^a}\frac{\partial X^\beta}{\partial y^b}$. The first junction condition is simply that the two manifolds $\mathcal{M}^\pm$ are joined at the boundary Σ in a geometrical sense. More formally, it is that the hypersurface has a well-defined geometry, so the induced metric calculated from the location of Σ in $\mathcal{M}^+$ must be equivalent to the induced metric calculated from its location in $\mathcal{M}^-$, i.e. related by a coordinate transformation. We shall use such a coordinate transformation to write $h^+_{ab} = h^-_{ab} = h_{ab}$. For the remaining coordinate we use geodesic distance from Σ. Imagine that Σ is pierced orthogonally by a congruence of geodesics, and that points not on Σ are labelled by l, defined as the proper time/proper distance from Σ along a geodesic, such that l is positive in $\mathcal{M}^+$, negative in $\mathcal{M}^-$, and 0 on Σ. In this way we define a set of continuous coordinates that we may use on both sides of the hypersurface. This is an example of what Israel called "natural coordinates" and they will make calculations much easier. Next we consider requiring the space-time to be a solution to some gravitational equations of motion. In the literature the equations of motion are usually the

Einstein equation, but the discussion can be adapted to other equations such as the equations of higher derivative gravity.

We allow the stress-energy tensor to be distribution-valued, that is featuring Heaviside step functions Θ and Dirac delta functions δ. [6] So we will solve for stress-energy tensors of the form

$$T_{\alpha\beta} = \Theta(l)T^{+}_{\alpha\beta} + \Theta(-l)T^{-}_{\alpha\beta} + \delta(l)S_{\alpha\beta} \tag{1.2.1}$$

where to write this we implicitly needed a coordinate basis that exists in both $\mathcal{M}^+$ and $\mathcal{M}^-$, such as the one we constructed. The quantity $S_{\alpha\beta}$ can be shown to be tangent to the hypersurface and it has the interpretation of the stress-energy of the hypersurface Σ. If we use the Einstein equation then we have $R_{\alpha\beta} = 8\pi G\left(T_{\alpha\beta} - \frac{1}{2}g_{\alpha\beta}(T_{\gamma\delta}g^{\gamma\delta})\right)$. So $R_{\alpha\beta}$ must also be distribution-valued. Schematically, R is two derivatives of the metric. We make an ansatz that in general relativity a distribution-valued R will arise from a metric of the form

$$g_{\alpha\beta} = \Theta(l)g^{+}_{\alpha\beta} + \Theta(-l)g^{-}_{\alpha\beta}\ . \tag{1.2.2}$$

Let us define a notation for the difference of a tensor $A^{\nu\cdots}_{\mu\cdots}$ across the hypersurface

$$\left[A^{\nu\cdots}_{\mu\cdots}\right] := A^{\nu\cdots}_{\mu\cdots}(\mathcal{M}^+)\big|_\Sigma - A^{\nu\cdots}_{\mu\cdots}(\mathcal{M}^-)\big|_\Sigma\ . \tag{1.2.3}$$

Computing the Christoffel symbols gives us terms like $g^{\cdot\cdot}\partial_\cdot g_{\cdot\cdot}$ where therefore $\partial_\cdot g_{\cdot\cdot}$ is of the form

$$\partial_\gamma g_{\alpha\beta} = \Theta(l)\partial_\gamma g^{+}_{\alpha\beta} + \Theta(-l)\partial_\gamma g^{-}_{\alpha\beta} + \epsilon\delta(l)[g_{\alpha\beta}]n_\gamma \tag{1.2.4}$$

but we recall that the value of g on Σ is given by the pull-back, h, and that h is continuous across Σ. This means that the $\delta(l)$ term vanishes and the Christoffel symbols are of the form

$$\Gamma^{\gamma}_{\alpha\beta} = \Theta(l)\Gamma^{(+)\gamma}{}_{\alpha\beta} + \Theta(-l)\Gamma^{(-)\gamma}{}_{\alpha\beta}\ , \tag{1.2.5}$$

where $\Gamma^{(\pm)}$ are calculated with $g^{\pm}$, respectively. Computing the Riemann tensor gives us terms like $\partial_\cdot\Gamma^{\cdot}_{\cdot\cdot} + \Gamma^{\cdot}_{\cdot\cdot}\Gamma^{\cdot}_{\cdot\cdot}$ and it is of the form

$$R_{\gamma\delta}{}^{\alpha}{}_{\beta} = \Theta(l)R^{(+)\alpha}_{\gamma\delta\ \ \beta} + \Theta(-l)R^{(-)\alpha}_{\gamma\delta\ \ \beta} + \delta(l)\left(n_\gamma[\Gamma^{\alpha}_{\beta\delta}] - n_\delta[\Gamma^{\alpha}_{\beta\gamma}]\right)\ , \tag{1.2.6}$$

where we used that $\partial_\alpha l = n_\alpha$ (since the hypersurface is time-like), and where $R^{(\pm)}$ are calculated with $\Gamma^{\pm}$, respectively. Note that $[\Gamma^{\alpha}_{\beta\delta}]$ is the difference of two Christoffel symbols in the same coordinate system, so is a tensor. From these results we can calculate the stress-energy, and we do indeed find it to be of the form (1.2.1). One can derive that $S_{\alpha\beta}$ is tangent to the

[6] Recall the properties $\Theta(l)^2 = \Theta(l)$ and $\Theta(l)\Theta(-l) = 0$

hypersurface Σ, and that its components are related to the discontinuities of the extrinsic curvature across Σ:

$$S_{ab} = -\frac{1}{8\pi G}\left([K_{ab}] - [K]\, h_{ab}\right) \ . \tag{1.2.7}$$

In section 3.1 we discuss coupling and in section 3.1.2.1 we find it useful to work through an explicit example of coupling to a source in general relativity.

The higher derivative equations of motion, which we shall see later, have equations of motion of a different form. They go as $8\pi G\, T_{\alpha\beta} \sim R + \nabla\nabla R + R^2$. This significantly changes the construction because the right-hand side is schematically four derivatives of the metric. We still need the stress-energy tensor to be of the form (1.2.1), so we must calculate what form the metric should take. We shall not calculate the general form of such a metric here, but later on when we deal with junction conditions (section 3.1) we shall consider a specific example. There we shall find that the metric is continuous across the hypersurface, but it has discontinuities in the second derivative of the normal component and in the third derivative of the tangential component. There is another case, the Einstein-Weyl theory, whose linearised solutions are considered in section 2.3.4.1, where the metric has discontinuities in the normal component and in the first derivative of the tangential component. Interestingly, this Einstein-Weyl example therefore seems to have the same junction conditions as general relativity, despite the higher differential order, but a general discussion of this is beyond the scope of the present work.

1.2.2 Uniqueness theorems in general relativity

Black holes in general relativity are tightly constrained by powerful uniqueness theorems. The simplest is Birkhoff's theorem, which proves that there is a single spherically symmetric vacuum solution to Einstein's equations, which must be static, and the total mass of the gravitating object is its only free parameter.

Birkhoff's theorem can be shown as follows. Consider the most general four-dimensional spherically symmetric metric. The requirement of spherical symmetry means that it must have at least the isometries and Killing vectors of the metric on a sphere $d\Omega^2 = d\theta^2 + \sin^2(\theta)d\phi^2$, where θ and ϕ are the usual spherical polar coordinates. One can show that a spherically symmetric metric must be of this form

$$ds^2 = f_1(\tau,\rho)d\tau^2 + f_2(\tau,\rho)d\rho^2 + f_3(\tau,\rho)d\tau d\rho + r^2 d\Omega^2 \tag{1.2.8}$$

and a coordinate transformation to $t(\tau,\rho)$, $r(\tau,\rho)$ can always bring it into this form

$$ds^2 = -B(t,r)dt^2 + A(t,r)dr^2 + r^2 d\Omega^2 \tag{1.2.9}$$

which is therefore the most general spherically symmetric metric. The Einstein tensor of this metric in four dimensions has non-zero components:

$$\begin{aligned}
G_{tt} =& \frac{B}{r^2A^2}\left(rA' + A(A-1)\right)\\
G_{tr} =& \frac{\dot{A}}{rA}\\
G_{rr} =& \frac{1}{Br^2}\left(rB' + B(1-A)\right)\\
G_{\theta\theta} =& \frac{r}{4A^2B^2}\left(r\left[A\dot{A}\dot{B} + B\dot{A}^2 - 2BA\ddot{A} - BA'B' - AB'^2\right] - 2B^2A' + 2AB\left[B' + rB''\right]\right)\\
G_{\phi\phi} =& \sin^2(\theta)G_{\theta\theta}\ ,
\end{aligned}$$

where dots denote derivatives with respect to t, and primes denote derivatives with respect to r. Note that by the Bianchi identity $G_{\theta\theta}$ is not independent of G_{tt} and G_{rr}. We assume that outside some radius r_0 there is a vacuum. The $G_{tr} = 0$ component immediately tells us then that (in that region) A has no time-dependence. The combination $G_{tt}\frac{A}{B}r^2 + G_{rr}r^2$ is equal to $\frac{A'}{A} + \frac{B'}{B}$. The vanishing of this implies that $\frac{B'}{B} = -\frac{A'}{A}$, and therefore that the ratio $\frac{B'}{B}$ is time independent, and therefore that B is of the form $B = B_t(t) \times B_r(r)$. Therefore $B(t,r) = \frac{C'(t)^2}{A(r)}$ where we have chosen to write the time-dependent function as $C'(t)^2$ instead of $B_t(t)$, but it is still true that $C(t)$ is simply a constant of integration for integration with respect to r. Simplifying the metric using what we have derived, the metric is:

$$ds^2 = -\frac{C'(t)^2}{A(r)}dt^2 + A(r)dr^2 + r^2 d\Omega^2 \tag{1.2.10}$$

and changing to a different time coordinate $t_2 = t_2(t) = C(t)$ makes the metric

$$ds^2 = -\frac{1}{A(r)}dt_2^2 + A(r)dr^2 + r^2 d\Omega^2 \ . \tag{1.2.11}$$

So starting from the Einstein equation of a spherically symmetric metric we need nearly no calculation to show that all spherically symmetric metrics are also static. If we stop being shy about calculation then we can solve the first-order non-linear ordinary differential equation $G_{tt} = 0$ to yield the Schwarzschild solution

$$g_{rr} = A(r) = \frac{1}{1 - \frac{2GM}{r}} \tag{1.2.12}$$

(where the constant of integration has been related to the mass by correspondence with Newtonian gravity). Birkhoff's theorem is that all spherically symmetric vacuum solutions to GR are also static, and that the unique solution is the Schwarzschild solution. Remarkably, the solution outside a spherically symmetric source is independent of the details of the source and of its evolution.

The proof of the converse, that static vacuum solutions must be spherically symmetric, is much more difficult. It was originally proven by Israel in [38] for pure gravity and in [39] for gravity coupled to a electric field, subject to some assumptions. A space-time is static if it admits a hypersurface-orthogonal Killing field which is time-like over some domain. The metric of a static space-time can always be written in the form

$$ds^2 = g_{ab}(x^c)dx^a dx^b - V^2(x^c)dt^2 \ , \tag{1.2.13}$$

where t is the time-like (in the exterior region) coordinate, roman indices run over the other coordinates $1, 2, 3$, and greek indices run over all four coordinates $1, 2, 3, 4$. Spatial hypersurfaces Σ of constant t are considered. Israel's proofs are subject to the following assumptions

- Everywhere outside the horizon there is vacuum, or if considering EM fields there is an "electrovacuum" meaning there are no charges but there is the energy density of the EM fields.
- There is an infinite red-shift surface, i.e. a surface where $g_{tt} = 0$ and the Killing vector becomes null, that bounds Σ (this will also be the horizon, but infinite red-shift surfaces are not always the same as horizons).
- Σ is asymptotically Euclidean, i.e. the space-time is asymptotically flat
- The curvature invariant $R_{\mu\nu\rho\sigma}R^{\mu\nu\rho\sigma}$ is bounded on Σ.
- (If considering EM fields) The EM fields are either purely electric, or purely magnetic, and admit a scalar potential that is asymptotically that of a monopole.

- The equipotential surfaces $V = c = \text{const.} > 0$ within Σ, are 2-spaces that are simply connected. This condition can be expressed alternatively as the condition that magnitude of the Killing vector must have non-zero gradient everywhere outside the horizon, or as the condition that there is no point outside the horizon where a non-accelerating particle can remain at rest.

- If the lower bound of V on Σ is zero, then as $c \to 0+$ the limiting 2-space is closed and has a finite area (the case where the lower bound is positive need not be considered since this implies that the space-time is everywhere flat).

If these are given, then it is proven that the only solution is the Reissner-Nordstrom solution, or if there are no EM fields, its special case, the Schwarzschild solution. The last three conditions are technical restrictions that mean the proof cannot be used in the case of a horizon with different topology (other than spherical), and cannot rule out solutions with equilibrium points, where a test particle would experience no force. Hawking [40] later showed that a space-time that is asymptotically flat and asymptotically predictable (meaning that from a Cauchy surface one can determine what happens at future null infinity) and has a time-like Killing vector (i.e. that is stationary), and where the matter satisfies the weak energy condition [7], must also have a second Killing vector, that near infinity corresponds to a Poincare transformation, so it must correspond to a rotation. Thus stationary black holes must be either static (if not rotating) or axisymmetric (if rotating). He then uses this to prove that in such stationary space-times with sources obeying the dominant energy condition [8], the connected components of the horizon must have topology S^2, i.e. that black holes are spherical but there may be multiple black holes. This addresses the last condition of Israel's proof by deriving it from a more physical statement. The last three, technical restrictions of Israel's proof were removed later by long proofs by Muller Zum Hagen, Robinson and Seifert in [41] for pure gravity and in [42] for gravity coupled to EM fields, and later again by simple proofs by Robinson in [43]. Thus the final result is that it can be proved that static solutions must be spherically symmetric Reissner-Nordstrom solutions using only intuitive, physically reasonable assumptions.

The similar result for stationary black holes is a lot harder to prove. In 1971 [44] Carter showed that black holes that are stationary, asymptotically flat, vacuum, with spherical topology, have only two free parameters - the mass M and angular momentum J. Solutions were shown to fall into discrete (M, J) families - that is, perturbations of solutions could only shift M and J but not deform it into a different family. The Kerr black hole solution is of course one such family. Its zero-angular-momentum limit, Schwarzschild, has been proven to be unique,

[7] The weak energy condition is a constraint on the stress-energy tensor requiring that $T_{\mu\nu}v^\mu v^\nu \geq 0$ for v^μ an arbitrary future-directed time-like vector, meaning that any observer would measure the energy density to be non-negative.

[8] The dominant energy condition is a constraint on the stress-energy tensor requiring that $-T^\mu{}_\nu v^\nu$ should be a future-directed time-like or null vector field, for v^μ an arbitrary future-directed time-like vector, meaning that any observer would measure the momentum density to be time-like or null.

so the other families cannot have zero-angular-momentum limits (at least not ones that satisfy the assumptions) and are thus argued to be unlikely to be physically realistic solutions. Soon afterwards Hawking's paper removed the need to assume spherical topology. The further step of proving that the Kerr black hole is indeed the only stationary solution was made by Robinson in 1975 [45]. The question of a charged stationary black hole is harder again. Robinson [46] was also able to show that charged rotating black holes fall into discrete (M, J, Q) solution families, which include the Kerr-Newman solution. Since the above theorems prove that there are unique solutions in the zero charge and/or zero angular momentum limits, and that the Kerr-Newman solution limits to those, then solutions discretely different from Kerr-Newman cannot have admissable limits of zero charge and/or zero angular momentum, and are therefore physically unappealing. The full proof was completed by Mazur [47] and Bunting [unpublished] , who showed that in fact there are no such other solutions, i.e. that the Kerr-Newman solution is the only such black hole solution. For reviews of uniqueness theorems in general relativity see, for example, [48], [49], [50] and [51], which were useful to the author.

The theory of higher derivative gravity treated in this thesis, in contrast, has no such uniqueness theorems. Comparison to the uniqueness theorems available in general relativity highlights how much more difficult it will be to make physical statements about higher derivative gravity. The uniqueness theorems in general relativity assumed at various places throughout the literature that there are no naked singularities. There is no proof that there cannot be naked singularities in general relativity, it is called the "cosmic censorship conjecture". One example of a way in which the higher derivative theory is less clear is that later on we shall actually find static spherically symmetric solutions with naked singularities, and even argue that they may be in some respects more physical than black holes. We also have no proof that black hole solutions must have spherical topology, nor that static solutions must be spherically symmetric, nor that spherically symmetric solutions must be static. This means that restricting consideration to the static spherically symmetric solutions constitutes a considerable assumption, even though it seems physically reasonable. We also note that in the higher derivative theory an important unresolved matter is whether charged solutions or rotating solutions can limit to any of the static spherically symmetric solutions that we will find, and if so, which ones. There is only a single no-hair theorem that we are aware of in the higher derivative theory, which is that black holes that are static and asymptotically flat must have $R = 0$. We shall present this proof later in section 2.1.1 and we shall also modify it to find constraints on a variety of solution families that do not (or may not) have horizons. Generally though the higher derivative theory has few proofs that certain important symmetries must exist, and lacks knowledge of the full range of solutions, so when we find solutions with both properties that make them seem unphysical and properties that make them seem physically plausible we will keenly feel the absence of uniqueness theorems and their clarifying power.

1.2.3 Frobenius' method for finding series solutions to differential equations

The focus of this work is to find the static spherically symmetric solutions of higher derivative gravity. By definition in such solutions the metric does not depend on time or angle, so depends only on a single radial coordinate. The problem, therefore, amounts to solving coupled non-linear ordinary differential equations for the metric components in terms of the radial coordinate. We shall see the equations later in section 1.3, and find that they are extremely large and extremely non-linear. There is no general procedure for finding solutions to such differential equations. One method we shall use to tackle the equations is to study solutions perturbatively close to the solutions to GR. But we also wish to learn about solutions *not* perturbatively close to the solutions of GR. We shall use another method, which is borrowed from the study of linear second-order ordinary differential equations, Frobenius' method. In this section we discuss some definitions and theorems for linear second-order ordinary differential equations, but do not delve into too much detail since our goal is only to justify the way we will use the same approach to solve unrelated non-linear differential equations. When writing this explanation of Frobenius' method [52] and [53] were useful to the author.

Define a second-order linear ordinary differential equation as

$$y''(x) + p(x)y'(x) + q(x)y(x) = 0 \tag{1.2.14}$$

for general functions $p(x)$ and $q(x)$. For convenience of notation let us define the differential operator

$$\mathcal{L}y := y''(x) + p(x)y'(x) + q(x)y(x) \ . \tag{1.2.15}$$

This definition of a general second-order linear ODE is invariant under shifts of the dependent variable $x \to x - x_0$, so without loss of generality let us consider the solutions around the point $x = 0$.

1.2.3.1 Ordinary points of the differential equation

If the functions $p(x)$ and $q(x)$ are analytic about the point $x = 0$, then this is an ordinary point of the differential equation. It can be shown that if $x = 0$ is an ordinary point then every solution $y(x)$ is analytic about $x = 0$, and its solutions can be written as

$$y(x) = \sum_{n=0}^{\infty} a_n x^n \ , \tag{1.2.16}$$

where the series expansion for y converges in all of the region where the series expansions for p and q converge. This solution can be substituted into the differential equation (1.2.14) to get

$$\begin{aligned}\mathcal{L}y = &(a_1 p(0) + a_0 q(0) + 2a_2) \\ &+ x\left(a_1 p'(0) + 2a_2 p(0) + a_0 q'(0) + a_1 q(0) + 6a_3\right) \\ &+ \frac{1}{2}x^2\left(a_1 p''(0) + 4a_2 p'(0) + 6a_3 p(0) + a_0 q''(0) + 2a_1 q'(0) + 2a_2 q(0) + 24a_4\right) + O(x^3)\ .\end{aligned}$$

So we see that by solving order-by-order in x we fix the coefficients a_n. The differential equation is of second order, so the solution must have two arbitrary constants, so two of the a_n remain free. Rather than having some undetermined a_n it is more usual to write the general solution as the sum of two completely determined functions, y_1 and y_2,

$$y(x) = c_1 y_1(x) + c_2 y_2(x)\ , \tag{1.2.17}$$

where c_1 and c_2 are arbitrary constants.

1.2.3.2 Regular singular points of the differential equation

If the functions $p(x)$ and/or $q(x)$ diverge at $x = 0$ then it is a singular point of the differential equation. A necessary and sufficient condition that the solution $y(x)$ is finite is that the functions $P(x) := xp(x)$ and $Q(x) := x^2 q(x)$ are analytic at $x = 0$. We shall use the following re-writing of the differential equation

$$0 = x^2\,\mathcal{L}y = x^2\,y''(x) + x\,P(x)\,y'(x) + Q(x)\,y(x)\ , \tag{1.2.18}$$

where we have simply multiplied to remove a denominator. For analytic $P(x)$, $Q(x)$, this point is called a *regular singular point* (if either of these is not analytic then then it is called an *irregular singular point*). Frobenius' method for finding series solutions of differential equations is designed to find the solutions around a regular singular point. There is at least one solution to the differential equation of the form

$$y = x^s \sum_{n=0}^{\infty} a_n x^n \quad , \quad a_0 \neq 0\ , \tag{1.2.19}$$

where this series converges in all of the region where $P(x)$ and $Q(x)$ converge, as stated by Fuch's theorem. Substituting this into the differential equation we get

$$x^2\,\mathcal{L}y = x^s\Bigg(a_0(s(P(0)+s-1)+Q(0)) \\ + x\left(a_0\left(sP'(0)+Q'(0)\right)+a_1((s+1)(P(0)+s)+Q(0))\right)+O(x^2)\Bigg)\,.$$

Since the differential equation is linear, the lowest-order term is $a_0(s(P(0)+s-1)+Q(0))$, so making this vanish leaves a_0 arbitrary but gives us a quadratic equation for s. This is called the *indicial equation*. The two roots of this equation are $s=\alpha$ and $s=\beta$, and let us say W.L.O.G. that $\alpha \leq \beta$. The proposed solutions of the differential equation corresponding to each root are

$$y_\alpha = x^\alpha \sum a_n^{(\alpha)} x^n \qquad \text{and} \qquad y_\beta = x^\beta \sum a_n^{(\beta)} x^n\,.$$

If the two roots differ by a non-integer amount, then the full solution is a simple sum of these two functions

$$y = c_1 y_\alpha + c_2 y_\beta \quad , \quad \alpha - \beta \notin \mathbb{Z}\,. \tag{1.2.20}$$

However, if the roots are the same or differ by an integer then things are more complicated; let us consider it now.

Consider the series expansion of the equation (1.2.18). Write $P(x) = \sum p_m x^m$ and $Q(x) = \sum q_m x^m$, and substitute the ansatz (1.2.19) into (1.2.18). This gives:

$$\begin{aligned} x^2\mathcal{L}y &= x^s\Bigg(\left(\sum_n (s+n)(s+n-1)a_n x^n\right) \\ &\quad + \left(\sum_m p_m x^m\right)\left(\sum_n (s+n)a_n x^n\right) + \left(\sum_m q_m x^m\right)\left(\sum_n a_n x^n\right)\Bigg) \\ &=: x^s \sum_n g_n x^n\,, \end{aligned}$$

where we define the g_n as a series expansion of the differential equation. To write the g_n explicitly define a convenient notation

$$\begin{aligned} f(n) &:= (s+n)(s+n-1) + p_0(s+n) + q_0 \\ h(n,m) &:= p_m(s+n) + q_m \end{aligned}$$

so that the series coefficients of the differential equation are

$$\begin{aligned} g_0 &= a_0 f(0) \\ g_1 &= a_1 f(1) + a_0 h(0,1) \\ g_2 &= a_2 f(2) + a_1 h(1,1) + a_0 h(0,2) \\ &\vdots \\ g_n &= a_n f(n) + \sum_{k=1}^{n} a_{n-k}\ h(n-k,k)\ . \end{aligned}$$

The solution method is to solve the equation order by order, setting each $g_n = 0$ to fix each a_n, respectively, and this completely fixes the series for the s we are using (up to a_0). However, this is not possible if one of the $f(n)$ is zero. What is the condition for this to happen? Consider the indicial equation and use it to re-express $f(n)$ in terms of the roots

$$\begin{aligned} f(0) &= s(s-1) + p_0 s + q_0 \\ &= (s-\alpha)(s-\beta) \\ \therefore q_0 &= \alpha\beta \\ p_0 &= 1-\alpha-\beta \\ \therefore f(n) &= (s+n-\alpha)(s+n-\beta) \\ f(n)|_{s=\alpha} &= n\,(n-(\beta-\alpha))\ . \end{aligned}$$

If $\beta - \alpha \notin \mathbb{Z}$ then $f(n) \neq 0$ and the method can determine all the $a_n^{(\alpha)}$ and there is no problem, but if not then we can now see the complication: if $\beta - \alpha = i \in \mathbb{Z}^+$ then $f(i)|_{s=\alpha} = 0$. Let us say that we solve the equations $g_{n\leq i-1} = 0$ for the variables $s, a_{1\leq n\leq i-1}$ (remember that it is a linear ODE so a_0 must be arbitrary), and then consider the equation $g_i = 0$. If $f(i) = 0$ then the equation $g_i = 0$ is a function only of $s, a_{1\leq n\leq i-1}$ and there are two possibilities. The first possibility is that the equation $g_i = 0$ is identically satisfied, and then the system is consistent but a_i is free. In the y_α solution a_i is the coefficient of $x^{\alpha+i} = x^\beta$, and it is free simply because we can always add a multiple of y_β to y_α and have it still be a solution. In this case the full solution is again simply

$$y = c_1 y_\alpha + c_2 y_\beta\ , \tag{1.2.21}$$

where, unlike equation (1.2.20), these series mingle together for the terms $x^{n\geq\beta}$ [9]. The second possibility is the generic one, it is that the equation $g_i = 0$ makes the system *overconstrained*, and y_α is not a solution. We see that in the case where $\beta - \alpha = i \in \mathbb{Z}^+$ then generically y_α is not the second solution. In the case of equal roots $\alpha = \beta$ then $y_\alpha = y_\beta$ is not independent, and again, the second solution is not y_α. We therefore say that there is always one solution of the

[9] this is what happens if one applies this method to an ordinary point of the ODE

form (1.2.19), for the *larger* root, $\beta \geq \alpha$. But if the second solution is not also of the form (1.2.19) then what form does it have? We now search for the second solution.

Consider the case of equal roots $\alpha = \beta$. Apply the differential operator $\mathcal{L}$ to y to get

$$x^2\mathcal{L}y = x^s \sum_n g_n x^n \,, \qquad\qquad g_n = a_n f(n) + \sum_{k=1}^{n} a_{n-k}\; h(n-k,k) \;.$$

For now let us *not* solve the equation $g_0 = 0$ for s, but let us solve the other equations $g_{n>0} = 0$ for the $a_n = a_n(a_0, s)$. We now have

$$x^2\mathcal{L}y\big|_{g_{n>0}=0} = x^s \; g_0 \; x^0 = x^s a_0 f(0) = x^s a_0 (s-\alpha)^2 \;.$$

We already know that the first solution to this is y_α, because we can see that $x^2\mathcal{L}y_\alpha = x^2\mathcal{L}y\big|_{s=\alpha} = 0$. We find a second solution using differentiation to exploit the second zero of the $(s-\alpha)^2$ term thus:

$$\begin{aligned} x^2\mathcal{L}\left(\partial_s y(x,s)\right)\big|_{g_{n>0}=0} &= \partial_s\left(x^2\mathcal{L}y\big|_{g_{n>0}=0}\right) \\ &= \partial_s\left(x^s a_0 (s-\alpha)^2\right) \\ &= x^s a_0 \;\left[\ln(x)(s-\alpha)+2\right](s-\alpha) \;, \end{aligned}$$

which vanishes when $s = \alpha$. So we see that the function $y_2(x) := \partial_s y(x,s)|_{s=\alpha}$ also satisfies $\mathcal{L}y_2 = 0$. Inspection of the form of this solution makes it clear that it is independent, and is therefore the only other solution:

$$\begin{aligned} y_2 :=\; \partial_s y(x,s)|_{s=\alpha} &= \partial_s\left(x^s \sum a_n(s) x^n\right)\Big|_{s=\alpha} = \ln(x)\; x^\alpha \sum a_n x^n + x^s \sum a_n'(\alpha) x^n \\ &= \ln(x)\; y_\alpha + x^\alpha \sum a_n'\, x^n \;. \end{aligned}$$

The full solution is

$$y = \; c_1 y_\alpha + c_2\left[\ln(x) y_\alpha + x^\alpha \sum a_n'\, x^n\right] \;. \tag{1.2.22}$$

Written out this is of the form

$$y = x^\alpha\Big(\Big(a_0 + k_0\ln(x)\Big) + \Big(a_1 + k_1\ln(x)\Big)x^1 + \Big(a_2 + k_2\ln(x)\Big)x^2 + \ldots\Big) \;. \tag{1.2.23}$$

We note that there is a logarithm in the leading order term $x^\alpha(a_0 + k_0\ln(x))$.

Consider the case of roots that differ by an integer, $\beta - \alpha = i \in \mathbb{Z}^+$. Recall that solving the differential equation order by order, $x^2\mathcal{L}y = x^s\sum_n g_n x^n$, where $g_n = a_n f(n) + \ldots$, where $f(n) = (s+n-\alpha)(s+n-\beta)$, could not give all the a_n of the $s = \alpha$ solution, because of a zero of $f(n)|_{s=\alpha}$. Let us now look at the problem in a different way. Expand the differential equation, order by order and let us *not* solve $g_0 = 0$ for s, but solve the other $g_{n>0} = 0$ for the $a_n = a_n(s)$.

We now have

$$x^2\mathcal{L}y\big|_{g_{n>0}=0} = x^s a_0 f(0) = x^s a_0(s-\alpha)(s-\beta)$$
$$a_n(s) = -\frac{1}{f(n)}\sum_{k=1}^{n} a_{n-k}\, h(n-k,k)\ .$$

By inspection, the general solution for the coefficients $a_n = a_n(a_0, s)$ is of the form

$$\begin{aligned} a_n(a_0,s) &= a_0 \sum_{\{p_j\}} \frac{h(\dots)\dots h(\dots)}{f(1)^{p_1} f(2)^{p_2}\dots f(n-1)^{p_{n-1}}}\ \frac{1}{f(n)} \quad , \quad p_j = \{0,1\} \\ &= a_0\ \frac{F\Big(h(\dots),\ \dots\ , h(\dots), f(1), f(2),\ \dots\ , f(n-1)\Big)}{f(1)f(2)\dots f(n)}\ , \end{aligned}$$

where the first line is a sum of many terms with products of $f(1<k<n-1)$ in the denominator and products of $h(k,l)$ in the numerator, and the second line has been rearranged to a single fraction with unspecified function F being a polynomial function of its arguments that the reader can work out exactly if desired. The problem with determining a_i now manifests as the factor $\frac{1}{f(i)} \sim \frac{1}{s+i-\beta} = \frac{1}{s-\alpha}$ in its solution, which blows up when one tries to set $s=\alpha$ while keeping a_0 finite. By inspection of the solution we can see that such a factor will also be present in every term $a_{n\geq i}$. We are therefore led to define a function

$$\begin{aligned} y_b(x,s) &= (s-\alpha)\, x^s \sum a_n(s) x^n \\ &=: x^s \sum b_n(s) x^n\ . \end{aligned}$$

This, where the $a_n(a_0,s)$ are the same as above, is straightforwardly also a solution of the differential equation when either $s=\beta$ or $s=\alpha$

$$x^2\mathcal{L}y_b\big|_{g_{n>0}=0} = x^s a_0 f(0) = x^s a_0(s-\alpha)^2(s-\beta)\ .$$

The factor $(s-\alpha)$ in y_b means that the coefficients of x^n are $b_n := (s-\alpha)a_n$. The factors $\frac{1}{f(i)} \sim \frac{1}{s+i-\beta} = \frac{1}{s-\alpha}$, which are present in all $a_{n\geq i}$, are therefore cancelled in the b_n which remain finite when we set $s=\alpha$. However, for the lower-order terms $b_{n<i}$ there is no $\frac{1}{f(i)}$ factor, and the $(s-\alpha)$ makes these vanish. The first non-zero term in y_b is therefore $(s-\alpha)x^s a_i(s)x^i = \frac{\dots}{f(1)\,\dots\,f(i-1)} x^{s+i} \sim x^\beta$. This means that we have simply found the $s=\beta$ solution again:

$$y_b(x, s=\alpha) = (s-\alpha)\, x^s \sum a_n(s) x^n \Big|_{s=\alpha} \ =\ y(\,x\,, s=\beta\,)\ =\ y_\beta\ . \tag{1.2.24}$$

As in the case of equal roots, in the case of roots differing by an integer we find the only way to generate a second *independent* solution is differentiation with respect to s.

$$\begin{aligned} x^2\mathcal{L}\left(\partial_s y_b(x,s)\right)\big|_{g_{n>0}=0} &= \partial_s\left(x^2\mathcal{L}y_b(x,s)\big|_{g_{n>0}=0}\right) \\ &= \partial_s\left(x^s a_0(s-\alpha)^2(s-\beta)\right) \\ &= x^s a_0\ \left[\ln(x)(s-\alpha)(s-\beta)+(s-\alpha)+2(s-\beta)\right]\ (s-\alpha)\ . \end{aligned}$$

Which vanishes when $s=\alpha$. Writing this new solution explicitly:

$$\begin{aligned} y_2 := \left(\partial_s y_b(x,s)\right)\big|_{s=\alpha} &= \partial_s\left(x^s\sum b_n(s)x^n\right)\Big|_{s=\alpha} \\ &= \left(\ln(x)\,x^s\sum b_n(s)x^n + x^s\sum b_n'(s)x^n\right)\Big|_{s=\alpha} \\ &= \ln(x)y_\beta + x^\alpha\sum b_n' x^n\ , \end{aligned} \tag{1.2.25}$$

where in the third line we recalled that $(s-\alpha)\,x^s\sum a_n(s)x^n|_{s=\alpha} = x^s\sum b_n(s)x^n|_{s=\alpha} = y_\beta$. Inspection of the form of this solution makes it clear that it is linearly independent of y_β, and is therefore the only other solution. The full solution is therefore

$$y = c_1 y_\beta + c_2\left(\ln(x)y_\beta + x^\alpha\sum b_n' x^n\right) = y_\beta\left(c_1 + c_2\ln(x)\right) + c_2 x^\alpha\sum d_n\,x^n\ . \tag{1.2.26}$$

Note that the leading order term is still x^α, and the logs appear later. Written out this is of the form

$$y = x^\alpha\Big(d_0 + d_1 x + \cdots + d_{i-1}x^{i-1} + \Big(a_0 + k_0\ln(x)\Big)x^i + \Big(a_1 + k_1\ln(x)\Big)x^{i+1} + \ldots\Big)\ . \tag{1.2.27}$$

The formalism described here applied to general second-order linear ordinary differential equations, but it can be generalised to higher-order linear ordinary differential equations, which follows similarly but where we differentiate more times, so terms like $\ln(x)^2, \ln(x)^3$, etc., appear as well. For higher order equations there is no proof that such solutions are guaranteed to exist, but the method can still be useful. Later in chapter 3.2.1 this formalism will be applied to a second-order linear ordinary differential equation, but more often we shall simply draw inspiration from this formalism when we are working on third-order and second-order pairs of non-linear coupled ODEs. We shall expand our two functions in the form of (1.2.19) and find series solutions. Seeing the alternative solutions (1.2.22) and (1.2.25) we also use trial functions with $\ln(x)$ terms and $\ln(x)^n$ terms. Trial solutions of the Frobenius form will actually prove very successful. However, unfortunately, in the non-linear case we have no theorems to tell us about the convergence properties of such solutions.

1.3 Equations of motion

1.3.1 The general case

Consider the four-dimensional higher-derivative action (1.1.7)

$$I = \int d^4x\sqrt{-g}\left(\gamma(R-2\Lambda) - \alpha C_{\mu\nu\rho\sigma}C^{\mu\nu\rho\sigma} + \beta R^2\right) .$$

Varying it with respect to the metric $\frac{1}{\sqrt{-g}}\frac{\delta\mathcal{I}}{\delta g^{\mu\nu}}$ produces the equations of motion [6]

$$\begin{aligned}\frac{1}{2}T_{\mu\nu} = H_{\mu\nu} :=& \gamma\left(R_{\mu\nu} - \frac{1}{2}g_{\mu\nu}R + \Lambda g_{\mu\nu}\right) + \frac{2}{3}(\alpha-3\beta)\nabla_\mu\nabla_\nu R - 2\alpha\Box R_{\mu\nu} + \frac{1}{3}(\alpha+6\beta)g_{\mu\nu}\Box R \\ &- 4\alpha R^{\eta\lambda}R_{\mu\eta\nu\lambda} + 2\left(\beta+\frac{2}{3}\alpha\right)RR_{\mu\nu} + \frac{1}{2}g_{\mu\nu}\left(2\alpha R^{\eta\lambda}R_{\eta\lambda} - \left(\beta+\frac{2}{3}\alpha\right)R^2\right) ,\end{aligned} \tag{1.3.1a}$$

Where the identity

$$R^{\rho\sigma}R_{\mu\rho\nu\sigma} = R_{\mu\rho}R_\nu{}^\rho - \nabla_\rho\nabla_{(\mu}R_{\nu)}{}^\rho + \frac{1}{2}\nabla_\mu\nabla_\nu R \tag{1.3.2}$$

can be used to write them in an alternative way. We consider only the case where $\Lambda = 0$ except where specified. Note that all vacuum solutions to general relativity ($R_{\mu\nu} = 0$) are still vacuum solutions of the higher-derivative theory. In particular note that this implies that the Schwarzschild solution is still a vacuum solution. The equations of motion satisfy generalised Bianchi identity:

$$\nabla^\nu H_{\mu\nu} \equiv 0 \tag{1.3.3}$$

and have trace

$$H_\mu{}^\mu = 6\beta\Box R - \gamma R = \frac{1}{2}T_\mu{}^\mu , \tag{1.3.4}$$

which is of fourth-order in derivatives of the metric for $\beta \neq 0$ and of second-order for $\beta = 0$.

As already stated the work in [7] showed that the theory describes two massive particles beyond the massless graviton of GR, one spin-2 particle and one spin-0 particle

$$m_2^2 := \frac{\gamma}{2\alpha} , \tag{1.3.5a}$$

$$m_0^2 := \frac{\gamma}{6\beta} , , \tag{1.3.5b}$$

providing an intuitive rewriting of (1.3.4)

$$H_\mu{}^\mu = 6\beta\left(\Box - m_0^2\right)R . \tag{1.3.6}$$

1.3.1.1 Comparison to the solutions of general relativity

The solutions to the Einstein field equations of general relativity are

$$R_{\mu\nu} = \frac{T_{\mu\nu}}{2\gamma} + g_{\mu\nu}\frac{1}{d-2}\left(2\Lambda - \frac{T}{2\gamma}\right) .$$

Substituting these into the fields equations of the higher-derivative theory, (1.3.1), gives

$$\begin{aligned} H_{\mu\nu} = {} & \frac{1}{2}T_{\mu\nu} + \frac{1}{d-2}\frac{4}{6\gamma}(\alpha - 3\beta)\left(g_{\mu\nu}\Box T - \nabla_\mu\nabla_\nu T\right) - \frac{\alpha}{\gamma}\Box T_{\mu\nu} + \frac{2\alpha}{\gamma}\nabla_\rho\nabla_{(\mu}T^{\rho}_{\nu)} \\ & - \frac{\alpha}{\gamma^2}T_{\rho\mu}T_\nu{}^\rho + g_{\mu\nu}\frac{T^2}{4\gamma^2}\frac{1}{d-2}\left(-\alpha + \frac{1}{d-2}\frac{2}{3}(3\beta - \alpha)\right) \\ & + TT_{\mu\nu}\frac{1}{3\gamma^2}\frac{1}{d-2}(4\alpha - 3\beta) + \frac{\alpha}{4\gamma}g_{\mu\nu}T_{\rho\sigma}T^{\rho\sigma} \\ & - \Lambda T_{\mu\nu}\frac{2}{3\gamma}\left(3\beta + \alpha + \frac{2}{d-2}\left[3\beta - 4\alpha\right]\right) + \Lambda T g_{\mu\nu}\frac{4}{3\gamma}\frac{1}{(d-2)^2}(\alpha - 3\beta) \\ & + g_{\mu\nu}\Lambda^2\frac{4}{3}\left(-\alpha - \frac{3}{2}\beta + \frac{1}{d-2}3\alpha + \frac{1}{(d-2)^2}2(3\beta - \alpha)\right) . \end{aligned}$$

This has to be equal to $\frac{1}{2}T_{\mu\nu}$ for it to be a solution to the theory, so we see that it misses being a solution by terms like T^2, $\nabla\nabla T$, ΛT or Λ^2. If, however, we simplify this by considering the Einstein space solutions $R_{\mu\nu} = \frac{2}{d-2}(\Lambda - \lambda)g_{\mu\nu}$, corresponding in general relativity to $T^{(\mathrm{GR})}_{\mu\nu} = 2\gamma\lambda\, g_{\mu\nu}$, then we find the energy-momentum density of this solution in the higher derivative theory is

$$\frac{1}{2}T_{\mu\nu} = H_{\mu\nu} = \gamma\,\lambda\,g_{\mu\nu} - g_{\mu\nu}\,\frac{2}{3}\,\frac{d-4}{(d-2)^2}\,(\Lambda-\lambda)^2\left(2\alpha\,(d-3) + 3\beta\,d\right) \tag{1.3.7a}$$

$$= \frac{1}{2}\,T^{(\mathrm{GR})}_{\mu\nu} - g_{\mu\nu}\,\frac{2}{3}\,\frac{d-4}{(d-2)^2}\,(\Lambda-\lambda)^2\left(2\alpha\,(d-3) + 3\beta\,d\right) . \tag{1.3.7b}$$

So we see that in $d = 4$ an Einstein space is sourced by the same stress-energy in higher-derivative gravity as in general relativity. In $d \neq 4$ Einstein spaces only have the same energy-momentum density in the two theories if $\lambda = \Lambda$.

Unless stated, we shall always be considering the theory with no cosmological constant and for a vacuum $T_{\mu\nu}$, for which the solutions to general relativity are all also solutions to the higher derivative theory in any dimension.

1.3.2 The static spherically-symmetric case

We shall be studying the static spherically-symmetric solutions of the equations of motion (1.3.1), so we shall use Schwarzschild coordinates:

$$ds^2 = -B(r)\,dt^2 + A(r)\,dr^2 + r^2 d\theta^2 + r^2\sin^2\theta\,d\phi^2 . \tag{1.3.8}$$

In this ansatz we have two independent equations of motion, corresponding to the two free functions in the metric (1.3.8). The purpose of this work is to attempt a complete description of static spherically-symmetric solutions, so we emphasise that we leave A and B completely general, and do not choose any simplifying assumptions (e.g. $AB = \text{const.}$) as is often done.

The static spherically-symmetric H tensor has the form

$$H_{\mu\nu} = \begin{pmatrix} H_{tt}(r) & 0 & 0 & 0 \\ 0 & H_{rr}(r) & 0 & 0 \\ 0 & 0 & H_{\theta\theta}(r) & 0 \\ 0 & 0 & 0 & H_{\theta\theta}(r)\sin^2\theta \end{pmatrix} , \tag{1.3.9}$$

where the three different components are related by the r component of (1.3.3):

$$\left(\frac{H_{rr}}{A}\right)' + \frac{2H_{rr}}{Ar} + \frac{B'H_{rr}}{2AB} - \frac{2H_{\theta\theta}}{r^3} + \frac{B'H_{tt}}{2B^2} \equiv 0 . \tag{1.3.10}$$

Accordingly the system is described by just two independent equations:

$$H_{tt} = \frac{1}{2}T_{tt} , \tag{1.3.11a}$$

$$H_{rr} = \frac{1}{2}T_{rr} . \tag{1.3.11b}$$

This restriction to the static spherically-symmetric case is a consistent truncation. This can be checked by substituting in the static spherically-symmetric ansatz (1.3.8) into the Lagrangian and checking that the equations of motion implied by

$$\frac{1}{\sqrt{-g}}\frac{\delta\mathcal{I}}{\delta A} \quad \text{and} \quad \frac{1}{\sqrt{-g}}\frac{\delta\mathcal{I}}{\delta B} \tag{1.3.12}$$

match those from (1.3.1) evaluated for (1.3.8).

We shall usually study the vacuum solutions with $T_{\mu\nu} = 0$.

1.3.3 Differential Order

1.3.3.1 For the generic higher-derivative theory

The higher-derivative equations of motion are complex and highly nonlinear. The equations of motion H_{tt} and H_{rr} are functions of $A(r), B(r), A'(r), B'(r), A''(r), B''(r), A^{(3)}, B^{(3)}$ but H_{tt} is a function also of $B^{(4)}$, but this dependence can be eliminated in a suitable combination of the equations.

$$0 = H_{rr} , \tag{1.3.13a}$$

$$0 = H_{tt} - X(r)H_{rr} - Y(r)\partial_r H_{rr} , \tag{1.3.13b}$$

where the appropriate $X(r)$ and $Y(r)$ are

$$X = \frac{(\alpha-3\beta)B}{A^2\left(r(\alpha-3\beta)B' - 2(\alpha+6\beta)B\right)^2}\Bigg(2r(\alpha-3\beta)B\left(rA'-2A\right)B' + 4(\alpha+6\beta)B^2\left(3A-rA'\right) - r^2(\alpha-3\beta)AB'^2\Bigg) \tag{1.3.14a}$$

$$Y = \frac{2r(\alpha-3\beta)B^2}{A\left(2(\alpha+6\beta)B - r(\alpha-3\beta)B'\right)}\,. \tag{1.3.14b}$$

In full, these equations are

$$\begin{aligned}
24r^4A^3B^4H_{rr} = {}& 8r^3A^2B^2B^{(3)}\left(r(\alpha-3\beta)B' - 2(\alpha+6\beta)B\right)\\
&- 4r^2AB^2A''\left(r^2(\alpha-3\beta)B'^2 - 4r(\alpha+6\beta)BB' + 4(\alpha-12\beta)B^2\right)\\
&- 4r^4(\alpha-3\beta)A^2B^2B''^2\\
&- 4r^2ABB''\Big(2rBA'\left(r(\alpha-3\beta)B' - 2(\alpha+6\beta)B\right)\\
&\quad + A\left(3r^2(\alpha-3\beta)B'^2 - 12r(\alpha+3\beta)BB' + 8(\alpha+6\beta)B^2\right)\Big)\\
&+ 7r^2B^2A'^2\left(r^2(\alpha-3\beta)B'^2 - 4r(\alpha+6\beta)BB' + 4(\alpha-12\beta)B^2\right)\\
&+ 2r^2ABA'B'\left(3r^2(\alpha-3\beta)B'^2 - 4r(2\alpha+3\beta)BB' + 4(\alpha+24\beta)B^2\right)\\
&+ 24A^3B^3\left(\gamma r^3B' + B\left(\gamma r^2 - 12\beta\right)\right)\\
&+ A^2\Big(7r^4(\alpha-3\beta)B'^4 - 4r^3(5\alpha+12\beta)BB'^3\\
&\quad - 4r^2(\alpha-48\beta)B^2B'^2 + 32r(\alpha+6\beta)B^3B' - 16(\alpha-21\beta)B^4\Big)\\
&+ 8A^4B^4\left(2\alpha-6\beta-3\gamma r^2\right)\,,
\end{aligned} \tag{1.3.15}$$

a function of $A, B, A', B', A'', B'', B^{(3)}$ and the other equation

$$
\begin{aligned}
&2r^4A^5B^2\left(\alpha rB' - 3\beta rB' - 2\alpha B - 12\beta B\right)^2\left(H_{tt} - X(r)H_{rr} - Y(r)\partial_r H_{rr}\right) = \\
&\quad 72\alpha\beta r^3A^2A^{(3)}B^4\left(r(\alpha-3\beta)B' - 2(\alpha+6\beta)B\right) \\
&\quad + 36\alpha\beta r^2AB^3A''\Big(13rBA'\left(2(\alpha+6\beta)B - r(\alpha-3\beta)B'\right) \\
&\quad\quad - 2A(-r^2(\alpha-3\beta)B'^2 + r(\alpha+6\beta)BB' + 2(\alpha+6\beta)B^2)\Big) \\
&\quad + 12\beta r^4(\alpha-3\beta)A^3B^2B''^2\left((\alpha+6\beta)B - r(\alpha-3\beta)B'\right) \\
&\quad + 4r^3A^2BB''\Big(3\beta BA'\left(r^2(\alpha-3\beta)^2B'^2 + r\left(\alpha^2 - 15\alpha\beta + 36\beta^2\right)BB' - 6\alpha(\alpha+6\beta)B^2\right) \\
&\quad\quad - 3\beta AB'\left(-r^2(\alpha-3\beta)^2B'^2 - 6\alpha r(\alpha-3\beta)BB' + 2\left(7\alpha^2 + 48\alpha\beta + 36\beta^2\right)B^2\right) \\
&\quad\quad + \gamma(-r)(\alpha-3\beta)A^2B^2\left(2(\alpha+6\beta)B - r(\alpha-3\beta)B'\right)\Big) \\
&\quad + 504\alpha\beta r^3B^4A'^3\left(r(\alpha-3\beta)B' - 2(\alpha+6\beta)B\right) \\
&\quad - 3\beta r^2AB^2A'^2\Big(r^3(\alpha-3\beta)^2B'^3 + 3r^2\left(17\alpha^2 - 57\alpha\beta + 18\beta^2\right)BB'^2 \\
&\quad\quad - 60\alpha r(\alpha+6\beta)B^2B' - 4\left(23\alpha^2 + 150\alpha\beta + 72\beta^2\right)B^3\Big) \\
&\quad - 6\beta rA^2BA'\Big(r^4(\alpha-3\beta)^2B'^4 + r^3\left(11\alpha^2 - 39\alpha\beta + 18\beta^2\right)BB'^3 - 4r^2\left(8\alpha^2 + 51\alpha\beta + 18\beta^2\right)B^2B'^2 \\
&\quad\quad + 4r\left(11\alpha^2 - 12\alpha\beta + 18\beta^2\right)B^3B' - 16\left(4\alpha^2 + 21\alpha\beta - 18\beta^2\right)B^4\Big) \\
&\quad + A^3\Big(-4r(\alpha-3\beta)B^4B'\left(12\beta(5\alpha+3\beta) + r(\alpha-3\beta)A'\left(\gamma r^2 - 12\beta\right)\right) \\
&\quad\quad - 2r^2B^3B'^2\left(6\beta\left(\alpha^2 + 66\alpha\beta + 36\beta^2\right) + \gamma r^3(\alpha-3\beta)^2A'\right) \\
&\quad\quad - 8(\alpha+6\beta)B^5\left(-6\beta(5\alpha+3\beta) - rA'\left(2\alpha\left(\gamma r^2 - 6\beta\right) + 3\beta\left(12\beta + \gamma r^2\right)\right)\right) \\
&\quad\quad - 3\beta r^5(\alpha-3\beta)^2B'^5 + 3\beta r^4\left(-19\alpha^2 + 51\alpha\beta + 18\beta^2\right)BB'^4 + 12\beta r^3\left(13\alpha^2 + 84\alpha\beta + 36\beta^2\right)B^2B'^3\Big) \\
&\quad - 8A^5B^4\Big(r(\alpha-3\beta)B'\left(\alpha\left(\gamma r^2 - 6\beta\right) + 6\beta\left(3\beta + \gamma r^2\right)\right) \\
&\quad\quad + (\alpha+6\beta)B\left(\alpha\left(6\beta - 2\gamma r^2\right) - 3\beta\left(6\beta + \gamma r^2\right)\right)\Big) \\
&\quad - 2A^4B^2\Big(\gamma r^5(\alpha-3\beta)^2B'^3 - 6r^2(\alpha-3\beta)BB'^2\left(\alpha\left(\gamma r^2 - 4\beta\right) + 3\beta\left(4\beta + \gamma r^2\right)\right) \\
&\quad + 4r(\alpha-3\beta)B^2B'\left(\alpha\left(\gamma r^2 - 24\beta\right) + 6\beta\left(\gamma r^2 - 6\beta\right)\right) + 4\left(2\alpha^2 + 15\alpha\beta + 18\beta^2\right)B^3\left(12\beta + \gamma r^2\right)\Big),
\end{aligned}
\tag{1.3.16}
$$

a function of $A, B, A', B', A'', B'', A^{(3)}$.

The reader will not be surprised to hear that it is too difficult to solve these in closed form.

The main focus of this work shall be to learn as much as possible about the solutions of these two coupled non-linear differential equations, use various analytic and numerical techniques. These equations of motion are two coupled third-order ordinary differential equations, so we expect that they will have six free parameters. It would be possible to reduce a pair of *linear* coupled third-order ordinary differential equations to a single sixth-order ordinary differential equation, but for the non-linear equations we can merely outline the equivalent procedure:

$$\begin{aligned}
(1.3.15) : 0 &= f_1(r, A, B, A', B', A'', B'', B''') \\
(1.3.16) : 0 &= g_1(r, A, B, A', B', A'', B'', A''') \\
\partial_r(1.3.16) : 0 &= \partial_r g_1(r, A, B, A', B', A'', B'', A''') \\
&= g_2(r, A, B, A', B', A'', B'', A''', B''', A^{(4)}) \\
\therefore B''' &= g_2^{-1}(r, A, B, A', B', A'', B'', A''', A^{(4)}) \\
\text{sub into } (1.3.15) : 0 &= f_2(r, A, B, A', B', A'', B'', A''', A^{(4)}) \\
\therefore B'' &= f_2^{-1}(r, A, B, A', B', A'', A''', A^{(4)}) \\
\text{sub into } (1.3.16) : 0 &= g_3(r, A, B, A', B', A'', A''', A^{(4)}) \\
\therefore B' &= g_3^{-1}(r, A, B, A', A'', A''', A^{(4)}) \\
\text{sub } f_2^{-1} \text{ and } g_3^{-1} \text{ into } (1.3.16) : 0 &= g_4(r, A, B, A', A'', A''', A^{(4)}) \\
\therefore B &= g_4^{-1}(r, A, A', A'', A''', A^{(4)}) \\
\text{sub into } (1.3.16) : 0 &= g_5(r, A, A', A'', A''', A^{(4)}, A^{(5)}, A^{(6)}) \ .
\end{aligned}$$

but this would require inversion of high-order polynomials, so we cannot prove that it is possible. However, later we shall find various perturbative solutions and see that there are six free parameters, so we believe that this is the order of the system.

1.3.3.2 For the Einstein-Weyl theory

We shall see later that the $\beta = 0$, or Einstein-Weyl, case with Lagrangian density $\gamma R - \alpha C^2$ is of particular interest to us. In this case the system is simpler and in fact has a lower differential order. The simplification is clearly visible in the fourth-order trace equation (1.3.4) which becomes simply the second-order equation

$$R = -\frac{1}{2\gamma} T_\mu{}^\mu \ , \tag{1.3.17}$$

and the absence of the massive scalar particle (1.3.5b). In this case the vacuum equations of motion are equivalent to the two equations

$$0 = H_\mu^{\ \mu}\,, \tag{1.3.18a}$$

$$0 = \frac{H_{rr}}{\alpha} + H_\mu^{\ \mu}\frac{3rBA' - 2A\left(rB' + B\right) + 2A^2B}{3\gamma r^2AB} - (H_\mu^{\ \mu})^2\frac{A}{6\gamma^2} - \partial_r(H_\mu^{\ \mu})\frac{2B - rB'}{3\gamma rB}\,, \tag{1.3.18b}$$

which are second order in B and first order in A, and second order in A and first order in B, respectively.

In full, these equations are

$$-\frac{2}{\gamma}r^2A^2B^2 \text{(1.3.18a)} = rBA'\left(rB' + 4B\right) + A\left(r^2B'^2 - 2rB\left(rB'' + 2B'\right) - 4B^2\right) + 4A^2B^2 \tag{1.3.19a}$$

$$\begin{aligned} 2\alpha r^4A^3B^3 \text{(1.3.18b)} =& \alpha r^2B^2A'^2\left(5B - 4rB'\right) + \alpha A^2\left(-4B^3\left(rA' + 2\right) + r^3B'^3 - 3r^2BB'^2\right) \\ &+ \alpha rAB\left(r^2A'B'^2 + 2rBB'\left(rA'' + A'\right) + 4B^2\left(A' - rA''\right)\right) \\ &+ 2A^3B^2\left(\gamma r^3B' + B\left(4\alpha + \gamma r^2\right)\right) - 2\gamma r^2A^4B^3\,. \end{aligned} \tag{1.3.19b}$$

So we expect four free parameters in the Einstein-Weyl case.

Chapter 2

Properties of Solution Families

2.1 Constraining the Ricci scalar

2.1.1 The proof

In [34] an important result was proved about the Ricci scalar in higher derivative gravity in static vacuum space-times. We now discuss and extend that result. The starting point for the proof is the trace of the equations of motion (1.3.4).

$$0 \;=\; H_\mu^{\ \mu} \;=\; 6\beta\Box R - \gamma R \;=\; 6\beta\left(\Box - m_0^2\right) R\,. \tag{2.1.1}$$

It is clear that for $\beta = 0$ we can immediately say $R = 0$ for all vacuum space, whereas for $\beta \neq 0$ we can only say that $\left(\Box - m_0^2\right) R = 0$ for all vacuum space. In [34] static symmetry and appropriate boundary conditions were used to show that this still implies $R = 0$. The argument is presented here in a different style using a time-like dimensional reduction instead of a time-like Killing vector field. Using static symmetry write the metric as [1].

$$ds^2 = -\lambda(x)^2 dt^2 + h_{ab}(x) dx^a dx^b\,, \tag{2.1.2}$$

where the indices a, b run over the spatial coordinates x. It follows straightforwardly that

$$\Box R := g^{\mu\nu}\nabla_\mu\nabla_\nu R = D^a D_a R + \frac{1}{\lambda}\left(D^a\lambda\right)\left(D_a R\right)\,, \tag{2.1.3}$$

where D_a is the covariant derivative for the spatial metric h_{ab}, and thus that

$$0 = \frac{H_\mu^{\ \mu}}{6\,\beta} = D^a D_a R + \frac{1}{\lambda}\left(D^a\lambda\right)\left(D_a R\right) - m_0^2 R\,. \tag{2.1.4}$$

Multiply this by λR and integrate over a volume $\mathcal{S}$ of the spatial dimensions

$$0 = \int_{\mathcal{S}} \sqrt{h}\,\mathrm{d}^3x \frac{H_\mu^{\ \mu}}{6\,\beta}\lambda R = \int_{\mathcal{S}} \sqrt{h}\,\mathrm{d}^3x \left[\lambda R\ \left(D^a D_a R\right) + R\left(D^a\lambda\right)\left(D_a R\right) - m_0^2\ \lambda R^2\right]\,, \tag{2.1.5}$$

and then integrate by parts:

$$0 = \int_{\mathcal{S}} \sqrt{h}\,\mathrm{d}^3x \left[D^a\left(\lambda R\, D_a R\right) - \lambda\ \left(D^a R\right)\left(D_a R\right) - m_0^2\ \lambda R^2\right]\,. \tag{2.1.6}$$

The integrand consists of a boundary term and two bulk terms. The theorem is then: If the space-time has Minkowski signature and the boundary term contribution vanishes, then $R = 0$ throughout the integration region. Strictly, the proof requires that $m_0^2 > 0 \Leftrightarrow \beta > 0$, and that the spatial metric h_{ab} is positive definite, for which Minkowski signature is sufficient. Then the proof simply states that since the two bulk terms obviously have the same sign, therefore they must vanish everywhere because of the vanishing of the boundary term and of the integral as

[1] Note that in the proof in [34] the metric was written differently, with λdt^2, so our λ is not the same as theirs

a whole. In the space-times we consider we shall often be able to choose a suitable integration region such that the boundary term vanishes. An example is a boundary at infinity, assuming asymptotic flatness, so that $D_a R = 0$ on the boundary and the contribution to the integral vanishes. We discuss some example space-times in the next subsection.

Later we shall need the explicit expression for the contribution of the boundary term to (2.1.6) so we calculate it here:

$$\text{boundary contribution} = \int_{\mathcal{S}} \sqrt{h}\ [D_a\left(\lambda\ R\ D^a R\right)]\,\mathrm{d}^3x = \int_{\mathcal{S}} \partial_a \left[\sqrt{h}\ \lambda\ R\ D^a R\right]\mathrm{d}^3x\ . \tag{2.1.7}$$

So far the proof has been valid for all static space-times, but in particular we shall be interested in the specialisation to the static spherically symmetric case, where only the r component is non-zero, and we find a simplification of the boundary contribution:

$$\text{boundary contribution} = \int_{\mathcal{S}} \partial_r \left[\sqrt{AB}\ r^2 \sin(\theta) R\ D^r R\right]\mathrm{d}r\mathrm{d}\theta\mathrm{d}\phi = 4\pi \left[\sqrt{AB}\ r^2\ R\ D^r R\right]_{r_-}^{r_+} \tag{2.1.8}$$

so we define a function $C(r)$ as

$$C(r) := \sqrt{AB}\ r^2\ R\ D^r R\Big|_r\ , \tag{2.1.9}$$

and we shall evaluate it in the various solutions we find. The most general spherically symmetric application of the theorem is then that $R = 0$ at radii between two zeroes of $C(r)$. A generalisation of this proof to the case where there is a cosmological constant Λ was presented in [1] and [2] and is discussed in appendix A.

2.1.2 Physical implications

Being able to prove that the Ricci scalar vanishes affords a great simplification of the equations of motion. Consider the vacuum equations of motion (1.3.1) for $R = 0$:

$$0 = H_{\mu\nu}|_{R=0} = -2\alpha\left(\Box R_{\mu\nu} + 2R^{\rho}_{\mu}R_{\nu\rho} - 2\nabla_\rho\nabla_\mu R^\rho_\nu - \frac{1}{2}g_{\mu\nu}R^{\rho\sigma}R_{\rho\sigma}\right) + \gamma R_{\mu\nu}\ . \tag{2.1.10}$$

There is no dependence on β. The equations of motion for $R = 0$ are in fact identical to those of the Einstein-Weyl theory, i.e. the theory with $\beta = 0$. Thus this proof makes the Einstein-Weyl theory of considerable interest. We saw in section 1.3.3.2 that in the static spherically symmetric situation the Einstein-Weyl theory reduces to two coupled second-order ODEs, with four free parameters, instead of the third-order equations of and six free parameters of the full theory. At various places in this work we find that several calculations that are intractable in the full theory are tractable in the Einstein-Weyl theory.

We now consider two physical situations that stand out for consideration in light of the theorem (2.1.6). The first is a simply connected region covering all space, the second is the

region exterior to a horizon. In both of these the theorem (2.1.6) can be used to show that the Ricci scalar vanishes subject to some reasonable assumptions which we now discuss.

Firstly we consider an asymptotically flat space-time with vacuum and Minkowski signature throughout. We choose a simply connected spatial integration region covering all space i.e. with a single boundary at $r \to \infty$. On the boundary R and $D_a R$ vanish by asymptotic flatness. Thus $R = 0$ throughout all space-time.

Secondly we consider an asymptotically flat space-time containing a horizon. We choose the integration region to be a vacuum Minkowski-signature region outside the horizon, extending out to infinity. On the inner boundary (the horizon) since $\lambda(x)$ vanishes by definition the boundary contribution is again zero and it follows that $R = 0$ everywhere outside the horizon. [2]

This theorem will prove to be very useful because with every solution we find we will be able to use this theorem to relate local properties (of the boundary term) to bulk properties (R for some open range of r) and we shall see some more examples later on.

2.1.3 The trace-free part

In [34], after using the trace equation to prove $R = 0$ given certain assumptions, the trace-free part of the equations of motion was discussed. Unfortunately we find errors in that calculation [3] and we discuss a corrected version here.

Take the trace-free part of the equations of motion ,

$$0 = H_{\mu\nu}|_{R=0} = -2\alpha \left(\Box R_{\mu\nu} + 2R^{\rho}_{\mu} R_{\nu\rho} - 2\nabla_{\rho}\nabla_{\mu} R^{\rho}_{\nu} - \frac{1}{2} g_{\mu\nu} R^{\rho\sigma} R_{\rho\sigma} \right) + \gamma R_{\mu\nu} \ , \qquad (2.1.11)$$

and multiply it by $\lambda R^{\mu\nu}$ and break it up into the time and space parts. As a side note we present a list of identities involved in that calculation. The connection and curvature break up

[2] One might be concerned that although $\lambda(x)|_{\text{horizon}} = 0$ it may be that another quantity, e.g. $\partial^i R$ diverges on the horizon such that the combination is non-vanishing. Later, while assuming spherical symmetry, we shall explicitly calculate the whole boundary contribution $C(r)$ near to the horizon and find that it indeed vanishes on the horizon.

[3] Specifically, in [34] their equations (2.28) and (2.30) are written in the convention (1.1.8) for curvature tensors, but their equations of motion (2.1) would only be correct if the opposite convention was used. The resulting errors in the analysis of the equations of motion invalidate their conclusion regarding the trace-free part.

simply as

$$\Gamma^i_{00} = \lambda D^i \lambda \tag{2.1.12a}$$
$$\Gamma^0_{0i} = \frac{D_i \lambda}{\lambda} \tag{2.1.12b}$$
$$\Gamma^0_{ij} = 0 \tag{2.1.12c}$$
$$\Gamma^0_{00} = 0 \tag{2.1.12d}$$
$$\Gamma^i_{0j} = 0 \tag{2.1.12e}$$
$$R_{00} = \lambda D_i D^i \lambda \tag{2.1.12f}$$
$$R_{0i} = 0 \tag{2.1.12g}$$
$$R_{ij} = \bar{R}_{ij} - \frac{1}{\lambda} D_i D_j \lambda \,, \tag{2.1.12h}$$

where $\bar{R}_{ij}$ denotes the Ricci tensor of the spatial metric h_{ij}. We use these to find the more complex identities:

$$0 = \; R = 2g^{00} R_{00} + \bar{R} = \; \bar{R} - \frac{2}{\lambda^2} R_{00} \tag{2.1.13a}$$
$$\nabla_0 R_{00} = 0 \tag{2.1.13b}$$
$$\nabla_i R_{00} = \frac{\lambda^2}{2} D_i \bar{R} \tag{2.1.13c}$$
$$\nabla_0 R_{i0} = \; - \frac{\lambda}{2} \bar{R} D_i \lambda - \lambda R_{ij} D^j \lambda \tag{2.1.13d}$$
$$\nabla_0 R_{ij} = 0 \tag{2.1.13e}$$
$$\nabla_i R_{j0} = 0 \tag{2.1.13f}$$
$$\nabla_i R_{jk} = D_i R_{jk} \tag{2.1.13g}$$
$$\Box \phi = D^i D_i \phi + \frac{1}{\lambda} D^i \lambda D_i \phi \tag{2.1.13h}$$
$$\Box R_{00} = \frac{\lambda^2}{2} D^i D_i \bar{R} + \frac{\lambda}{2} D^i \lambda D_i \bar{R} - \bar{R} D^i \lambda D_i \lambda - 2 S_{ij} D^i \lambda D^j \lambda \tag{2.1.13i}$$
$$\Box R_{ij} = D^k D_k R_{ij} + \frac{1}{\lambda} D^k \lambda D_k R_{ij} - \frac{1}{\lambda^2} \bar{R} D_i \lambda D_j \lambda - \frac{2}{\lambda^2} D_{(i} \lambda R_{j)k} D^k \lambda \tag{2.1.13j}$$
$$\nabla_\rho \nabla_0 R^\rho_0 = \; - \frac{\lambda}{2} \bar{R} D^i D_i \lambda - \lambda S_{ij} D^i D^j \lambda - R_{ij} D^i \lambda D^j \lambda - \lambda D^j \lambda D^i R_{ij} - \frac{1}{2} \bar{R} D_i \lambda D^i \lambda \tag{2.1.13k}$$
$$\nabla_\rho \nabla_i R^\rho_j = D_k D_i R^k_j - \frac{1}{2\lambda^2} \bar{R} D_i \lambda D_j \lambda - \frac{1}{\lambda^2} D_i \lambda R_{jk} D^k \lambda + \frac{1}{\lambda} D^k \lambda D_i R_{jk} + \frac{1}{2\lambda} D_j \lambda D_i \bar{R} \tag{2.1.13l}$$
$$R^{\mu\nu} R_{\mu\nu} = \frac{\bar{R}^2}{4} + R^{ij} R_{ij} \tag{2.1.13m}$$
$$R^\mu_\nu R^\nu_\rho R^\rho_\mu = \; - \frac{\bar{R}^3}{8} + R^i_j R^j_k R^k_i \,, \tag{2.1.13n}$$

where $\bar{R}$ denotes the Ricci scalar of the spatial metric h_{ij}. In particular note that $R_{\mu\nu}$ is block-diagonal in the time and space parts. We also need the contracted Bianchi identity for $R = 0$:

$$\nabla^\mu R_{\mu\nu} = \frac{1}{2}\nabla_\nu R = 0 \tag{2.1.14a}$$

$$\therefore 0 = \nabla^\mu R_{\mu i} = D^j R_{ij} + \frac{1}{\lambda} R_{ij} D^j \lambda + \frac{\bar{R}}{2\lambda} D_i \lambda \,. \tag{2.1.14b}$$

The result of the calculation is

$$\begin{aligned} 0 &= \int_{\mathcal{S}} \sqrt{h}\, \mathrm{d}^3x \left[\lambda\, R^{\mu\nu} \frac{H_{\mu\nu}}{-2\alpha}\bigg|_{R=0} \right] \\ &= \int_{\mathcal{S}} \sqrt{h}\, \mathrm{d}^3x \Bigg[D_i \left(\frac{\lambda}{4} \bar{R} D^i \bar{R} + \lambda\, R^{\cdot\cdot} D^i R_{\cdot\cdot} - 2\lambda\, R_{\cdot\cdot} D^{\cdot} R^{\cdot i} - \lambda\, \bar{R} D_j R^{ji} \right) \\ &\quad - \frac{\lambda}{4}\, D^i \bar{R}\, D_i \bar{R} + 2\lambda\, D^i \bar{R} D^j R_{ji} - \lambda\, D^i R^{jk} \left[D_i R_{jk} - 2 D_j R_{ki} \right] \\ &\quad - \lambda \frac{\bar{R}^2}{4} \left(m_2^2 + \bar{R} \right) - \lambda\, R^{ij} R_{ij} \left(m_2^2 - 2\mathcal{R} \right) \Bigg] \,, \end{aligned}$$

where $\mathcal{R}$ is defined as

$$\mathcal{R} := \frac{R^i_j R^j_k R^k_i}{R^{mn} R_{mn}} \,. \tag{2.1.15}$$

For an asymptotically flat vacuum space-time the boundary term vanishes at spatial infinity, so the hope would be that the remaining bulk terms could be shown to be all positive- or negative-semi-definite, and therefore each to separately vanish. However, in our calculation this is not the case and we cannot conclude that $R_{\mu\nu}$ vanishes (nor any other new constraints on it). In fact in [2] an explicit numerical solution was found of an asymptotically flat solution with a horizon but non-vanishing Ricci curvature, and we will discuss and develop such black holes solutions in section 3.2. Although the Ricci tensor does not vanish, these solutions will only deviate from Ricci-flatness via a single parameter, so it may indeed be tractable to prove other constraints on the Ricci tensor but we have not succeeded in doing so.

A generalisation of all the expressions in this section to the case where there is a cosmological constant Λ was presented in [1] (repeated in more detail in [2]) and is discussed in appendix A. Unfortunately allowing non-zero Λ does not open up any new possibilities for proving constraints on the curvature.

2.2 Solutions near the origin

The static spherically-symmetric equations of motion were analysed near the origin in [6] and three solution families were found. We can now build on this, including using Mathematica to give confident statements about the number of free parameters in the solutions. We expect to always find at least one free parameter, because the static symmetry allows us to freely scale the B function by positive constants.

2.2.1 Frobenius analysis

In [6] they made the ansatz

$$\begin{aligned} A(r) &= a_s r^s + a_{s+1} r^{s+1} + a_{s+2} r^{s+2} + \dots \,, \\ B(r) &= b_t \left(r^t + b_{t+1} r^{t+1} + b_{t+2} r^{t+2} + \dots \right) \,, \end{aligned} \tag{2.2.1}$$

($a_s \neq 0, b_t \neq 0$) and attempt to find a suitable s, t and coefficients a_n, b_m. They found that the only solutions that exist for all α, β are the (s,t) pairs

- $(0, \quad 0)_0$
- $(1, -1)_0$
- $(2, \quad 2)_0$

where we write the 0 subscript to indicate that these are (s,t) of solutions (2.2.1) around the origin.

We find additional solution families that exist only for suitable $\alpha > 3\beta > 0$:

$$\frac{t-2}{3} = s \in \mathbb{Z}^+ \,, \qquad \alpha = \frac{(s^2+2s+2)^2}{s^4} 3\beta \,,$$

but since these require precise values for the couplings these solutions will not be considered further. We also do not consider the theory with $\alpha = 0$.

In [6] only the leading order terms in the expansions were found. In [33] the $(0,0)_0$ and $(2,2)_0$ families were expanded further, and the number of free parameters could be counted with confidence. We repeated the expansion analysis, for the general α, β theory and also for the $\beta = 0$ theory, and including the $(1,-1)_0$ family, and we show our results below. In each family we expanded out to at least 12 orders, and found that in each family all the free parameters had appeared by fourth order at the latest. The three short sections below present these solution families. There are a few physical comments but the most interesting points will wait slightly until section 2.2.2.

2.2.1.1 The $(0,0)_0$ family

The first few terms of this solution family are

$$\begin{aligned} A(r) &= 1 + a_2 r^2 \\ &\quad + r^4 \frac{a_2\left(\gamma(2\alpha+3\beta) - 36\alpha\beta b_2\right) + 18a_2^2\beta(10\alpha+3\beta) - 2b_2\left(\gamma(\alpha-3\beta) + 9\beta b_2(2\alpha+3\beta)\right)}{180\alpha\beta} \\ &\quad + O(r^6)\,, \end{aligned} \tag{2.2.2a}$$

$$\begin{aligned} \frac{B(r)}{b_0} &= 1 + b_2 r^2 \\ &\quad + \frac{r^4\left(54a_2^2\beta^2 + a_2\left(-\alpha\gamma + 108\alpha\beta b_2 + 3\beta\gamma\right) + b_2\left(\gamma(\alpha+6\beta) + 54\beta b_2(2\alpha-\beta)\right)\right)}{360\alpha\beta} \\ &\quad + O(r^6)\,. \end{aligned} \tag{2.2.2b}$$

which has 3=2+1 free parameters: a_2, b_2 and the trivial parameter b_0.

This solution can be compared to the $(0,0)_0$ solution of general relativity, which is Minkowski space (and the zero-mass limit of the Schwarzschild solution). In our coordinate ansatz (1.3.8) (where the r coordinate is fixed) Minkowski space has one free parameter, corresponding to its static symmetry.

For later reference we also present the $(0,0)_0$ solution for the $\beta = 0$ theory which is equal to (2.2.2) fixing $b_2 = a_2$:

$$A(r) = 1 + a_2\left(r^2 + r^4\frac{12\alpha a_2 + \gamma}{20\alpha} + r^6\frac{320\alpha^2 a_2^2 + 100\alpha a_2\gamma + \gamma^2}{1120\alpha^2} + O(r^8)\right) \tag{2.2.3a}$$

$$\frac{B(r)}{b_0} = 1 + a_2\left(r^2 + r^4\frac{24\alpha a_2 + \gamma}{40\alpha} + r^6\frac{960\alpha^2 a_2^2 + 144\alpha a_2\gamma + \gamma^2}{3360\alpha^2} + O(r^8)\right)\,, \tag{2.2.3b}$$

and has 2=1+1 free parameters. Note that we have $R_{\mu\nu} = 0$ if and only if Minkowski space, if and only if $a_2 = 0$.

We consider this solution family to be the vacuum. Being of $(0,0)_0$ type is sufficient for the metric to be non-singular. Further, if one looks at the Riemann curvature tensor related to local orthonormal frame, $R_{abcd} = R_{\mu\nu\rho\sigma}e_a^\mu e_b^\nu e_c^\rho e_d^\sigma$, we find that the non-zero components are

$$R_{yzyz} = \frac{A-1}{Ar^2} \tag{2.2.4a}$$

$$R_{xyxy} = R_{xzxz} = \frac{A'}{2rA^2} \tag{2.2.4b}$$

$$R_{tyty} = R_{tztz} = \frac{B'}{2rAB} \tag{2.2.4c}$$

$$R_{txtx} = \frac{1}{4A^2B^2}\left(-AB'^2 - BA'B' + 2BAB''\right)\,, \tag{2.2.4d}$$

and others related by symmetry, where t, x, y, z are the chosen orthonormal coordinates for the

local inertial frame. We can see that R_{abcd} is non-diverging in the limit $r \to 0$ if and only if $A(r) \to 1, A'(r) \to 0, B(r) \to$ constant, $B'(r) \to 0$ and $B''(r)$ non-diverging. So the necessary and sufficient condition for being non-singular is that A and B are of the form $c_1 + c_2 r^2 + O(r^3)$. Additionally being a solution of the field equations implies that A and B are elements of this solution family.

Later in section 2.3.6 we discuss this family further using comparisons to perturbative solutions.

2.2.1.2 The $(1,-1)_0$ family

The first few terms of this solution family are:

$$\begin{aligned} A(r) &= a_1 r - a_1^2 r^2 + a_1^3 r^3 + a_4 r^4 - \frac{1}{16} r^5 \left(a_1 \left(3 a_1 b_2 + 19 a_1^4 + 35 a_4\right)\right) \\ &\quad + \frac{1}{40} a_1^2 r^6 \left(21 a_1 b_2 + 101 a_1^4 + 141 a_4\right) + O(r^7)\,, \end{aligned} \tag{2.2.5a}$$

$$\begin{aligned} \frac{B(r)}{b_{-1}} &= \frac{1}{r} + a_1 + b_2 r^2 + \frac{1}{16} r^3 \left(a_1 b_2 + a_1^4 + a_4\right) \\ &\quad - \frac{1}{40} 3 r^4 \left(a_1 \left(a_1 b_2 + a_1^4 + a_4\right)\right) + O(r^5)\,, \end{aligned} \tag{2.2.5b}$$

which has 4=3+1 free parameters: a_1, a_4, b_2 and the trivial parameter b_{-1}.

The $(1,-1)_0$ family is clearly the family that contains the classic Schwarzschild solution of Einstein theory. For later reference we also present the $(1,-1)_0$ solution to the $\beta = 0$ theory which is equal to (2.2.5) fixing $a_4 = \frac{5}{3} a_1 b_2 - a_1^4$.

$$A(r) = a_1 r - a_1^2 r^2 + a_1^3 r^3 + r^4 \left(\frac{5}{3} a_1 b_2 - a_1^4\right) + r^5 \left(a_1^5 - \frac{23}{6} a_1^2 b_2\right) + O(r^6) \tag{2.2.6a}$$

$$\frac{B(r)}{b_{-1}} = \frac{1}{r} + a_1 + b_2 r^2 + \frac{1}{6} a_1 b_2 r^3 - \frac{1}{5} r^4 a_1^2 b_2 + O(r^5)\,. \tag{2.2.6b}$$

Where we have chosen the parameterisation so that there is a clear similarity between a_1 and the Schwarzschild mass of the Schwarzschild solution, and $b_2 \neq 0$ describes the space of deviation from Schwarzschild. Specifically, $b_2 = 0$ is necessary and sufficient for $R_{\mu\nu} = 0$, in which case $a_1 = -\frac{1}{2}(G M_{\text{Schwarzschild}})^{-1}$.

At the origin, the $(1,-1)_0$ indicial structure gives rise to a curvature singularity, with $R_{\mu\nu\rho\sigma} R^{\mu\nu\rho\sigma}$ going like r^{-6} as $r \to 0$ [6].

2.2.1.3 The $(2,2)_0$ family

The first few terms of this solution family are

$$\begin{aligned} A(r) = {} & a_2 r^2 + a_2 b_3 r^3 - \frac{a_2 r^4}{6}\left(2a_2 + b_3^2 - 8b_4\right) + a_5 r^5 \\ & + \frac{r^6}{1296\alpha\beta}\Bigg(- 12\alpha^2 a_2^3 - 2a_2^2\left(b_3^2\left(\alpha^2 - 603\alpha\beta - 252\beta^2\right) + 27\alpha\left(20\beta b_4 + \gamma\right)\right) \\ & + a_2\Big(b_3^4\left(-16\alpha^2 + 1413\alpha\beta - 72\beta^2\right) + 2b_4 b_3^2\left(19\alpha^2 - 2223\alpha\beta + 180\beta^2\right) \\ & - 36 b_5 b_3\left(\alpha^2 + 45\beta^2\right) + 12\alpha b_4^2(\alpha + 162\beta)\Big) + 324 a_5 \beta b_3(7\alpha + 3\beta)\Bigg) \\ & + O(r^7)\,, \end{aligned} \tag{2.2.7a}$$

$$\begin{aligned} \frac{B(r)}{b_2} = {} & r^2 + b_3 r^3 + b_4 r^4 + b_5 r^5 \\ & + \frac{r^6}{216\alpha a_2}\Bigg(- 12\alpha a_2^3 + a_2^2\left(14 b_3^2(2\alpha + 3\beta) - 24\alpha b_4\right) \\ & + a_2\left(2b_3^4(67\alpha - 3\beta) + 2b_4 b_3^2(15\beta - 227\alpha) + 45 b_5 b_3(7\alpha - 3\beta) + 180\alpha b_4^2\right) + 27 a_5 b_3(\alpha + 3\beta)\Bigg) \\ & + O(r^7)\,, \end{aligned} \tag{2.2.7b}$$

which has 6=5+1 free parameters a_2, b_3, b_4, b_5, a_5 and the trivial parameter b_2.

This family does not appear in General Relativity. It is singular at the origin, with $R_{\mu\nu\rho\sigma}R^{\mu\nu\rho\sigma} \sim r^{-8}$ as $r \to 0$ [6].

For later reference we also present the $(2,2)_0$ solution to the $\beta = 0$ theory which is equal to (2.2.7) fixing

$$a_5 = -\frac{a_2}{18\alpha b_3}\left(10\alpha a_2^2 + a_2\left(11\alpha b_3^2 + 45\gamma\right) + \alpha\left(12 b_3^4 - 25 b_4 b_3^2 - 10 b_4^2\right)\right) \tag{2.2.8a}$$

$$b_5 = -\frac{1}{18\alpha b_3}\left(6\alpha a_2^2 + a_2\left(\alpha b_3^2 + 27\gamma\right) + \alpha\left(8 b_3^4 - 19 b_4 b_3^2 - 6 b_4^2\right)\right)\,, \tag{2.2.8b}$$

and begins with

$$\begin{aligned} A(r) = {} & a_2 r^2 + a_2 b_3 r^3 - \frac{1}{6} r^4 \left(a_2 \left(2a_2 + b_3^2 - 8b_4\right)\right) \\ & - \frac{r^5 \left(a_2 \left(10\alpha a_2^2 + a_2 \left(11\alpha b_3^2 + 45\gamma\right) + \alpha \left(12b_3^4 - 25b_4 b_3^2 - 10b_4^2\right)\right)\right)}{18\left(\alpha b_3\right)} \\ & - \frac{r^6 \left(a_2 \left(140\alpha a_2^2 + 10a_2 \left(2\alpha b_3^2 + 12\alpha b_4 + 63\gamma\right) + \alpha \left(11b_3^4 + 144 b_4 b_3^2 - 356 b_4^2\right)\right)\right)}{144\alpha} \\ & + O(r^7)\,. \end{aligned} \tag{2.2.9a}$$

$$\begin{aligned} \frac{B(r)}{b_2} = {} & r^2 + b_3 r^3 + b_4 r^4 - \frac{r^5 \left(6\alpha a_2^2 + a_2 \left(\alpha b_3^2 + 27\gamma\right) + \alpha \left(8b_3^4 - 19 b_4 b_3^2 - 6 b_4^2\right)\right)}{18\left(\alpha b_3\right)} \\ & + \frac{1}{36} r^6 \left(-\frac{a_2 \left(\alpha b_3^2 + 4\alpha b_4 + 90\gamma\right)}{\alpha} - 22 a_2^2 - 4 b_3^4 - 14 b_4 b_3^2 + 50 b_4^2\right) \\ & + O(r^7)\,. \end{aligned} \tag{2.2.9b}$$

2.2.2 Constraints on the Ricci scalar for the near-origin solution families

We shall also consider the solutions in the light of the theorem (2.1.6). Consider a spherically-symmetric space-time with a vacuum everywhere except perhaps the origin, and integrate over $\epsilon < r < \infty$, taking $\epsilon \to 0$. The inner boundary is near the origin and is described by these near-origin solutions, but at the origin itself the space-time may be singular or non-vacuum so we exclude it from the integration region. If we find (possibly subject to conditions) that the contribution from the inner boundary vanishes, then we would also need to show that the space-time has Minkowski signature before we could prove that R must vanish. The boundary term contribution is given by $C(r)$ (2.1.9) with $r_+ \to \infty$ and $r_- = \epsilon \to 0$. The contribution from $r \to \infty$ vanishes by asymptotic flatness, so we must determine if

$$C(r = \epsilon \to 0) = \sqrt{AB}\, r^2\, R\, \partial^r\, R\Big|_{r=\epsilon\to 0} \tag{2.2.10}$$

vanishes. We calculate it in the three solution families below.

Solution family	$R\partial^r R$	$C(r)$
$(0,0)_0$	$\frac{2\gamma}{\beta}\left(a_2 - b_2\right)^2 r + O(r^3)$	$\sim O(r^3)$
$(1,-1)_0$	$-\frac{3\gamma}{8a_1^4\beta}\left(\frac{5}{3}a_1 b_2 - a_1^4 - a_4\right)^2 r + O(r^3)$	$\sim O(r^3)$
$(2,2)_0$	$-\frac{\left(a_2\left(14a_2 b_3 - 2b_3^3 + 10 b_4 b_3 - 45 b_5\right) + 27 a_5\right)^2}{9a_2^5} r^{-5} + O(r^{-4})$	$\sim O(r^{-1})$

The table shows that the $(0,0)_0$ and $(1,-1)_0$ families have the boundary contribution at $r = \epsilon$ tend to zero as ϵ tends to zero, so in the region $r > 0$ the space-time has $R = 0$ (if it

has Minkowski signature throughout). This is consistent with our claim that the $(0,0)_0$ family represents the vacuum, in that we find that the theorem applies equally well if the origin is excluded from the integration region, or included (i.e. a simply connected region with a single boundary at $r \to \infty$). The $(0,0)_0$ and $(1,-1)_0$ solutions for $R = 0 \Leftrightarrow \beta = 0$ were given already in (2.2.3) and (2.2.6). They are obtained from their general expressions by setting to zero $(a_2 - b_2)$ and $(a_4 - \frac{5}{3}a_1 b_2 + a_1^4)$, respectively, so we can say that these quantities parameterise asymptotic non-flatness in the $R \neq 0$ parts of these families (at least they do when the other conditions of the theory are met, if possibly not always). This does not necessarily imply that the $R = 0$ parts of these families are asymptotically flat.

On the other hand, for the $(2,2)_0$ family the boundary term contribution is generically not zero, and in fact blows up as $\epsilon \to 0$, and the proof fails. However, the $(2,2)_0$ family is a (5+1)-parameter space of solutions and R does in fact vanish in a subspace of its parameter space. In the $(2,2)_0$ family R and $C(r)$ generically go as r^{-1}. The condition on the parameters to remove the divergent term in R is also necessary and sufficient to remove the divergence from $C(r)$ (such that $C(r) \sim r^5$). We can use the theorem within this subspace. This is a (4+1)-parameter space given by $b_5 = \tilde{b_5}$ where

$$\tilde{b_5} := \frac{1}{45}\left(14a_2b_3 + \frac{27a_5}{a_2} - 2b_3^3 + 10b_4b_3\right) . \tag{2.2.11}$$

This can be compared to the space of $(2,2)_0$ solutions where R vanishes, which is of course a subspace of the space where R is non-divergent, which is a (3+1)-parameter space (given by (2.2.8)), where $a_5 = \tilde{a_5}$ as well as $b_5 = \tilde{b_5}$

$$\begin{aligned}
\tilde{a_5} :=& -\frac{a_2}{18\alpha b_3}\left(10\alpha a_2^2 + a_2\left(11\alpha b_3^2 + 45\gamma\right) + \alpha\left(12b_3^4 - 25b_4b_3^2 - 10b_4^2\right)\right) \\
\tilde{b_5} =& \frac{1}{45}\left(14a_2b_3 + \frac{27\tilde{a_5}}{a_2} - 2b_3^3 + 10b_4b_3\right) \\
=& -\frac{1}{18\alpha b_3}\left(6\alpha a_2^2 + a_2\left(\alpha b_3^2 + 27\gamma\right) + \alpha\left(8b_3^4 - 19b_4b_3^2 - 6b_4^2\right)\right) .
\end{aligned}$$

We learn that if $b_5 = \tilde{b_5}$, and the space-time has Minkowski signature for $r > 0$, and D_aR vanishes at infinity, then a_5 is constrained. Conversely, it follows that if $b_5 = \tilde{b_5}$, and the space-time has Minkowski signature for $r > 0$ and $a_5 \neq \tilde{a_5}$ then D_aR does not vanish at infinity, and the space-time is not asymptotically flat. So within the solution space $b_5 = \tilde{b_5}$ (Minkowski signature) we can say that $(a_5 - \tilde{a_5})$ is one of the two parameters controlling asymptotic non-flatness, analogous to C_{0+} in the linearised solution from [6] which we shall see later in section 2.3.

2.2.3 Non-Frobenius solutions

One should worry that there are other solution families not described by the Frobenius ansatz (2.2.1). We do in fact find a solution family more like the form (1.2.27), which we name $(1,-1)_{\ln}$, which we detail next before moving on to a description of the searches that did not yield new solution families.

2.2.3.1 A wider $(1,-1)_0$ family : $(1,-1)_{\ln}$

The Frobenius solution (1.2.27), had logs appearing at sub-leading orders. We also consider an ansatz of that form. We note, however, that the $(2,2)_0$ family already has the full number of free parameters of the theory, so we do not expect to be able to add terms of the form $k\ln(x)$ to it. The $(0,0)_0$ family has been determined to be the vacuum (an analysis which depended on its first two terms only), and its number of free parameters is the same as the vacuum family in the linearised theory, so we do not expect to be able to include any log terms, since they would have to be associated with additional free parameters. That leaves the $(1,-1)_0$ family. We write the following ansatz

$$\begin{aligned} A &= r\left(a_0 + p_0\ln(r) + (a_1 + p_1\ln(r))r + (a_2 + p_2\ln(r))r^2 + ...\right) \\ \frac{B}{b_0} &= \frac{1}{r}\left(1 + q_0\ln(r) + (b_1 + q_1\ln(r))r + (b_2 + q_2\ln(r))r^2 + ...\right) \ . \end{aligned}$$

For $\beta = 0$ we find that all the p_i and q_i are zero for $i \leq 9$. For $\beta \neq 0$, however, we find that logs are admissible in the third order terms.

$$\begin{aligned} A &= r\left(a_1 + a_2 r + a_3 r^2 + (a_4 + p_4\ln(r))r^3 + (a_5 + p_5\ln(r))r^4 + \dots\right) \\ \frac{B}{b_{-1}} &= \frac{1}{r}\left(1 + b_0 r + b_1 r^2 + (b_2 + q_2\ln(r))r^3 + (b_3 + q_3\ln(r))r^4\dots\right) \ , \end{aligned}$$

where there are 4+1 free parameters $b_{-1}, a_1, a_4, b_2, p_4$. At sixth order we find that $p_4 = 0$ appears to be required. We note that we are solving coupled non-linear third-order ODEs, and we take inspiration from the generalisation of Frobenius' method from second-order linear ODEs (see section 1.2.3) to third-order linear ODEs, which causes $\ln(r)^2$ terms to appear. Generalising our ansatz to allow $\ln(r)^2$ terms allows it to remain a solution for $p_4 \neq 0$, and makes the solution of the form:

$$\begin{aligned} A &= r\left(a_1 + a_2 r + a_3 r^2 + \dots\right) + \ln(r)\sum_{p=4} c_p r^p + \ln(r)^2 f_7 r^7 + \dots \\ \frac{B}{b_{-1}} &= \frac{1}{r}\left(1 + b_0 r + b_1 r^2 + \dots\right) + \ln(r)\sum_{q=2} d_q r^q + g_5 r^5\ln(r)^2 + \dots \ , \end{aligned}$$

where $f_7 = f_7(a_1, a_4, b_2, p_4)$ and $g_5 = g_5(a_1, a_4, b_2, p_4)$ so there are 4+1 free parameters.

The boundary term of the theorem (2.1.6) went as $O(r^3)$ in the $(1,-1)_0$ family, but in this wider family it goes as

$$C(r) = \sqrt{\frac{b_{-1}}{a_1}}\,\frac{81p_4^2}{a_1^4(7\alpha+15\beta)^2}\Bigg(36\alpha^2\ln(r) + \frac{\alpha}{p_4}\left((7\alpha+15\beta)\left(3\left(a_1^4+a_4\right)-5a_1b_2\right)+18p_4(\alpha-\beta)\right) - ra_1 36\alpha^2 + r^2a_1^2 18\alpha^2\Bigg) + O(r^3) + O(r^3\ln(r)) + O(r^3\ln(r)^2) + \dots \ .$$

The leading order is $p_4(\sim r^0 + \sim \ln(r))$. This boundary contribution does not vanish for $p_4 \neq 0$ The $R = 0 \Leftrightarrow \beta = 0$ sub-family has $p_4 = 0$ and is the same as the $(1,-1)_0$ family. In the $(1,-1)_{\ln}$ family we assume $p_4 \neq 0$, so we cannot say that R must vanish for asymptotically flat solutions in this family. In this family the Ricci scalar goes as

$$\frac{54}{a_1^2}\frac{\alpha}{7\alpha+15\beta}p_4\ln(r) + O(r^0)\ . \tag{2.2.13}$$

It is interesting to note that although the $\ln(r)$ expressions appeared at third-order in the metric, they are the leading order in the Ricci scalar. In the $(1,-1)_0$ family the Ricci scalar went as $\sim O(r^0)$ but in the $(1,-1)_{\ln}$ family the leading order is lower, $p_4\ln(r)$. This gives us a sense in which we can say that these are different families, rather than interpreting the $(1,-1)_0$ family as merely a sub-family of the $(1,-1)_{\ln}$ family: though the p_4 term is sub-leading in the metric it is the leading order term in the curvature.

2.2.3.2 Searching for other non-Frobenius solutions

We have tried various other ansatzes but found no other solution families. We detail the outcome of the search below. Note that it is usually not possible to rule out a solution of a particular form, but only to say that no such solution is positively confirmed.

The Frobenius analysis of linear differential equations in fact involves solutions of another form, that we haven't mentioned so far, the form of (1.2.23) or (1.2.27). We are now dealing with non-linear differential equations, to let us consider an ansatz that allows logs to any power, but for now we restrict consideration to the leading order, to make the problem tractable.

$$A = r^{n_a}\left(a_0\ln(r)^{m_a} + O(\epsilon)\right) \tag{2.2.14}$$

$$B = b_t r^{n_b}\left(\ln(r)^{m_b} + O(\epsilon)\right)\ . \tag{2.2.15}$$

The only allowed (n_a, n_b) cases are $(0,0)_0$, $(1,-1)_0$, $(2,2)_0$, and for each it can be shown that neither $m_a \neq 0$ nor $m_b \neq 0$ are admissible, and this follows for both the $\beta \neq 0$ theory and the $\beta = 0$ theory. So we see that there are no logs in the leading order terms.

One ansatz we have tried uses exponentials. This has been tried only in the simpler $\beta = 0$ theory. The form is

$$A = e^{S(r)} \tag{2.2.16a}$$
$$B = e^{T(r)} \,, \tag{2.2.16b}$$

where $S(r)$ and/or $T(r)$ are large near the origin. For $S(r \to 0) >> 0$ there is no solution. For $S(r \to 0) << 0$ we must choose an ansatz for S, T in order to say more. We choose

$$S = s_0 r^{n_a} ln(r)^{m_a} (1 + \epsilon_s(r)) \tag{2.2.17a}$$
$$T = t_0 r^{n_b} ln(r)^{m_b} (1 + \epsilon_t(r)) \tag{2.2.17b}$$

and look for n_a, n_b, m_a, m_b such that the leading order is not of the Frobenius form for both A and B. There are no solutions except possibly the special cases $n_a = 0$ and/or $n_b = 0$. However, in these cases the NLO becomes relevant so to examine these cases we need to use an ansatz for the NLO as well. We use the ansatz

$$S = s_0 r^{n_a} ln(r)^{m_a} + s_1 r^{p_a} ln(r)^{q_a} (1 + \epsilon_s(r)) \tag{2.2.18a}$$
$$T = t_0 r^{n_b} ln(r)^{m_b} + t_1 r^{p_b} ln(r)^{q_b} (1 + \epsilon_t(r)) \,, \tag{2.2.18b}$$

where $n_a = 0$ and/or $n_b = 0$. There is now a very large variety of possible cases of combinations of $n_a, n_b, m_a, m_b, p_a, p_b, q_a, q_b$, which cannot be examined exhaustively. In the case $n_a = 0$ we can eliminate most solutions, but we cannot eliminate the solutions

$$n_b = p_b \tag{2.2.19a}$$
$$n_b = p_a \tag{2.2.19b}$$
$$p_a = 0 \tag{2.2.19c}$$
$$p_b = 0 \,, m_a = 0 = m_b \tag{2.2.19d}$$

because an examination of them requires consideration of the NNLO as well. Similarly in the case $n_b = 0$ we can eliminate most solutions, but we cannot eliminate the solutions

$$n_a = p_a \tag{2.2.20a}$$
$$n_a = p_b \tag{2.2.20b}$$
$$p_a = 0 \tag{2.2.20c}$$
$$m_b = 0 \tag{2.2.20d}$$

because an examination of them requires consideration of the NNLO as well. In the case $n_a =$

$0 = n_b$ then there are no non-Frobenius cases except possibly the special case $p_a = 0 = p_b$, where further examination requires consideration of the NNLO too. We cannot conclude that this non-Frobenius form for A and B is not a solution, but since the LO and NLO fail to give specific values for the indices we decide to not consider it further.

Another ansatz considered in the $\beta = 0$ theory is one similar to the solution around an irregular singular point of a linear ODE.

$$A = e^{S(r)} E(r) \tag{2.2.21a}$$
$$B = e^{T(r)} F(r) \,, \tag{2.2.21b}$$

where $S(r), T(r), E(r), F(r)$ are Frobenius series, and we require that at least one of S and T is large near the origin (we will not discuss the case where they are both finite). For $S(r \to 0) >> 0$ there is no solution. To discuss $S(r \to 0) << 0$ or $S(r \to 0)$ finite then we need to define terms in our ansatz

$$S(r) = \frac{1}{r^u} S_T(r) \tag{2.2.22a}$$
$$T(r) = \frac{1}{r^v} T_T(r) \tag{2.2.22b}$$
$$E(r) = r^s E_T(r) \tag{2.2.22c}$$
$$F(r) = r^t F_T(r) \,, \tag{2.2.22d}$$

where the T subscripts denote Taylor series, and we shall require that $u \geq 0$ and $v \geq 0$. Consider $S(r \to 0)$ finite - i.e. $u = 0$ - one finds that there is no solution. Next consider $S(r \to 0) << 0$, implying $u > 0$. Solving at next-to-leading order we learn that $v = u > 1$. At the next order we learn that $t = s + 2u + 2$ and going to higher orders we can rule out more of possible values for u, At the highest order studied $u < \frac{3}{2}$ is excluded, and we did not continue to check higher values of u.

Another ansatz considered is r powers not in integer steps, $A, B \sim r^a + r^{a+\delta}$. Write

$$A = a_s r^s + a_{s+x} r^{s+x} + \ldots \tag{2.2.23a}$$
$$B = b_t \left(r^t + b_{t+y} r^{t+y} + \ldots \right) \tag{2.2.23b}$$

and look for positive real non-integer x, y ($\{x, y \in \mathbb{R}^+ \mid x, y \notin \mathbb{Z}\}$). as before we find that the leading order has $(s,t) = (0,0)_0$ or $(1,-1)_0$ or $(2,2)_0$. For the $\beta = 0$ theory we can rule out any non-integer x, y. For the $\beta \neq 0$ theory we can eliminate non-integer x, y in the $(0,0)_0$ and

$(1,-1)_0$ cases but for the $(2,2)_0$ case there are possible solutions:

$$y = 2\,, x > 2\,, b_4 = \frac{1}{4}a_2 \tag{2.2.24}$$

$$\text{or } x = 2\,, y > 2\,, a_4 = -\frac{1}{3}a_s^{\,2} \tag{2.2.25}$$

$$\text{or } y = x\,, x < 2\,, a_{2+x} = \frac{x+2}{3}a_s b_{2+x}\,, \tag{2.2.26}$$

which would need consideration of the NNLO too before they could be ruled out. However, they are consistent with the Frobenius solution (2.2.7). (2.2.24) is consistent with (2.2.7) with $x = 3$, $b_3 = 0$, $b_4 = \frac{1}{4}a_2$ where one would have $A \sim r^2 + r^5$. (2.2.25) is consistent with (2.2.7) with $y = 3$, $b_3 = b_4 = 0$. (2.2.26) is consistent with (2.2.7) with $x = 1$, $b_3 \neq 0$. So although we cannot completely rule out solutions of this form we fail to find evidence for their existence.

So we do not find any non-Frobenius solutions. Our investigation indicated that the $\alpha = 3\beta$ ($m_2^2 = m_0^2$) theory is a special case and may be different, but we do not consider it here.

2.2.4 Summary

We present the key properties of all the families of solutions around the origin that we have found in table 2.1.

Solution family	$C(r)$	number of free parameters	
		(generic α, β)	($\beta = 0$)
$(0,\ \ 0)_0$	$O(r^3)$	2+1	1+1
$(1,-1)_0$	$O(r^3)$	3+1	2+1
$(2,\ \ 2)_0$	$O(r^{-1})$	5+1	3+1
$(1,-1)_{\ln}$	$O(r^0 \ln(r))$	4+1	N/A

TABLE 2.1: Summary of free parameter counts in the three families of solutions near the origin

2.3 The Linearised theory

In [6] perturbations about Minkowski space were studied. These solutions can be used for studying the large r regime when considering asymptotically flat solutions. When linearising around flat space we can obtain closed-form solutions and it becomes possible to study coupling to various matter sources, which is extremely difficult in the full nonlinear theory. We shall expand on the matter coupling solutions that appeared in [6] to show more detail and consider more situations.

The perturbations are written as

$$A = 1 + W(r) + O(W^2) \tag{2.3.1a}$$
$$B = 1 + V(r) + O(V^2)\ , \tag{2.3.1b}$$

where W and V are both assumed to be small, of order ϵ, and the equations of motion are solved to linear order in ϵ.

2.3.1 Solving the vacuum for $r > 0$

The first task is to find the vacuum solutions to the theory. To solve the vacuum equations it is convenient to make the substitution

$$Y(r) = \frac{(rW)'}{r^2}\ , \tag{2.3.2}$$

but one should take note that while we require that the metric does not contain any delta functions, with this substitution it is permitted for Y to contain delta functions. Specifically, $\frac{1}{r}$ terms in W do not give rise to bulk terms in Y but do give rise to delta functions, while $\frac{e^{\pm mr}}{r}$ terms in W give bulk and delta terms.

$$W \sim \frac{k}{r} \quad \text{implies} \quad Y = \frac{(rW)'}{r^2} \sim k\, 4\pi\delta^3(\vec{r})\ . \tag{2.3.3}$$

To solve note that the equations of motion (1.3.1) imply the pair of equations [6]

$$H_\mu^{\ \mu} = 2(3\beta - \alpha)\nabla^2\nabla^2 V - \gamma\nabla^2 V - 4(3\beta - \alpha)\nabla^2 Y + 2\gamma Y + O((W,V)^2) \tag{2.3.4a}$$
$$H_i^{\ i} - H_t^{\ t} = 2\beta\nabla^2\nabla^2 V - \gamma\nabla^2 V + 2(\alpha - 2\beta)\nabla^2 Y + O((W,V)^2)\ , \tag{2.3.4b}$$

where ∇^2 is the three-dimensional Laplacian operator. Note that although this is a very convenient form of the equations of motion, by (1.3.10) the equations (2.3.4) contain both H_{rr} and H'_{rr}, forming a first order differential equation for H_{rr} (specifically, $\frac{1}{2}$((2.3.4a) + (2.3.4b)) $=$ $3H_{rr}(r) + rH'_{rr}(r) + O((W,V)^2)$). So solutions to (2.3.4) must be refined with $H_{rr} = 0$ as an extra condition.

These vacuum equations of motion for $r > 0$ can be solved using normal methods, giving terms like $V, Y \sim \frac{e^{\pm mr}}{r}$. This was done in [6] but featured a typo; the correct solutions are given by

$$V = C + \frac{C_{2,0}}{r} + C_{0-}\frac{e^{-m_0 r}}{r} + C_{0+}\frac{e^{m_0 r}}{r} + C_{2-}\frac{e^{-m_2 r}}{r} + C_{2+}\frac{e^{m_2 r}}{r} , \tag{2.3.5a}$$

$$\begin{aligned} W = &- \frac{C_{2,0}}{r} + C_{0-}\frac{e^{-m_0 r}}{r}(1 + m_0 r) + C_{0+}\frac{e^{m_0 r}}{r}(1 - m_0 r) \\ &- \frac{1}{2}C_{2-}\frac{e^{-m_2 r}}{r}(1 + m_2 r) - \frac{1}{2}C_{2+}\frac{e^{m_2 r}}{r}(1 - m_2 r) , \end{aligned} \tag{2.3.5b}$$

$$\begin{aligned} Y = &- m_0^2\left(C_{0-}\frac{e^{-m_0 r}}{r} + C_{0+}\frac{e^{m_0 r}}{r}\right) + \frac{m_2^2}{2}\left(C_{2-}\frac{e^{-m_2 r}}{r} + C_{2+}\frac{e^{m_2 r}}{r}\right) \\ &- 4\pi\delta^3(\vec{r})\left(C_{2,0} - (C_{0-} + C_{0+}) + \frac{1}{2}(C_{2-} + C_{2+})\right) . \end{aligned} \tag{2.3.5c}$$

There are six free parameters in these solutions, which can be broken up as one parameter, C, corresponding to the time scaling symmetry, and five physical parameters.

By inspection of these solutions we see that we should restrict our consideration to positive couplings α, β. For negative α or negative β we would have pure imaginary masses m_2 or m_0, respectively. Then W would have terms that went as $\sim \sin(im_n r)$ and $\sim \cos(im_n r)$ $(n = 0, 2)$ which are non-diminishing oscillations that are mutually exclusive with the the asymptotically flat solutions that we wish to consider.

For a generic solution to the linearised theory the Ricci curvature is given by

$$R = -\frac{3m_0^2}{r}\left(C_{0-}e^{-m_0 r} + C_{0+}e^{m_0 r}\right) + O((W,V)^2) \tag{2.3.6a}$$

$$R_{tt} = \frac{1}{2r}\left(C_{0-}m_0^2 e^{-m_0 r} + C_{0+}m_0^2 e^{m_0 r} + C_{2-}m_2^2 e^{-m_2 r} + C_{2+}m_2^2 e^{m_2 r}\right) + O((W,V)^2) \tag{2.3.6b}$$

$$\begin{aligned} R_{rr} = &\frac{1}{2r^3}\Big(- C_{0-}e^{-m_0 r}\left(3(m_0 r)^2 + 4m_0 r + 4\right) + C_{0+}e^{m_0 r}\left(-3(m_0 r)^2 + 4m_0 r - 4\right) \\ &- C_{2-}e^{-m_2 r}(1 + m_2 r) - C_{2+}e^{m_2 r}((1 - m_2 r) + O((W,V)^2)\Big) , \end{aligned} \tag{2.3.6c}$$

which are all generically divergent, as are the curvature invariants constructed from the Riemann and Ricci tensors

$$R_{\mu\nu}R^{\mu\nu} \sim \frac{3(4C_{0-} + 4C_{0+} + C_{2-} + C_{2+})^2}{8r^6} + O(r^{-5}) + O((W,V)^3) \tag{2.3.7}$$

$$\begin{aligned} R_{\mu\nu\rho\sigma}R^{\mu\nu\rho\sigma} \sim &\frac{3}{2r^6}\Big(8(C_{0-})^2 + 4C_{0-}(4C_{0+} + C_{2-} + C_{2+}) + 8(C_{0+})^2 + 4C_{0+}(C_{2-} + C_{2+}) \\ &+ 8(C_{2,0})^2 + (C_{2-} + C_{2+})(12C_{2,0} + 5(C_{2-} + C_{2+}))\Big) \\ &+ O(r^{-4}) + O((W,V)^3) . \end{aligned} \tag{2.3.8}$$

The three curvature scalars R , $R_{\mu\nu}R^{\mu\nu}$ and $R_{\mu\nu\rho\sigma}R^{\mu\nu\rho\sigma}$ and non-divergent at the origin if and only if $0 = C_{2,0} = C_{2-} + C_{2+} = C_{0-} + C_{0+}$. We do not expect the linearised theory to

approximate the full theory if the curvature grows large, but it may be a good approximation in this case of non-singular curvature. We comment on this again in section 2.3.6.

We can compare to the theorem (2.1.6) where we find that the boundary contribution $C(r)$ goes as

$$C(r) = -\frac{9m_0^4}{r}\left(C_{0-}e^{-m_0 r} + C_{0+}e^{m_0 r}\right)\left(C_{0-}e^{-m_0 r}(1+m_0 r) + C_{0+}e^{m_0 r}(1-m_0 r)\right) + O((W,V)^2)\,, \tag{2.3.9}$$

which has two zeroes (at distinct radii $0 \leq r \leq \infty$) only if $C_{0-} = 0 = C_{0+}$ which is clearly necessary and sufficient for R (2.3.6a) to vanish everywhere, clearly reflecting the statement of the theorem.

Note that here $\alpha = 3\beta$ is a special case where $m_2 = m_0$ coincide. In this case the solutions (2.3.5) would have only four independent functions of r. This is an artefact of the linearised theory; there are still 5+1 free parameters in the static spherically symmetric theory. The free parameter count for the non-linear $\alpha = 3\beta$ theory is found from an expansion around r_0, called the $(0,0)_{r_0}$ family, that we shall see later in section 2.4.1.1, and it finds that there are still 5+1 free parameters.

We now couple this vacuum solution to different matter distributions. Since we can only do this in the linearised theory this will provide most of our intuition about matter coupling in the higher derivative theory.

2.3.2 Vacuum for $r \geq 0$

The solutions (2.3.5) describe a vacuum for $r > 0$. To include the origin we can use Stokes' theorem on (2.3.4) to find:

$$\begin{aligned} H_\mu^{\ \mu} =& 4\pi\delta^3(\vec{r})\,\gamma\, C_{2,0} \\ &+ 4\pi\nabla^2\delta^3(\vec{r})6\beta\,(3(C_{0-}+C_{0+}) - C_{2,0}) \qquad (2.3.10a) \\ H_i^{\ i} - H_t^{\ t} =& -4\pi\delta^3(\vec{r})\,\gamma\, C_{2,0} \\ &+ 4\pi\nabla^2\delta^3(\vec{r})2\left(\alpha(C_{2-}+C_{2+}) + 3\beta(C_{0-}+C_{0+}) + \left[\frac{4}{3}\alpha - \beta\right]C_{2,0}\right)\,, \qquad (2.3.10b) \end{aligned}$$

and one can also show that

$$\lim_{r_0\to 0}\int_{r\leq r_0} r^2 H_{rr}\,dV = 12\pi\,\left(\alpha(C_{2-}+C_{2+}) + 12\beta(C_{0-}+C_{0+}) + \frac{4}{3}(\alpha - 3\beta)C_{2,0}\right)\,, \tag{2.3.11}$$

so the true vacuum solution, i.e. vacuum for $r \geq 0$, has $0 = C_{2,0} = C_{2-} + C_{2+} = C_{0-} + C_{0+}$

$$V_{\text{vacuum}} = C + 2C_{0+}\frac{\sinh(m_0 r)}{r} + 2C_{2+}\frac{\sinh(m_2 r)}{r} \tag{2.3.12a}$$

$$W_{\text{vacuum}} = 2C_{0+}\left(\frac{\sinh(m_0 r)}{r} - m_0\cosh(m_0 r)\right) - C_{2+}\left(\frac{\sinh(m_2 r)}{r} - m_2\cosh(m_2 r)\right) . \tag{2.3.12b}$$

One can clearly see that the vacuum solution is the Minkowski solution ($V = C, W = 0$) if and only if it is asymptotically flat.

This solution has 2+1 free parameters, because there are three independent constraints for there to be a vacuum at the origin. This count agrees with the near-origin expansions, which found the vacuum family to be the (2+1)-parameter $(0,0)_0$ family (2.2.2). This point will be reinforced again in section 2.3.6.

2.3.3 A point source at the origin

In [6] the discussion of coupling to sources began with the simple and understandable example of the point source. We will expand on the discussion of sources in [6] and begin by repeating the point source example. We show the curvatures of this solution too. Take as source a point mass at the origin,

$$T_{\mu\nu} = \delta^0_\mu \delta^0_\nu M \delta^3(\vec{r}) , \tag{2.3.13}$$

so that by

$$H_{\mu\nu} = \frac{1}{2}T_{\mu\nu} \tag{2.3.14}$$

we can compare to (2.3.10) to get

$$H^\mu_\mu = -\frac{1}{2}M\delta^3(\vec{r}) \tag{2.3.15a}$$

$$H^i_i - H^t_t = \frac{1}{2}M\delta^3(\vec{r}) , \tag{2.3.15b}$$

and therefore

$$C_{2,0} = -3\frac{M}{24\pi\gamma} \tag{2.3.16a}$$

$$C_{0-} + C_{0+} = -\frac{M}{24\pi\gamma} \tag{2.3.16b}$$

$$C_{2-} + C_{2+} = 4\frac{M}{24\pi\gamma} , \tag{2.3.16c}$$

and for an asymptotically flat matter distribution we say $C_{2+} = C_{0+} = 0$.

So the metric of a point source is [6]:

$$V = C - \frac{M}{24\pi\gamma r}\left(e^{-m_0 r} - 4e^{-m_2 r} + 3\right) \tag{2.3.17a}$$

$$W = -\frac{M}{24\pi\gamma r}\left(e^{-m_0 r}\left(1 + m_0 r\right) + 2e^{-m_2 r}\left(1 + m_2 r\right) - 3\right) \ , \tag{2.3.17b}$$

indicating that $\gamma = \frac{1}{16\pi G}$ to match with the Schwarzschild result in the limit $\alpha, \beta \to 0$, i.e. $m_0, m_2 \to \infty$.

The curvatures of a point source are:

$$R = \frac{M}{8\pi\gamma r}\, m_0^2\, e^{-m_0 r} + O(W, V^2) \tag{2.3.18a}$$

$$R_{tt} = \frac{M}{48\pi\gamma r}\left(4m_2^2 e^{-m_2 r} - m_0^2 e^{-m_0 r}\right) + O((W, V)^2) \tag{2.3.18b}$$

$$R_{rr} = \frac{M}{48\pi\gamma r^3}\left(e^{-m_0 r}\left[3(m_0 r)^2 + 4m_0 r + 4\right] - 4e^{-m_2 r}\left[1 + m_2 r\right]\right) + O((W, V)^2) \tag{2.3.18c}$$

$$R_{\mu\nu\rho\sigma}R^{\mu\nu\rho\sigma} \sim \frac{\left(m_0^4 + m_2^2 m_0^2 + 7m_2^4\right) M^2}{288\pi^2\gamma^2 r^2} + O(r^{-1}) + O((W, V)^2) \ . \tag{2.3.18d}$$

The curvatures diverge towards the origin and tend to zero at large r.

This stress-energy solution is not persuasive enough, however, since there are two main reasons to doubt its reliability. The first is that in general relativity there is a problem with codimension 2 sources like this, in that they are not properly defined [37]. To be properly defined the source should be codimension 0 or 1. The second is that the source is located at $r = 0$, a region where the linearised theory may not be valid because we see that the curvatures become large, and in fact we shall see in section 2.3.6 that indeed, the non-vacuum linearised solution is only valid for large r. Hence we turn to other examples of sources, macroscopic and with codimension 1, for more confident statements about source coupling in the theory.

2.3.4 Shell source

We now turn to extended sources, whose solutions will illustrate the important point that there is no uniqueness theorem for spherically symmetric solutions - in fact we shall explicitly see that the exterior solution depends on the details of the source. We start with a simple example, a thin spherical shell of matter of radius ℓ:

$$T_{tt} = \frac{M}{4\pi\ell^2}\delta(r - \ell) \tag{2.3.19a}$$

$$T_{rr} = 0 \ , \tag{2.3.19b}$$

where by the linearised $\nabla^\mu T_{\mu\nu} = 0$ condition we must have

$$T_{\theta\theta} = 0 + O((W, V)^2) \,. \tag{2.3.20}$$

For $r < \ell$ we use the vacuum solution (2.3.12) with free parameters D, D_{0-}, D_{2-}:

$$V_{\text{in}} = D - \frac{2D_{0-}\sinh(m_0 r)}{r} - \frac{2D_{2-}\sinh(m_2 r)}{r} \,, \tag{2.3.21a}$$

$$W_{\text{in}} = -2D_{0-}\left(\frac{\sinh(m_0 r)}{r} - m_0\cosh(m_0 r)\right) + D_{2-}\left(\frac{\sinh(m_2 r)}{r} - m_2\cosh(m_2 r)\right) \,, \tag{2.3.21b}$$

and for the exterior solution ($r > \ell$) we use the generic solutions (2.3.5) for V_{out} and W_{out} with the free parameters C, C_{0-}, C_{0+}, C_{2-}, C_{2+}.

For $\alpha \neq 0$ and $\beta \neq 0$ we require step discontinuities (of the form $\Theta(r-\ell)$) in W'' and V''' (equivalently A'' and B'''), with the following discontinuity structure

$$\begin{aligned}
W &\sim \text{(continuous)} \\
W' &\sim \text{(continuous)} \\
W'' &\sim \text{(continuous part)} - \frac{\ell M(\alpha+6\beta)}{144\pi\alpha\beta}\Theta(r-\ell) \\
V &\sim \text{(continuous)} \\
V' &\sim \text{(continuous)} \\
V'' &\sim \text{(continuous)} \\
V''' &\sim \text{(continuous part)} - \frac{\ell M(\alpha-12\beta)}{144\pi\alpha\beta}\Theta(r-\ell) \,.
\end{aligned}$$

The solution in full is

$$V_{\text{in}} = D + \frac{\sinh(m_0 r)}{r}\left(2C_{0+} - \frac{Me^{-m_0\ell}}{24\pi\gamma m_0\ell}\right) + \frac{\sinh(m_2 r)}{r}\left(2C_{2+} + \frac{Me^{-m_2\ell}}{6\pi\gamma m_2\ell}\right) \tag{2.3.22a}$$

$$\begin{aligned}
W_{\text{in}} = &\left(\frac{\sinh(m_0 r)}{r} - m_0\cosh(m_0 r)\right)\left(2C_{0+} - \frac{Me^{-m_0\ell}}{24\pi\gamma m_0\ell}\right) \\
&- \left(\frac{\sinh(m_2 r)}{r} - m_2\cosh(m_2 r)\right)\left(C_{2+} + \frac{Me^{-m_2\ell}}{12\pi\gamma m_0\ell}\right)
\end{aligned} \tag{2.3.22b}$$

$$\begin{aligned}
V_{\text{out}} = &D + \frac{M}{8\pi\gamma\ell} - \frac{M}{24\pi\gamma r}\left(3 + \frac{\sinh(m_0\ell)}{m_0\ell}e^{-m_0 r} - 4\frac{\sinh(m_2\ell)}{m_2\ell}e^{-m_2 r}\right) \\
&+ 2C_{0+}\frac{\sinh(m_0 r)}{r} + 2C_{2+}\frac{\sinh(m_2 r)}{r}
\end{aligned} \tag{2.3.22c}$$

$$\begin{aligned}
W_{\text{out}} = &\frac{M}{24\pi\gamma r}\left(3 - 2\frac{\sinh(m_2\ell)}{m_2\ell}e^{-m_2 r}(1+m_2 r) - \frac{\sinh(m_0\ell)}{m_0\ell}e^{-m_0 r}(1+m_0 r)\right) \\
&C_{0+}\frac{e^{m_0 r}}{r}(1-m_0 r) - C_{0+}\frac{e^{-m_0 r}}{r}(1+m_0 r) - \frac{1}{2}C_{2+}\frac{e^{m_2 r}}{r}(1-m_2 r) + \frac{1}{2}C_{2+}\frac{e^{-m_2 r}}{r}(1+m_2 r) \,,
\end{aligned} \tag{2.3.22d}$$

with Ricci scalar

$$R_{\text{out}} = \frac{M}{8\pi\gamma r}\, m_0^2\, e^{-m_0 r}\, \frac{\sinh(m_0\ell)}{m_0\ell} + O((W,V)^2)\ , \tag{2.3.23}$$

So we see that the exterior metric and curvature of the spherical shell are of the same form as the metric and curvature of the point source, with $\frac{\sinh(m_n\ell)}{m_n\ell}$ terms multiplying the functions. Since terms of this form appear both with m_2 and with m_0 the dependence on ℓ cannot be absorbed by any of the other free parameters, and we see the unlike General Relativity there is no Birkhoff theorem - the exterior metric depends not just on the total mass of the source but also on its structure through the parameter ℓ. In the $\ell \to 0$ limit the $\frac{\sinh(m_n\ell)}{m_n\ell}$ terms tend to 1 and the solutions corresponds with the point source expressions. The interior metric is divergent in the limit $\ell \to 0$ but this does not worry us since the volume of space that is described by that metric would vanish.

The lack of a Birkhoff theorem was noted already in [6] using as example source a "balloon", which we shall also cover in section 2.3.5.

2.3.4.1 The shell source in the $\beta = 0$ case

We find that in the limit $\beta \to 0$ the coupling to sources is changed slightly. We shall see that although the final result is changed simply, and is given by taking the same expression and removing the m_0 terms, the derivation is changed significantly because the discontinuities are different. We shall take the hollow shell source as an example and see that in the $\beta = 0$ case there is actually in discontinuity in the normal component of the metric (g_{rr}) itself. The reader may wish to refer back to the introduction to the topic of junction conditions in section 1.2.1. The simpler equations of motion for the Einstein-Weyl theory reveal that the appropriate discontinuity structure for the linearised shell is the following:

$$\begin{aligned}
W &\sim (\text{continuous part}) + \frac{M}{24\pi\gamma\ell}\Theta(r-\ell) \\
W' &\sim (\text{continuous part}) + \frac{M}{24\pi\gamma\ell}\delta(r-\ell) - \frac{M}{24\pi\gamma\ell^2}\Theta(r-\ell) \\
V &\sim (\text{continuous}) \\
V' &\sim (\text{continuous part}) - \frac{M}{24\pi\gamma\ell^2}\Theta(r-\ell) \\
V'' &\sim (\text{continuous part}) - \frac{M}{24\pi\gamma\ell^2}\delta(r-\ell) + \frac{M}{12\pi\gamma\ell^3}\Theta(r-\ell)\ .
\end{aligned}$$

The solution is:

$$V_{\text{in}} = D + \frac{\sinh(m_2 r)}{r}\left(2C_{2+} + \frac{Me^{-m_2\ell}}{6\pi\gamma m_2 \ell}\right) \tag{2.3.24a}$$

$$W_{\text{in}} = -\left(\frac{\sinh(m_2 r)}{r} - m_2\cosh(m_2 r)\right)\left(C_{2+} + \frac{Me^{-m_2\ell}}{12\pi\gamma m_0 \ell}\right)$$

$$V_{\text{out}} = D + \frac{M}{8\pi\gamma\ell} - \frac{M}{24\pi\gamma r}\left(3 - 4\frac{\sinh(m_2\ell)}{m_2\ell}e^{-m_2 r}\right) + 2C_{2+}\frac{\sinh(m_2 r)}{r} \tag{2.3.24b}$$

$$W_{\text{out}} = \frac{M}{24\pi\gamma r}\left(3 - 2\frac{\sinh(m_2\ell)}{m_2\ell}e^{-m_2 r}(1+m_2 r)\right) - \frac{1}{2}C_{2+}\frac{e^{m_2 r}}{r}(1-m_2 r) + \frac{1}{2}C_{2+}\frac{e^{-m_2 r}}{r}(1+m_2 r)\ . \tag{2.3.24c}$$

Despite the different discontinuity structure, The only difference from the solution (2.3.22) is that m_0 terms do not appear.

2.3.5 Balloon source

The next source we shall consider is a balloon of radius ℓ. This expands upon the discussion of the balloon in [6]. By balloon we mean a uniform mass and pressure for $r < \ell$ and vacuum outside:

$$T_{\mu\nu} = \begin{pmatrix} \frac{3M}{4\pi\ell^3}\Theta(\ell - r) & 0 & 0 & 0 \\ 0 & P\Theta(\ell - r) & 0 & 0 \\ 0 & 0 & T_{\theta\theta} & 0 \\ 0 & 0 & 0 & T_{\theta\theta}\sin^2\theta \end{pmatrix}, \tag{2.3.25}$$

where $\Theta(r)$ is the Heaviside theta function. $T_{\theta\theta}$ is fixed by the condition (1.3.3)

$$T_{\theta\theta} = Pr^2\Theta(\ell - r) - \frac{1}{2}Pr^3\delta(\ell - r) \tag{2.3.26}$$

(plus higher-order terms). The interior solution is now modified to solve (2.3.4) for non-zero $H_{\mu\nu}$:

$$V_{\text{in}}(r) = -\frac{2D_{0-}\sinh(m_0 r)}{r} - \frac{2D_{2-}\sinh(m_2 r)}{r} + D + \frac{r^2\left(4\pi\ell^3 P + M\right)}{16\pi\gamma\ell^3} \tag{2.3.27}$$

$$W_{\text{in}}(r) = -2D_{0-}\left(\frac{\sinh(m_0 r)}{r} - m_0\cosh(m_0 r)\right) + D_{2-}\left(\frac{\sinh(m_2 r)}{r} - m_2\cosh(m_2 r)\right) + \frac{Mr^2}{8\pi\gamma\ell^3}\ . \tag{2.3.28}$$

Note that the new terms that produce the bulk mass and pressure are proportional to r^2, and so near the origin V, W, V', W' are not different from the discussion in 2.3.1 above and the

discussion of section 2.3.2 (regarding the condition to have no delta functions at the origin) is unmodified for the balloon, i.e. $0 = D_{2,0} = D_{2-} + D_{2+} = D_{0-} + D_{0+}$ still applies to the interior solution.

The discontinuity structure of the balloon is similar to that of the hollow shell, with discontinuities in $V'''(r)$ and $W''(r)$ at $r = \ell$:

$$V'''_{\text{out}}(\ell_+) = V'''_{\text{in}}(\ell_-) + \frac{\ell P(\alpha + 6\beta)}{36\alpha\beta} \tag{2.3.29a}$$

$$W''_{\text{out}}(\ell_+) = W''_{\text{in}}(\ell_-) - \frac{\ell^2 P(\alpha - 3\beta)}{36\alpha\beta} \,. \tag{2.3.29b}$$

We also enforce continuity of the lower order derivatives and the metric itself. The continuity and discontinuity conditions form a system of six independent constraints, as one might expect from the nature of the system, which is sixth order in differentials.

To present the solution, we shall enforce asymptotic flatness and use a shorthand notation

$$M_n := M + n\, 2\pi\ell^3 P \,, \tag{2.3.30}$$

making the interior and exterior metrics of a balloon

$$\begin{aligned}
V_{\text{in}} =& D + \frac{1}{48\pi\gamma\ell^3}\left(3M_2 r^2 + 2\left[3\frac{1+m_0\ell}{m_0^2}M_{-2} - 4\pi\ell^5 P\right]\frac{\sinh(m_0 r)}{m_0 r}e^{-m_0\ell}\right.\\
&\left. - 8\left[3\frac{1+m_2\ell}{m_2^2}M_1 + 2\pi\ell^5 P\right]\frac{\sinh(m_2 r)}{m_2 r}e^{-m_2\ell}\right)\\
W_{\text{in}} =& \frac{1}{24\pi\gamma\ell^3}\left(3M_0 r^2 + \left[3\frac{1+m_0\ell}{m_0^2}M_{-2} - 4\pi\ell^5 P\right]\left[\frac{\sinh(m_0 r)}{m_0 r} - \cosh(m_0 r)\right]e^{-m_0\ell}\right.\\
&\left. + 2\left[3\frac{1+m_2\ell}{m_2^2}M_1 + 2\pi\ell^5 P\right]\left[\frac{\sinh(m_2 r)}{m_2 r} - \cosh(m_2 r)\right]e^{-m_2\ell}\right)\\
V_{out} =& D + \frac{1}{16\pi\gamma\ell}\left(2\frac{M_{-2}}{\ell^2 m_0^2} - 8\frac{M_1}{\ell^2 m_2^2} + 3M + 4\pi\ell^3 P\right) - \frac{M}{8\pi\gamma r}\\
&+ \frac{e^{-m_0 r}}{24\pi\gamma r}\left(3\frac{M_{-2}}{\ell^2 m_0^2}\left[\frac{\sinh(m_0\ell)}{m_0\ell} - \cosh(m_0\ell)\right] - 4\pi\ell^3 P\frac{\sinh(m_0\ell)}{m_0\ell}\right)\\
&- \frac{e^{-m_2 r}}{6\pi\gamma r}\left(3\frac{M_1}{\ell^2 m_2^2}\left[\frac{\sinh(m_2\ell)}{m_2\ell} - \cosh(m_2\ell)\right] + 2\pi\ell^3 P\frac{\sinh(m_2\ell)}{m_2\ell}\right)\\
W_{out} =& \frac{M}{8\pi\gamma r}\\
&+ \frac{e^{-m_0 r}(1+m_0 r)}{24\pi\gamma r}\left(3\frac{M_{-2}}{\ell^2 m_0^2}\left[\frac{\sinh(m_0\ell)}{m_0\ell} - \cosh(m_0\ell)\right] - 4\pi\ell^3 P\frac{\sinh(m_0\ell)}{m_0\ell}\right)\\
&+ \frac{e^{-m_2 r}(1+m_2 r)}{12\pi\gamma r}\left(3\frac{M_1}{\ell^2 m_2^2}\left[\frac{\sinh(m_2\ell)}{m_2\ell} - \cosh(m_2\ell)\right] + 2\pi\ell^3 P\frac{\sinh(m_2\ell)}{m_2\ell}\right)
\end{aligned}$$

(where the exterior metric appeared already in [6])

Like the hollow spherical shell, we see that the exterior metric depends on the details of the source. The hollow spherical shell depended on the mass and size, M and ℓ. The balloon has these and also a third parameter describing it, the pressure P, and the result for the exterior metric depends on M, ℓ and P as independent quantities. The exterior metric necessarily has free parameters corresponding to static symmetry (D) and asymptotic non-flatness (C_{0+}, C_{2+}, here constrained to vanish). Since it also depends on multiple parameters of the source then we see that all six free parameters of the theory are needed to describe the solution of a matter source in the linearised theory. This is in contrast to general relativity where Birkhoff's theorem implies that spherically symmetric solutions depend on the matter distribution through only one parameter.

2.3.6 Next correction to the linearised theory

For the $\beta = 0$ theory it is actually tractable to find the second-order perturbations around flat space, too. Let us define precisely what we mean. Write A, B as

$$A = 1 + \epsilon W(r) + \epsilon^2 W_2(r) + O(\epsilon^3) \tag{2.3.32a}$$

$$B = 1 + \epsilon V(r) + \epsilon^2 V_2(r) + O(\epsilon^3) \tag{2.3.32b}$$

and solve the equations of motion to order ϵ^2, neglecting order ϵ^3. The solution is

$$
\begin{aligned}
V_2 =& \mathrm{Ei}\left(-2rm_2\right)\frac{1}{8}C_{2-}m_2\left(3C_{2-}m_2-4C_{2,0}\frac{e^{m_2r}}{r}\right)\\
&+\mathrm{Ei}\left(2rm_2\right)\frac{1}{8}C_{2+}m_2\left(3C_{2+}m_2+4C_{2,0}\frac{e^{-m_2r}}{r}\right)\\
&+\frac{e^{-m_2r}}{r}\frac{1}{4}C_{2-}\left(2C_{2,0}m_2\ln(r)+\frac{C_{2,0}}{r}+4C\right)\\
&+\frac{e^{m_2r}}{r}\frac{1}{4}C_{2+}\left(-C_{2,0}m_2\ln(r)+\frac{C_{2,0}}{r}+4C\right)\\
&+\mathrm{Ei}\left(-rm_2\right)C_{2-}m_2\frac{69}{128}\left(C_{2-}\frac{e^{-m_2r}}{r}-2C_{2+}\frac{e^{m_2r}}{r}\right)\\
&+\mathrm{Ei}\left(rm_2\right)C_{2+}m_2\frac{69}{128}\left(2C_{2-}\frac{e^{-m_2r}}{r}-C_{2+}\frac{e^{m_2r}}{r}\right)\\
&+\frac{e^{-2m_2r}}{r^2}\frac{1}{64}C_{2-}^2\left(15-4m_2r\right)+\frac{e^{2m_2r}}{r^2}\frac{1}{64}C_{2+}^2\left(15+4m_2r\right)\\
&-\mathrm{Ei}\left(-3rm_2\right)\frac{69}{128}C_{2-}^2m_2\frac{e^{m_2r}}{r}+\mathrm{Ei}\left(3rm_2\right)\frac{69}{128}C_{2+}^2m_2\frac{e^{-m_2r}}{r}\\
&+\frac{3}{4}C_{2-}C_{2+}m_2^2\ln(r)+\frac{15C_{2-}C_{2+}}{32r^2}+\frac{C_{2,0}C}{r}\\
W_2 =& +\frac{1}{4}\frac{e^{m_2r}}{r}\mathrm{Ei}\left(-2rm_2\right)C_{2-}C_{2,0}m_2\left(1-m_2r\right)\\
&-\frac{1}{4}\frac{e^{-m_2r}}{r}\mathrm{Ei}\left(2rm_2\right)C_{2,0}C_{2+}m_2\left(1+m_2r\right)\\
&+\mathrm{Ei}\left(-rm_2\right)\frac{69}{256}C_{2-}m_2\left(-C_{2-}\frac{e^{-m_2r}}{r}\left(1+m_2r\right)+C_{2+}\frac{e^{m_2r}}{r}2\left(1-m_2r\right)\right)\\
&+\mathrm{Ei}\left(rm_2\right)\frac{69}{256}C_{2+}m_2\left(-C_{2-}\frac{e^{-m_2r}}{r}2\left(1+m_2r\right)+C_{2+}\frac{e^{m_2r}}{r}\left(1-m_2r\right)\right)\\
&+\frac{1}{8}\frac{e^{-m_2r}}{r}C_{2,0}C_{2-}\left(6m_2-2m_2\ln(r)\left(1+m_2r\right)+\frac{7}{r}\right)\\
&+\frac{1}{8}\frac{e^{m_2r}}{r}C_{2,0}C_{2+}\left(-6m_2+2m_2\ln(r)\left(1-m_2r\right)+\frac{7}{r}\right)\\
&+\mathrm{Ei}\left(-3rm_2\right)\frac{69}{256}C_{2-}^2m_2\frac{e^{m_2r}}{r}\left(1-m_2r\right)-\mathrm{Ei}\left(3rm_2\right)\frac{69}{256}C_{2+}^2m_2\frac{e^{-m_2r}}{r}\left(1+m_2r\right)\\
&+\frac{1}{64}\frac{e^{-2m_2r}}{r^2}C_{2-}^2\left(9+21m_2r+20m_2^2r^2\right)\\
&+\frac{1}{64}\frac{e^{2m_2r}}{r^2}C_{2+}^2\left(9-21m_2r+20m_2^2r^2\right)\\
&-\frac{1}{8}C_{2-}C_{2+}m_2^2\frac{32C_{2,0}^2+9C_{2-}C_{2+}}{32r^2}\,,
\end{aligned}
$$

where Ei is the exponential integral function defined as the principal value of the integral

$$
\mathrm{Ei}(z)=-\int_{-z}^{\infty}\frac{e^{-t}}{t}dt\,. \tag{2.3.33}
$$

At large and small argument $\mathrm{Ei}(x)$ goes as

$$\mathrm{Ei}(x) \sim \begin{cases} \ln(|x|) + \gamma_E + O(x) & , \ 0 < |x| << 1 \\ e^x \left(x^{-1} + O(x^{-2})\right) & , \ 1 << |x| \end{cases} , \tag{2.3.34}$$

where γ_E is the Euler constant $\gamma_E \approx 0.577$. So we can see that in the order ϵ^2 solution the terms that blow up as r gets large are still controlled by C_{2+}. We also see that the corrections blow up for small r except in the vacuum case $0 = C_{2,0} = C_{2-} + C_{2+}$ (2.3.12). Generically, for all non-vacuum space-times the linearised solutions (2.3.5) only approximate the full theory away from the origin. This is an important point since it is the reason why we have not compared the linearised solutions (2.3.5) to the small-r solutions of section 2.2, though this would have been extremely useful if it were possible.

Although generic solutions to the non-linear theory are not approximated by solutions to the linearised theory, there should certainly exist a subset of solutions that are perturbatively close to Minkowski for all r, that *can* be consistently described with the linearised solution. The next-to-leading order corrections are non-divergent only for the vacuum solution family $0 = C_{2,0} = C_{2-} + C_{2+}$, so it must be this family that is consistent for all finite r. Recall that the condition for the linearised solution to be vacuum is the same as the condition for its curvatures to be non-singular at the origin. The vacuum family can therefore be compared to the $(0,0)_0$ solution of section 2.2.1.1. We can only use linearised solutions near the origin in the non-singular, vacuum case, and all such linearised solutions have a $(0,0)$ behaviour at small r. In the non-linear theory the $(0,0)_0$ family is necessary and sufficient for being non-singular at the origin. We feel justified in identifying the linearised vacuum solutions as the perturbative approximation of the $(0,0)_0$ family at any radius.

The $(0,0)_0$ family had 2+1 free parameters in the general theory and 1+1 in the $\beta = 0$ theory. From the discussion in section 2.2.2 we saw that in the $(0,0)_0$ family asymptotic flatness (with or without any horizons) implies that the family reduces to its $\beta = 0$ version and that $a_2 = b_2$. This implies that the parameter $(a_2 - b_2)$ describes a deviation from asymptotic flatness analogous to C_{0+}. Within the linearised $\beta = 0$ theory, the vacuum solutions are only asymptotically flat if they are flat space, and we recall that in the non-linear $\beta = 0$ theory the $(0,0)_0$ solutions are flat space if and only if $a_2 = 0$, so we believe that a_2 corresponds to C_{2+}. In summary, we believe that the two non-trivial free parameters of the $(0,0)_0$ family, a_2 and b_2, both describe asymptotic non-flatness, and the only asymptotically flat member of the $(0,0)_0$ family is Minkowski space.

The next-to-leading-order expressions found here will appear again in section 3.3 which deals with asymptotically flat numerical solutions in the $\beta = 0$ theory.

2.4 Solutions around $r_0 \neq 0$.

We gain further insight into solutions of the theory by studying expansions around an arbitrary radius r_0. This will include radii where special things happen, e.g. a horizon. A Frobenius analysis is very successful but we shall find other very important non-Frobenius solutions too.

2.4.1 Frobenius Analysis

We write the metric functions as expansions about an arbitrary point, i.e. series in $(r-r_0)$. This will be much easier using a different radial function:

$$ds^2 = -B(r)\,dt^2 + \frac{dr^2}{f(r)} + r^2 d\Omega_2^2\,, \tag{2.4.1}$$

simply related to (1.3.8) by $A(r) = 1/f(r)$.

The Frobenius ansatz we shall use is

$$f = f_u(r-r_0)^u + f_{u+1}(r-r_0)^{u+1} + \cdots \tag{2.4.2a}$$

$$\frac{B}{b_t} = (r-r_0)^t + b_{t+1}(r-r_0)^{t+1} + \cdots \tag{2.4.2b}$$

for some u and t, not confusing these undetermined placeholders (u,t) with the undetermined placeholders (s,t) we wrote earlier (2.2.1)

In the $\beta = 0$ case the equations of motion imply the two relatively simple coupled second-order ODEs (c.f. equations (1.3.19))

$$0 = -2\gamma r^2 B^3 \tag{2.4.3a}$$

$$-3\alpha r^2 B^3 f'^2 + 4\alpha r^2 f B^3 f'' \tag{2.4.3b}$$

$$-2\alpha r^3 f B^2 f'' B' \tag{2.4.3c}$$

$$-r^3\alpha f B f' B'^2 + \alpha r^3 f^2 B'^3 \tag{2.4.3d}$$

$$+8\alpha f B^3 + 2\gamma r^2 f B^3 - 8\alpha f^2 B^3 + 4\alpha r B^3 f' \tag{2.4.3e}$$

$$-4\alpha r f B^3 f' + 2\gamma r^3 f B^2 B' - 2\alpha r^2 f B^2 f' B' - 3\alpha r^2 f^2 B B'^2\,, \tag{2.4.3f}$$

$$0 = \frac{H^{\mu}_{\mu}}{\gamma} = -r^2 f^3 B'^2 + 2r^2 f^3 B B'' \tag{2.4.4a}$$
$$+ r^2 f^2 B f' B' \tag{2.4.4b}$$
$$+ 4r f^2 B^2 f' \tag{2.4.4c}$$
$$- 4 f^2 B^2 \tag{2.4.4d}$$
$$+ 4 f^3 B^2 + 4r f^3 B B' \ , \tag{2.4.4e}$$

These equations are simple and the reader can easily use a paper calculation to gain insight into the method we use to determine u and t. Substituting the ansatz (2.4.2) into (2.4.3) we find that if $\frac{3}{2} < u$ then the term (2.4.3a) contributes the leading order behaviour, but does not vanish, so we conclude that $u \leq \frac{3}{2}$. In (2.4.4) we find that for all $u < 2$ the terms (2.4.4a) and (2.4.4b) lead, and vanish only for $t = 0$ or $t = 2 - u$. Now we must examine the next-to-leading order. For $t = 2 - u$ the leading-order terms are contributed by (2.4.4a) and (2.4.4b), and (2.4.3c) and (2.4.3d), and vanish only for $u = 1$. On the other hand, for $t = 0$, if $1 < u$ then the leading order appears in (2.4.3a) and (2.4.4d) but never vanishes. For $t = 0$ and $u < 1$ then the leading order comes from the terms (2.4.3b) and (2.4.3c), and (2.4.4b) and (2.4.4c), and vanish only for $u = 0$. Thus we rule out all Frobenius solutions except the (u, t) pairs

- $(u, t) = (1, 1)_{r_0}$
- $(u, t) = (0, 0)_{r_0}$
- $(u, t) = (1, 0)_{r_0}$

where we write the r_0 subscript to indicate that these are (u, t) of solutions (2.4.2) around $r = r_0 \neq 0$.

In the $\beta \neq 0$ theory there is a similar calculation producing the same (u, t) pairs. Details of the calculation find that the $\alpha = 3\beta$ case may have different properties (due to solving equations at leading order of the form $(\alpha - 3\beta)(\dots) = 0$), and that there may be a special radius $\tilde{r_0}$ s.t. $3\gamma\tilde{r_0}^{\,2} = 2(\alpha - 3\beta)$, though these may just be an artefact of the series approach. Note, however, that we will also find some solutions not described by a Frobenius ansatz, and these are detailed in section 2.4.2.

2.4.1.1 The $(0, 0)_{r_0}$ solution

This solution corresponds to no special point of the solution and since we impose no boundary conditions at $r \neq r_0$ we expect this expansion to see the full number of free parameters of the

theory. The first few terms in the solution are:

$$
\begin{aligned}
f(r) =& f_0 + f_1 (r-r_0) + f_2 (r-r_0)^2 \\
&+ \frac{(r-r_0)^3}{432\alpha\beta f_0 r_0^3 ((\alpha-3\beta)b_1 r_0 - 2(\alpha+6\beta))} \Bigg(-3\beta \Big((\alpha-3\beta)^2 b_1^5 r_0^5 + \left(19\alpha^2 - 51\beta\alpha - 18\beta^2\right) b_1^4 r_0^4 \\
&- 4b_1^3 \left(13\alpha^2 + 84\beta\alpha + 36\beta^2 + 2(\alpha-3\beta)^2 b_2 r_0^2\right) r_0^3 \\
&+ 4b_1^2 \left(\alpha^2 - 12(\alpha-3\beta)b_2 r_0^2 \alpha + 66\beta\alpha + 36\beta^2\right) r_0^2 \\
&+ 16 b_1 \left((\alpha-3\beta)^2 b_2^2 r_0^4 + \left(7\alpha^2 + 48\beta\alpha + 36\beta^2\right) b_2 r_0^2 + 5\alpha^2 - 9\beta^2 - 12\alpha\beta\right) r_0 \\
&- 16 \left(\left(\alpha^2 + 3\beta\alpha - 18\beta^2\right) b_2^2 r_0^4 + 5\alpha^2 + 18\beta^2 + 33\alpha\beta\right) \Big) f_0^2 \\
&+ 2 \Bigg(-\alpha^2\gamma b_1^3 r_0^5 - 9\beta^2\gamma b_1^3 r_0^5 + 6\alpha\beta\gamma b_1^3 r_0^5 + 4\alpha^2\gamma b_1 b_2 r_0^5 + 36\beta^2\gamma b_1 b_2 r_0^5 - 24\alpha\beta\gamma b_1 b_2 r_0^5 \\
&+ 6\alpha^2\gamma b_1^2 r_0^4 - 54\beta^2\gamma b_1^2 r_0^4 - 8\alpha^2\gamma b_2 r_0^4 + 144\beta^2\gamma b_2 r_0^4 - 24\alpha\beta\gamma b_2 r_0^4 - 4\alpha^2\gamma b_1 r_0^3 + 72\beta^2\gamma b_1 r_0^3 \\
&- 12\alpha\beta\gamma b_1 r_0^3 - 216\beta^3 b_1^2 r_0^2 + 144\alpha\beta^2 b_1^2 r_0^2 - 24\alpha^2\beta b_1^2 r_0^2 - 8\alpha^2\gamma r_0^2 - 72\beta^2\gamma r_0^2 - 60\alpha\beta\gamma r_0^2 \\
&- 72\alpha\beta f_2 \left((\alpha-3\beta)b_1^2 r_0^2 - (\alpha+6\beta)b_1 r_0 - 2(\alpha+6\beta)\right) r_0^2 \\
&- 432\beta^3 b_1 r_0 - 144\alpha\beta^2 b_1 r_0 + 96\alpha^2\beta b_1 r_0 + 3\beta f_1 \Big((\alpha-3\beta)^2 b_1^4 r_0^4 + \left(11\alpha^2 - 39\beta\alpha + 18\beta^2\right) b_1^3 r_0^3 \\
&- 4b_1^2 \left(8\alpha^2 + 51\beta\alpha + 18\beta^2 + (\alpha-3\beta)^2 b_2 r_0^2\right) r_0^2 \\
&- 4b_1 \left(-11\alpha^2 + 12\beta\alpha - 18\beta^2 + \left(\alpha^2 - 15\beta\alpha + 36\beta^2\right) b_2 r_0^2\right) r_0 + 8(\alpha+6\beta)\left(3\alpha b_2 r_0^2 - 8\alpha + 6\beta\right) \Big) r_0 \\
&- 864\beta^3 - 720\alpha\beta^2 - 96\alpha^2\beta \Bigg) f_0 \\
&+ 2 f_1 r_0 \left((\alpha-3\beta)b_1 r_0 - 2(\alpha+6\beta)\right) \left((\alpha-3\beta)\gamma b_1 r_0^3 + 4\alpha\gamma r_0^2 + 6\beta\gamma r_0^2 - 36\alpha\beta f_2 r_0^2 + 72\beta^2 - 24\alpha\beta\right) \\
&- 3\beta f_1^2 r_0^2 \Big((\alpha-3\beta)^2 b_1^3 r_0^3 + 3\left(\alpha^2 - 9\beta\alpha + 18\beta^2\right) b_1^2 r_0^2 - 12\alpha(\alpha+6\beta) b_1 r_0 + 4\left(\alpha^2 - 6\beta\alpha - 72\beta^2\right)\Big) \\
&+ 8\Big(-(\alpha-3\beta)b_1 r_0 \left(\alpha\left(\gamma r_0^2 - 6\beta\right) + 6\beta\left(\gamma r_0^2 + 3\beta\right)\right) - (\alpha+6\beta)\left(\alpha\left(6\beta - 2\gamma r_0^2\right) - 3\beta\left(\gamma r_0^2 + 6\beta\right)\right)\Big) \Bigg) \\
&+ O\left((r-r_0)^4\right)
\end{aligned}
\tag{2.4.5a}
$$

$$\begin{aligned}\frac{B(r)}{b_0} =& 1 + b_1 (r-r_0) + b_2 (r-r_0)^2 \\ &+ \frac{(r-r_0)^3}{48 f_0^2 r_0^3 \left(b_1 r_0(\alpha - 3\beta) - 2(\alpha + 6\beta)\right)} \\ &\times \Bigg(2f_0 \Bigg(4b_1 r_0^2 \left(f_1 \left(\alpha - 2b_2 r_0^2(\alpha - 3\beta) + 24\beta\right) - 3\gamma r_0\right) \\ &+ 4\left(4b_2 f_1 r_0^3(\alpha + 6\beta) + 36\beta - 3\gamma r_0^2\right) \\ &+ 3b_1^3 f_1 r_0^4(\alpha - 3\beta) - 4b_1^2 f_1 r_0^3(2\alpha + 3\beta) - 4f_2 r_0^2 \left(4(\alpha - 12\beta) + b_1^2 r_0^2(\alpha - 3\beta) - 4b_1 r_0(\alpha + 6\beta)\right) \Bigg) \\ &+ f_0^2 \Bigg(-7b_1^4 r_0^4(\alpha - 3\beta) + 4b_1^3 r_0^3(5\alpha + 12\beta) + 4b_1^2 r_0^2 \left(\alpha + 6b_2 r_0^2(\alpha - 3\beta) - 48\beta\right) \\ &- 32 b_1 r_0 \left(\alpha + 3b_2 r_0^2(\alpha + 3\beta) + 6\beta\right) + 16\left(\alpha + b_2^2 r_0^4(\alpha - 3\beta) + 4b_2 r_0^2(\alpha + 6\beta) - 21\beta\right) \Bigg) \\ &+ f_1^2 r_0^2 \left(4(\alpha - 12\beta) + b_1^2 r_0^2(\alpha - 3\beta) - 4b_1 r_0(\alpha + 6\beta)\right) + 8\left(-2\alpha + 6\beta + 3\gamma r_0^2\right) \Bigg) \\ &+ O\left((r-r_0)^4\right) \ , \end{aligned} \tag{2.4.5b}$$

which has 5+1 free parameters, f_0, f_1, f_2, b_1, b_2 and the trivial parameter b_0.

The boundary quantity $C(r)$ goes as a product of two functions $F(b_1, b_2, f_0, f_1, r_0)$ and $F(b_1, b_2, f_0, f_1, r_0, f_2, \alpha, \beta, \gamma)$ over a denominator:

$$\begin{aligned} C(r) =& \frac{\sqrt{\frac{b_0}{f_0}}}{16 r_0^3 \left(b_1 r_0(\alpha - 3\beta) - 2(\alpha + 6\beta)\right)} \times F(b_1, b_2, f_0, f_1, r_0) \times F(b_1, b_2, f_0, f_1, r_0, f_2, \alpha, \beta, \gamma) \\ &+ O(r - r_0) \ , \end{aligned} \tag{2.4.6}$$

so for a given r_0 there are two (4+1)-parameter sub-solutions (equivalently, there are two possibly constraints) where the $O((r-r_0)^0)$ term vanishes and therefore that this quantity vanishes at r_0. From the theorem (2.1.6) we see that if $C(r)$ vanishes at two radii r_1 and r_2 it implies that $R = 0$ for all $r_1 < r < r_2$. From (2.4.6) we expect that this would be one constraint at r_1 and a second (assumed independent) constraint at r_2, so the $R = 0$ solution has two fewer parameters than the generic solution. This agrees with the analysis of 1.3.3.2 where we found that the solution with $R = 0 \Leftrightarrow \beta = 0$ has 4 free parameters compared to 6 in the generic theory.

The fact that in this expansion around an arbitrary point r_0 the condition for the boundary term $C(r_0)$ to vanish is one constraint compares well with the information in section 2.2.4. Consider using (2.1.6) with integration region $0 < r < r_0$, and assume for the sake of argument that even matching onto a specified small-r solution family, it is still true that $C(r_0) = 0$ is exactly one constraint. We saw that the two families where $C(r \to 0)$ vanished had one fewer free parameter in the $R = 0$ theory than in the generic theory, which matches nicely with the idea that the single condition $C(r_0) = 0$ is sufficient to force R to vanish by (2.1.6).

We present the solution for the $\beta = 0$ theory too.

$$\begin{aligned} f(r) =& f_0 + f_1 (r - r_0) \\ &+ \frac{(r-r_0)^2}{4\alpha f_0 r_0^2 (b_1 r_0 - 2)} \Big(f_0 \left(2\left(4\alpha + b_1 \gamma r_0^3 + \gamma r_0^2\right) - \alpha f_1 r_0 \left(b_1^2 r_0^2 + 2 b_1 r_0 + 4\right)\right) \\ &+ \alpha f_0^2 \left(b_1^3 r_0^3 - 3 b_1^2 r_0^2 - 8\right) + r_0 \left(4\alpha f_1 - 3\alpha f_1^2 r_0 - 2\gamma r_0\right) \Big) \\ &+ O\left((r-r_0)^3\right) \end{aligned} \tag{2.4.7a}$$

$$\begin{aligned} \frac{B(r)}{b_0} =& 1 + b_1 (r - r_0) \\ &+ \frac{(r-r_0)^2}{4 f_0 r_0^2} \left(-f_1 r_0 (b_1 r_0 + 4) + f_0 \left(b_1^2 r_0^2 - 4 b_1 r_0 - 4\right) + 4\right) \\ &+ O\left((r-r_0)^3\right) \ , \end{aligned} \tag{2.4.7b}$$

which has 3+1 free parameters, b_0, b_1, f_0, f_1, as expected.

2.4.1.2 The $(1,1)_{r_0}$ solution

This solution family corresponds to a horizon and goes as:

$$f(r) = f_1 (r - r_0) + f_2 (r - r_0)^2 + O\left((r-r_0)^3\right) \tag{2.4.8a}$$

$$\begin{aligned} \frac{B(r)}{b_1} =& (r - r_0) \\ &+ \frac{(r-r_0)^2}{9\beta f_1 r_0^2 (\alpha - 3\beta)} \Big(- \pm \Big(+ (\alpha - 3\beta) \left(144\beta^2(\alpha - 3\beta) + \gamma^2 r_0^4 (\alpha - 3\beta) - 24\beta\gamma r_0^2 (\alpha + 6\beta)\right) \\ &+ 72\beta f_1 r_0 \left(2\beta f_1 r_0 (\alpha + 3\beta)^2 - (\alpha - 3\beta)\left(4\beta(\alpha - 3\beta) + 8\alpha\beta f_2 r_0^2 + \gamma r_0^2 (-(\alpha + 2\beta))\right)\right) \Big)^{\frac{1}{2}} \\ &+ r_0^2 (\alpha - 3\beta)(\gamma - 3\beta f_2) + 12\beta f_1 r_0 (\alpha + 3\beta) \Big) \\ &+ O\left((r-r_0)^3\right) \ . \end{aligned} \tag{2.4.8b}$$

It has 3+1 free parameters: f_1, f_2, b_1 and the location of the horizon, r_0.

In this solution family (2.1.9) goes as

$$
\begin{aligned}
C(r) =& (r-r_0)\,\frac{\sqrt{\frac{b_1}{f_1}}\gamma}{108\beta^3 r_0^2(\alpha-3\beta)^2}\Bigg(144\alpha^2\beta^2-864\alpha\beta^3+1296\beta^4+\\
&\pm\Big(144\beta^2 f_1^2 r_0^2(\alpha+3\beta)^2-72\beta f_1 r_0(\alpha-3\beta)\left(8\alpha\beta f_2 r_0^2+\alpha\left(4\beta-\gamma r_0^2\right)-2\beta\left(6\beta+\gamma r_0^2\right)\right)\\
&+\alpha^2\left(\gamma r_0^2-12\beta\right)^2-6\alpha\beta\left(144\beta^2+12\beta\gamma r_0^2+\gamma^2 r_0^4\right)\\
&+9\beta^2\left(144\beta^2+48\beta\gamma r_0^2+\gamma^2 r_0^4\right)\Big)^{\frac{1}{2}}\left((\alpha-3\beta)\left(12\beta-\gamma r_0^2\right)-36\beta f_1 r_0(\alpha-\beta)\right)\\
&-288\alpha^2\beta^2 f_1 f_2 r_0^3+720\alpha^2\beta^2 f_1^2 r_0^2-576\alpha^2\beta^2 f_1 r_0\\
&+72\alpha^2\beta\gamma f_1 r_0^3+864\alpha\beta^3 f_1 f_2 r_0^3-864\alpha\beta^3 f_1^2 r_0^2+2592\alpha\beta^3 f_1 r_0-180\alpha\beta^2\gamma f_1 r_0^3\\
&+1296\beta^4 f_1^2 r_0^2-2592\beta^4 f_1 r_0-108\beta^3\gamma f_1 r_0^3-24\alpha^2\beta\gamma r_0^2\\
&+\alpha^2\gamma^2 r_0^4+36\alpha\beta^2\gamma r_0^2-6\alpha\beta\gamma^2 r_0^4+108\beta^3\gamma r_0^2+9\beta^2\gamma^2 r_0^4\Bigg)\\
&+O\left((r-r_0)^2\right)\,, \qquad (2.4.9)
\end{aligned}
$$

which always vanishes as $r \to r_0$.

We present the solution for the $\beta = 0$ theory too:

$$
\begin{aligned}
f(r) =& f_1\,(r-r_0) \qquad (2.4.10a)\\
&+(r-r_0)^2\left(\frac{3\gamma}{8\alpha}+\frac{-\frac{3\gamma}{8\alpha f_1}-2f_1}{r_0}+\frac{1}{r_0^2}\right)\\
&+\frac{(r-r_0)^3}{288\alpha^2 f_1^3 r_0^3}\Bigg(f_1\Big(f_1\left(4\alpha f_1\left(-64\alpha+136\alpha f_1 r_0-5\gamma r_0^2\right)+\gamma r_0\left(\gamma r_0^2-28\alpha\right)\right)\\
&\qquad +8\gamma\left(6\alpha+\gamma r_0^2\right)\Big)-9\gamma^2 r_0\Bigg)\\
&+O\left((r-r_0)^4\right)\\
\frac{B(r)}{b_1} =& (r-r_0) \qquad (2.4.10b)\\
&+\frac{(r-r_0)^2}{8\alpha f_1^2 r_0^2}\left(\gamma r_0-f_1\left(-8\alpha+16\alpha f_1 r_0+\gamma r_0^2\right)\right)\\
&+\frac{(r-r_0)^3}{288\alpha^2 f_1^4 r_0^3}\Bigg(f_1\Big(f_1\left(4\alpha f_1\left(-160\alpha+232\alpha f_1 r_0+\gamma r_0^2\right)+\gamma r_0\left(7\gamma r_0^2-52\alpha\right)\right)\\
&\qquad -16\gamma\left(\gamma r_0^2-3\alpha\right)\Big)+9\gamma^2 r_0\Bigg)\\
&+O\left((r-r_0)^4\right)\,,
\end{aligned}
$$

which has 2+1 free parameters f_1, b_1 and r_0. It is related to the generic β theory by fixing $f_2 = \tilde{f}_2$ where $\tilde{f}_2 := \frac{3\gamma}{8\alpha} - \frac{3\gamma}{8\alpha f_1 r_0} - \frac{2f_1}{r_0} + \frac{1}{r_0^2}$ and the $\pm$ to the sign of $f_1\left(36\beta f_1 r_0(\alpha-\beta) - (\alpha-3\beta)\left(12\beta - \gamma r_0^2\right)\right)$

The $(1,1)_{r_0}$ family should be compared to the Schwarszchild solution. The $(1,1)_{r_0}$ behaviour has a smooth sign change of $f(r)$ and $B(r)$, describing a horizon. Consider the theorem (2.1.6) with the integration region having one boundary at $r = r_0$ and the other boundary at $r \to \infty$. The boundary contribution $C(r)$ (2.4.9) vanishes on both boundaries if the spacetime asymptotically flat, and tells us that $R = 0$, i.e. that we should restrict consideration to (2.4.10).

This family is a particularly important family because it describes black holes. There is a lot to say about the global structure of black hole solutions so the discussion is presented separately in section 3.2.

2.4.1.3 The $(1,0)_{r_0}$ solution

This solution family has $f \sim (r-r_0)$ and $B \sim 1+ \sim (r-r_0)$. We postpone a physical discussion of this family, however, until we consider its non-Frobenius generalisation, the $(1,0)_{1/2}$ family, in section 2.4.2.1. This family is better understood as an important special case of that more general family. In this section we simply present the solution, which goes as:

$$\begin{aligned} f =& f_1(r-r_0) - \frac{(r-r_0)^2}{18\alpha\beta f_1 r_0^2(\alpha-3\beta)}\Bigg(12\alpha^2\beta f_1 - 72\alpha\beta^2 f_1 + 108\beta^3 f_1 \\ &\pm\left(\gamma r_0(\alpha-3\beta) - 6\beta f_1(2\alpha+3\beta)\right)\sqrt{27\alpha\beta f_1^2 r_0^2 + 2(\alpha-3\beta)\left(2\alpha-6\beta-3\gamma r_0^2\right)} \\ &+ 9\alpha^2\beta f_1^2 r_0 - 3\alpha^2\gamma f_1 r_0^2 + 135\alpha\beta^2 f_1^2 r_0 + 27\beta^2\gamma f_1 r_0^2 + 2\gamma r_0(\alpha-3\beta)^2\Bigg) \\ &+ O\left((r-r_0)^3\right) \end{aligned} \tag{2.4.11a}$$

$$\frac{B}{b_0} = 1 + \frac{2(r-r_0)}{f_1 r_0^2(\alpha-3\beta)}\left(f_1 r_0(\alpha+6\beta) - \pm\sqrt{27\alpha\beta f_1^2 r_0^2 + 2(\alpha-3\beta)\left(2\alpha-6\beta-3\gamma r_0^2\right)}\right) + O\left((r-r_0)^2\right)\ , \tag{2.4.11b}$$

which has 2+1 free parameters, b_0, f_1, r_0.

In this solution family (2.1.9) goes as

$$\begin{aligned} C(r) =& \sqrt{r-r_0}\,\frac{\sqrt{\frac{b_0}{f_1}}\,\gamma}{3\beta r_0^2(\alpha-3\beta)^2}\Bigg(+36\alpha\beta f_1 r_0 + 2(\alpha-3\beta)\left(4\alpha - 3\left(4\beta+\gamma r_0^2\right)\right) \\ &+ 9\alpha^2 f_1^2 r_0^2 - 12\alpha^2 f_1 r_0 + 27\alpha\beta f_1^2 r_0^2 \\ &- 2 \pm (-2\alpha + 6\beta + 3\alpha f_1 r_0)\sqrt{27\alpha\beta f_1^2 r_0^2 + 2(\alpha-3\beta)\left(2\alpha-6\beta-3\gamma r_0^2\right)}\Bigg) + \dots\ , \end{aligned}$$

which vanishes at r_0.

We present the solution for the $\beta = 0$ theory too:

$$r_0 = \frac{4\alpha f_1}{3\alpha f_1^2 + 2\gamma} \tag{2.4.12a}$$

$$f(r) = f_1 (r - r_0) - \frac{\gamma (r - r_0)^2 \left(2\gamma + \alpha f_1^2\right)}{4\alpha^2 f_1^2} + O\left((r - r_0)^3\right) \tag{2.4.12b}$$

$$\begin{aligned} \frac{B(r)}{b_0} =& 1 + (r - r_0)\left(\frac{\gamma^2}{\alpha^2 f_1^3} + \frac{\gamma}{\alpha f_1} - \frac{3f_1}{4}\right) \\ &+ \frac{\gamma (r - r_0)^2}{16\alpha^4 f_1^6}\left(2\gamma + 3\alpha f_1^2\right)^2 \left(2\gamma - 3\alpha f_1^2\right) \\ &+ O\left((r - r_0)^3\right) \ , \end{aligned} \tag{2.4.12c}$$

which has only 1+1 free parameters, b_0 and f_1.

2.4.2 Non-Frobenius solutions

As in the analysis of solutions around the origin, one might think that there are other solutions around r_0 that are not described by the Frobenius ansatz $r^s \times$ (a Taylor series), but may be of the form of the Frobenius ansatz that uses logs or of an entirely different form.

We do, in fact, find two other solutions families, which we detail next, before moving on to a description of searches we did that came back negative (or inconclusive). Both of the new solutions are based on series of integer and half-integer powers of $(r - r_0)$. They are denoted with their (u, t) brackets as usual, but with a subscript to indicate that the powers go up in half-integer steps.

2.4.2.1 A consistent wormhole solution - $(1, 0)_{1/2}$

We find one solution similar to the solution (2.4.11), except it sees the full number of free parameters of the theory. For $\beta \neq 0$ the solution goes as

$$f(r) = f_1 (r - r_0) + f_2 (r - r_0)^{3/2} + O\left((r - r_0)^2\right) \tag{2.4.13}$$

$$\frac{B(r)}{b_0} = 1 + b_1\sqrt{r - r_0} + b_2 (r - r_0) + O\left((r - r_0)^{\frac{3}{2}}\right) \ . \tag{2.4.14}$$

This solution has 5+1 free parameters, f_1, f_2, b_1, b_2, r_0 and the trivial parameter b_0.

To talk about the theorem (2.1.6) we calculate the boundary term contribution:

$$\begin{aligned}C(r) = &-\frac{\sqrt{\frac{b_0}{f_1}}}{512 b_1 r_0^4(\alpha-3\beta)} \times \left(-b_1 f_2 r_0^2 + f_1 r_0\left(b_1^2 r_0 - 4\left(b_2 r_0+4\right)\right)+16\right)\\ &\times\Bigg(\left(\alpha-3\beta\right)\left(r_0^2\left(4b_2 f_1 + b_1\left(f_2 - b_1 f_1\right)\right)-16\right)\left(r_0^2\left(4b_2 f_1 + b_1\left(f_2 - b_1 f_1\right)\right)+16\right)+384\gamma r_0^2\\ &+32 f_1 r_0^2\Big(b_1^2 f_1 r_0(2\alpha+3\beta)+b_1 f_2 r_0(4\alpha-3\beta)-2b_2 f_1 r_0(\alpha+6\beta)+2f_1(\alpha-12\beta)\Big)\Bigg)\\ &+O\left((r-r_0)^{\frac{1}{2}}\right)\ .\end{aligned}$$

This tends to a finite value as $r \to r_0$, so the theorem (2.1.6) for asymptotically flat solutions does not apply. It tends to the $(r-r_0)^0$ term shown, which is a product of two large bracketed terms, and for a given r_0 either of the brackets could vanish for a choice of f_2 or b_2, however.

For $\beta = 0$ the solution is

$$f(r) = f_1\left(r-r_0\right) - \frac{\left(r-r_0\right)^{3/2}\left(\alpha f_1^2 r_0\left(b_1^2 r_0+12\right)-16\alpha f_1+8\gamma r_0\right)}{3\alpha b_1 f_1 r_0^2} + O\left((r-r_0)^2\right) \quad (2.4.15)$$

$$\frac{B(r)}{b_0} = 1 + b_1\sqrt{r-r_0} + \frac{(r-r_0)}{3\alpha f_1^2 r_0^2}\left(\alpha f_1^2 r_0\left(b_1^2 r_0-9\right)+8\alpha f_1+2\gamma r_0\right)+O\left((r-r_0)^{\frac{3}{2}}\right)\ , \quad (2.4.16)$$

which has 3+1 free parameters, f_1, r_0, b_1 and the trivial parameter b_0.

This $(1,0)_{1/2}$ family is interpreted as the generalisation of the $(1,0)_{r_0}$ family. To see this one would take the limit as the coefficients of half-integers powers go to zero. Taking the limit $f_2 \to 0$, $b_1 \to 0$ causes the $O\left((r-r_0)^{\frac{3}{2}}\right)$ term in B, which goes as $\frac{1}{b_1}$, to blow up unless the numerator is fixed to zero by constraining the value of b_2. Those three requirements are sufficient to reduce this family to the integer wormhole family $(1,0)_{r_0}$ already shown.

In [2] the $(1,0)_{r_0}$ solution was interpreted as a wormhole. We shall develop that discussion in the context of this generalisation of the family. Let us change coordinates to

$$r - r_0 = \frac{1}{4}\rho^2 \quad (2.4.17)$$

to write the metric near $r = r_0$ in the form

$$ds^2 = -b_0\left(1+\frac{b_1}{2}\rho+\frac{b_2}{4}\rho^2+\ldots\right)dt^2 + \frac{d\rho^2}{f_1+\frac{1}{2}f_2\rho+\frac{1}{4}f_3\rho^2+\ldots} + \left(\frac{1}{4}\rho^2+r_0\right)^2 d\Omega^2\ . \quad (2.4.18)$$

The interpretation of the coordinate transformation (2.4.17) is that a $\rho > 0$ patch is sewed on to a $\rho < 0$ patch. The natural next question then concerns the causal structure of the wormhole and how it works with this patch structure.

We can solve the geodesic equation

$$(X^\mu)''(\lambda) + \Gamma^\mu_{\rho\sigma}(X^\rho)'(\lambda)(X^\sigma)'(\lambda) = 0 \,,$$

in the vicinity of the wormhole, choosing a radial geodesic and use coordinates t, ρ. Pick an affine parameter such that $\rho(0) = 0$ and choose the time coordinate such that $t(0) = 0$. The geodesic is then:

$$\begin{aligned} t(\lambda) &= \lambda t'(0) - \frac{1}{4}\lambda^2 t'(0)^2 b_1 \frac{\rho'(0)^2}{t'(0)^2} + O(\lambda^3) \\ \rho(\lambda) &= \lambda t'(0)\frac{\rho'(0)}{t'(0)} + \frac{1}{8}\lambda^2 t'(0)^2 \left(\frac{f_2}{f_1}\frac{\rho'(0)^2}{t'(0)^2} - b_0 b_1 f_1\right) + O(\lambda^3) \,, \end{aligned}$$

which has length

$$(X^\mu)'(\lambda)(X_\mu)'(\lambda) = \frac{\rho'(0)^2}{f_1} - b_0 t'(0)^2 + O(\lambda^3) \,. \tag{2.4.19}$$

The signs of these terms are determined by the signs of f_1 and b_0, which are both positive if the signature of the space-time is to be $-+++$ at r just above r_0. So we see that there are geodesics that pass through from the $\rho > 0$ patch to the $\rho < 0$ patch, they have $\rho'(0) \neq 0$, $t'(0) > 0$, and they can be space-like, time-like or null. This underpins their interpretation as traversable wormholes, since a time-like observer could pass through from the $0 < \rho$ $(r_0 < r)$ region to the $\rho < 0$ $(r_0 < r)$ region. We see from the transformed metric (2.4.18) that these two patches have different metrics though, since it has terms odd in ρ. The integer wormhole $(1,0)_{r_0}$ is an important special case because in that family the same coordinate transformation shows us a metric with only even terms in ρ and so the two patches have the same metric.

What about the global structure of these solutions? Fixing the time coordinate so that asymptotically $g_{tt} \to -1$ must be one constraint by static symmetry. Since this family has 5+1 free parameters, the maximum allowed by the system, there must be a mapping between them and the 5+1 free parameters of the linearised solution (2.3.5) without any redundancy. Therefore the two constraints of asymptotic flatness, $C_{2+} = 0 = C_{2-}$, must be two constraints on this family, using only the reasonable assumption that a comparison to the linearised theory is valid. However, when considering asymptotic flatness in this family recall that there are *two* large-r regions, one in the $\rho > 0$ patch and one in the $\rho < 0$ patch. In the half-integer solution family $(1,0)_{1/2}$ these two regions do not have the same metric, and requiring asymptotic flatness and $g_{tt} \to -1$ in the other asymptotic region as well will be additional, independent constraints [4]. Thus there are six constraints on the 5+1 free parameters, and in this (5+1)-parameter family there is a single asymptotically flat solution (a zero-parameter family). In

[4] Note that usually, in the way we choose to parameterise our solutions, the constraint $g_{tt}(\rho \to \infty) \to -1$ is a constraint on what we call the trivial parameter, the parameter b_0 that corresponds to scaling the time coordinate. When there is a second patch with different metric, however, the requirement $g_{tt}(\rho \to -\infty) \to -1$ is an independent constraint on the whole system of parameters, not just b_0, and therefore does not make b_0 overconstrained.

the integer solution family $(1,0)_{r_0}$ there are only 2+1 free parameters, but the two asymptotic regions are the same, so the three conditions of asymptotic flatness and $g_{tt} \to -1$ in the one patch are the same as in the other patch, so there are only three independent constraints, so again we can find exactly one asymptotically flat solution in this family. Comparing, then, the half-integer wormhole $(1,0)_{1/2}$ with the integer wormhole $(1,0)_{r_0}$, it seems that within the system of six independent constraints on $(1,0)_{1/2}$ that we described, we can cast three of them as asymptotic flatness constraints and three as constraining the two patches to be identical i.e. as fixing it to the $(1,0)_{r_0}$ case.

Consider the theorem (2.1.6) for the integer wormhole $(1,0)_{r_0}$. The symmetry of the $(1,0)_{r_0}$ family can be used to prove that $C(r_0) = 0$ must vanish identically. Consider the following picture. The use of two patches means we can choose one boundary in each patch, one at $r_1, \rho > 0$ and one at $r_1, \rho < 0$. With some thought it is clear that this two-patch structure is compatible with the theorem as we derived it. If $C(r = r_1 > r_0)$ is zero in one patch, then by the symmetry of this solution it is also zero in the other patch, and by the theorem we can say that $R(r_0 < r < r_1) = 0$. The point is that in this family a single zero of $C(r = r_1 > r_0)$ is sufficient to prove the vanishing of the Ricci scalar, as opposed to the usual requirement of two zeroes. Now consider an alternative picture. Consider the theorem in a single patch, and put one boundary at $r = r_0$ and one at $r = r_1 > r_0$. In this picture we need $C(r_1) = 0$ and $C(r_0) = 0$ in order to prove that $R(r_0 < r < r_1) = 0$. However, from the previous picture we also know that $C(r_1) = 0$ is sufficient to prove this. The two pictures are obviously equivalent. So how can these two pictures be reconciled? The only way is if $C(r_0) = 0$ identically in this family. In the more general $(1,0)_{1/2}$ family the two patches are not identical and this proof fails, and indeed we see that $C(r_0)$ does not vanish identically in the wider family.

We believe we have a good picture of the global structure of these solutions, and although the discussion falls short of a proof, a numerical analysis can quickly corroborate our ideas. We shoot outwards from the $(1,0)_{r_0}$ family for $\beta = 0$, which has only 1+1 free parameters b_0 and f_1. Fix the trivial parameter $b_0 = 1$ and shoot from $1.01 \times r_0$ towards large r. Recall that r_0 and f_1 are related by (2.4.12a), so there is only a single non-trivial free parameter. We find that there are two behaviours. For large f_1 as you shoot outwards $f(r)$ will go to zero, at which point the numerical routines fail. For small f_1 as you shoot outwards $f(r)$ grows large while $B(r)$ asymptotes to zero. By interpolating between such a too-large value of f_1 and such a too-small value of f_1 a solution can be found that is regular out to a larger radius, and then by repeated interpolation solutions regular to larger and larger distances can be found. Ultimately precise tuning of f_1 will give us a single asymptotically flat solution. For values of the couplings $\alpha = \frac{1}{2}$ and $\gamma = 1$ the asymptotically flat solution appears around $f_1 \approx 1.18151794738$, corresponding to a wormhole radius of $r_0 \approx 0.577198137788$. The wormhole of this radius remains flat out to $r \approx 25$ and is plotted in figure 2.1. The numerical approach implies some uncertainty of the quoted value of f_1 that corresponds to an asymptotically flat solution, but the procedure of

interpolating between the two behaviours seems sound and could be carried out to arbitrary accuracy as required.

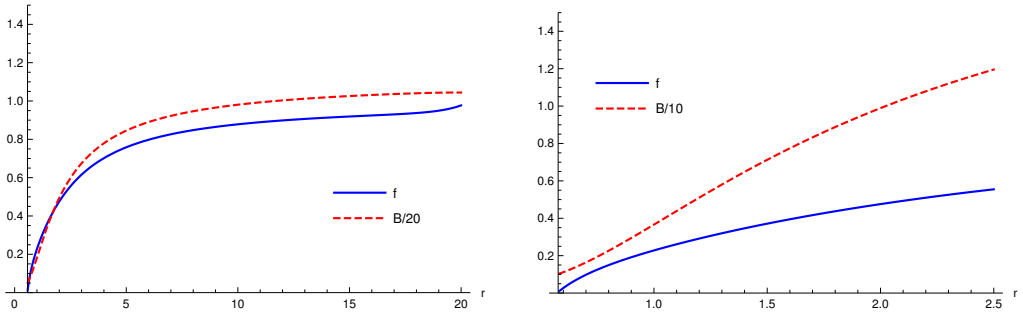

FIGURE 2.1: The asymptotically flat wormhole solution for $\alpha = \frac{1}{2}$ and $\gamma = 1$. The left-hand plot shows the space-time staying flat out to $r \approx 25$, with $f(r)$ tending to 1 and $B(r)$ tending to a constant. The right-hand plot shows detail around the wormhole, for $0.58 \lesssim r < 2.5$. In both graphs the function $B(r)$ has been scaled (as indicated), to make the functions of comparable size.

2.4.2.2 A consistent horizon solution - $(\frac{3}{2}, \frac{1}{2})_{1/2}$

We find another solution that is similar to a horizon in that it is a zero of both $B(r)$ and $f(r)$. The metric goes as:

$$\begin{aligned} f(r) =& f_0 \, (r - r_0)^{3/2} + \text{function}(\alpha, \beta, r_0, f_0, k)(r - r_0)^2 + O\left((r - r_0)^{\frac{5}{2}}\right) \\ \frac{B(r)}{b_0} =& \sqrt{r - r_0} + \text{function}(\alpha, \beta, r_0, f_0, k)(r - r_0)^1 + O\left((r - r_0)^{\frac{3}{2}}\right) \ , \end{aligned}$$

where

$$k = \pm r_0^2 \sqrt{(\alpha - 3\beta)\left(\alpha\left(-36\beta^2\left(3 f_0^2 r_0^3 - 4\right) - 24\beta\gamma r_0^2 + \gamma^2 r_0^4\right) - 3\beta\left(144\beta^2 + 48\beta\gamma r_0^2 + \gamma^2 r_0^4\right)\right)} \ , \tag{2.4.20}$$

which has 2+1 free parameters, f_0, r_0 and the trivial parameter b_0. This solution family does not appear in the $\beta = 0$ theory, and therefore it cannot have $R = 0$ for an open interval of r. However, evaluating the boundary quantity for the theorem (2.1.6) near r_0 gives

$$\begin{aligned} C(r) =& \sqrt{r - r_0} \frac{\gamma \sqrt{\frac{b_t}{a_0}}}{54\beta^3 r_0^4 (\alpha - 3\beta)} \Bigg(54\alpha a_0^2 \beta^2 r_0^5 - 12\beta k + r_0^2 \left(\gamma k - 144\beta^2(\alpha - 3\beta)\right) \\ & + \gamma^2 r_0^6 (-(\alpha - 3\beta)) + 12\beta\gamma r_0^4 (2\alpha + 3\beta) \Bigg) + \dots \ , \end{aligned}$$

which vanishes towards r_0. However, since solutions of the $\beta = 0$ theory are equivalent to the solutions with $R = 0 \ \forall r$, and this solution does not exist for $\beta = 0$, we can say that R cannot

vanish everywhere. In fact we can evaluate it near r_0 to find it goes as $O(1) + O(\sqrt{r - r_0})$:

$$R = \frac{k - \gamma r_0^4(\alpha - 3\beta) + 12\beta r_0^2(\alpha - 3\beta)}{6\beta r_0^4(\alpha - 3\beta)} + O(\sqrt{r - r_0}) \ , \tag{2.4.21}$$

and the leading order (the constant term) is never zero for the theory we wish to consider, which has positive α, γ, r_0, and real f. So we consider the theorem (2.1.6) with inner integration boundary at r_0+ and outer integration boundary $r \to \infty$, and take the fact that the Ricci scalar is not zero throughout the integration region, but the boundary term $C(r)$ does vanish at the inner integration boundary r_0. Taken together we can say that if there is Minkowski [5] signature for $r_0 < r < \infty$ then the boundary term cannot vanish at the outer boundary $r \to \infty$, i.e. the solution cannot be asymptotically flat. More generally we can say that (assuming Minkowski signature) there are no zeroes of C at radii larger than r_0 by obtaining a contradiction. Suppose that there is a zero of C at $r_1 > r_0$ s.t. $C(r_1) = 0$. By (2.1.6) this would imply that R vanishes for $r_0 < r < r_1$, which is not possible. Thus no such zero of $C(r > r_0)$ exists. Recall that (assuming $f \neq 0$) $C(r)$ would vanish either for $R = 0$ or $\partial_r R = 0$, and therefore there are no zeroes of either of these for $r > r_0$. So in fact, starting from the horizon at $r = r_0$, as you move towards increasing r either the Ricci scalar must monotonically increase or the Ricci scalar must monotonically decrease (without asymptotically approaching zero).

This solution family is interpreted as a horizon. To see this, change coordinates to

$$\sqrt{r - r_0} = \frac{f_0 \rho_0}{4}(\rho - \rho_0) \tag{2.4.22a}$$

$$r - r_0 = \frac{{f_0}^2 {\rho_0}^2}{16}(\rho - \rho_0)^2 \tag{2.4.22b}$$

so that the metric is explicitly of the Schwarzschild form for $\rho - \rho_0 << \rho_0$:

$$ds^2 = -b_0 \frac{f_0 \rho_0^2}{4} \left(\frac{\rho - \rho_0}{\rho_0} + \frac{b_1 f_0}{4}(\rho - \rho_0)^2 + \dots \right) dt^2 + \frac{d\rho^2}{\frac{\rho - \rho_0}{\rho_0} + \frac{f_1}{4}(\rho - \rho_0)^2 + \dots} + r(\rho)^2 d\Omega^2 \ . \tag{2.4.23}$$

Near this unusual "horizon" this fortunately allows us to use all the familiar apparatus of the Schwarzschild solution. The interpretation of the coordinate transformation (2.4.22a) is that a $\rho > \rho_0$ patch is sewed on to a $\rho < \rho_0$ patch. Because it is locally Schwarzschild we can say that time-like geodesics pass through from the $\rho > \rho_0$ patch to the $\rho < \rho_0$ patch (keeping the same θ and ϕ), and find the coordinates t and ρ changed from being time-like to being space-like and vice-versa. The $\rho < \rho_0$ patch also corresponds to $r > r_0$, and thus an observer on a time-like geodesic falls to a finite minimum radius and then touches this horizon and then continues to increasing radius. The fact that the coordinates change in nature between space-like and time-like when this happens makes further physical interpretation difficult, and it

[5] or Euclidean

should be borne in mind that we said that this solution cannot be asymptotically flat. The proof that it is not asymptotically flat, however, was conditional upon a $-+++$ signature for $r > r_0$. The physical interpretation just given complicates things, because the signature is different in the two patches, so the proof can apply to at most one patch. It may be possible to think of an interpretation where there are more creative signature changes at various radii, and that this interesting solution could appear at one radius in the space-time, with another of the interesting $(r - r_0)$ solution families at some other radius. In the current work we do not spend any longer finding interpretations of this solution, however, and leave it as a curiosity.

2.4.2.3 Searching for other non-Frobenius solutions

One possible ansatz is

$$f = f_u(r-r_0)^u + f_{u+x}(r-r_0)^{u+x} + \dots \tag{2.4.24a}$$

$$B = b_t\left((r-r_0)^t + b_{t+y}(r-r_0)^{t+y} + \dots\right) , \tag{2.4.24b}$$

however it proves very difficult to confirm or exclude any s, t, x, y range for this ansatz. We shall instead try the similar but simpler ansatz where the powers go up in steps $\frac{1}{n}$, for n some integer $n \geq 2$:

$$f = f_0(r-r_0)^u + f_1(r-r_0)^{u+\frac{1}{n}} + f_2(r-r_0)^{u+\frac{2}{n}} + \dots \tag{2.4.25a}$$

$$\frac{B}{b_0} = (r-r_0)^t + b_1(r-r_0)^{t+\frac{1}{n}} + b_2(r-r_0)^{t+\frac{2}{n}} + \dots . \tag{2.4.25b}$$

We cannot rule out solutions for all n, but trying the first few integers for n we can find no solutions except those $n = 2$ solutions already discussed, in either the $\beta = 0$ case or the $\beta \neq 0$ case.

Another possible ansatz has logs in the leading order term in the expansion:

$$A = (r-r_0)^{n_a}\left(a_0[\ln(r-r_0)]^{m_a} + \epsilon_a(r)\right) \tag{2.4.26}$$

$$\frac{B}{b_t} = (r-r_0)^{n_b}\left([\ln(r-r_0)]^{m_b} + \epsilon_b(r)\right) . \tag{2.4.27}$$

This proved difficult so only the $\beta = 0$ theory was examined. We can rule out solutions where such log terms appear in the leading order, but we did not check if the sub-leading terms could contain log terms of this form.

It is not possible to exhaustively exclude solutions families other than those already given, but we now have more confidence in the assumption that there are no such families.

2.4.3 Summary

The results for series expansions in $(r - r_0)$ are summarised in table 2.2 where the numbers in brackets refer to the leading-order behaviours of f and B, s.t. (u, t) corresponds to $f \sim (r-r_0)^u + \ldots$, $B \sim (r-r_0)^t + \ldots$, and where $(1,0)_{1/2}$ and $(\frac{3}{2}, \frac{1}{2})_{1/2}$ refer to the solution families with both integer and half-integer powers of $(r - r_0)$ appearing.

Solution family	$C(r)$	number of free parameters	
		(generic α, β)	($\beta = 0$)
$(0,0)_{r_0}$	$O(1)$	5+1	3+1
$(1,1)_{r_0}$	$O(r - r_0)$	3+1	2+1
$(1,0)_{r_0}$	$O(\sqrt{r - r_0})$	2+1	1+1
$(1,0)_{1/2}$	$O(1)$	5+1	3+1
$(\frac{3}{2}, \frac{1}{2})_{1/2}$	$O(\sqrt{r - r_0})$	2+1	N/A

TABLE 2.2: Summary of free parameter counts in the five families of solutions around $r = r_0$

Chapter 3

Key Physical Discussions

3.1 Coupling to matter in the full non-linear theory

Considering all our results so far, there is a stark difference between the matter coupling in the higher derivative theory and the matter coupling in GR. It is apparent from two of the simpler results. The first result is that the theorem (2.1.6) implies that static space-times that are asymptotically flat and have horizons must have $R = 0$ for all space above the horizon. The second result is that when we do matter coupling in the linearised theory, the Ricci scalars are not zero, for example (2.3.18a) and (2.3.23). Together these imply that matter coupled solutions do not have horizons, and follows for matter sources of any mass and radius. The contrast with General Relativity is clear. However, the weak link in the argument in the use of the linearised theory. We saw in section 2.3.6 that for non-vacuum solutions the linearised theory is only a valid approximation at large radii. In general relativity horizons only form for matter sources contained within a radius $2GM$, so therefore in the higher derivative theory we would wish to couple to matter at small radii, where the linear approximation may be poor. In any case linearised solutions would not be good at describing horizons since a horizon is a large deviation from flat space. The linearised theory is the only theory where we have found matter-coupled solutions in closed form, because of its simplicity, but that same simplicity causes us to doubt what it says about horizons.

The issue of horizons and matter coupling needs more examination, but the discussion will have to cope without closed-form solutions. We present a range of arguments about the features of the solutions in this section.

3.1.1 General arguments that matter fields in higher-derivative gravity are unlike those in general relativity

We have already seen in the linearised theory (section 2.3) that the solutions of matter sources have no Birkhoff theorem; the fields of extended sources depended on multiple parameters of the source. In the balloon source example, the source was described by three parameters, and the solution depended on all three of these, and had additionally one free parameter corresponding to time-scaling, and two free parameters corresponding to asymptotic non-flatness, totalling an irreducible dependence on 6 parameters, the maximum allowed by the theory. We also saw in the extended sources that the interior solutions were joined to the exterior solutions via six independent constraints. So we suppose that the vacuum exterior solution must have six free parameters in order for the coupling to work, i.e. it is not possible to couple to an exterior solution that has previously been constrained by some other consideration.

In the non-linear theory the coupling to matter is greatly more difficult than in the linearised theory, so we can only present a schematic discussion. Knowing the number of free parameters in each solution family will be key. Consider a shell source with a stress tensor like

(2.3.19):

$$T_{tt} = \frac{M}{4\pi\ell^2}\delta(r-\ell)\,, \tag{3.1.1a}$$

$$T_{rr} = 0\,, \tag{3.1.1b}$$

where the (non-linearised) conservation condition $\nabla^\mu T_{\mu\nu} = (0, \nabla^\mu T_{\mu r}, 0, 0) = 0$ requires the other component be

$$T_{\theta\theta} = \frac{r^3 B' T_{tt}}{4B^2}\,. \tag{3.1.1c}$$

The equations of motion (1.3.1) expand schematically as

$$H_{tt} = \sim B^{(4)} + \sim A^{(3)} + \sim B^{(3)} + \dots\,, \tag{3.1.2a}$$

$$H_{rr} = \sim B^{(3)} + \sim A'' + \sim B'' + \dots\,, \tag{3.1.2b}$$

$$H_{\theta\theta} = \sim B^{(4)} + \sim A^{(3)} + \sim B^{(3)} + \dots\,, \tag{3.1.2c}$$

where we show only the high-derivative terms, i.e. the dots stand for functions of lower derivatives of A, B, and the $\sim$ are also understood to indicate that similar functions multiply the high-derivative terms too. This suggests that we should consider

$$B^{(4)} \sim \delta(r-\ell) + \Theta(r-\ell)\,, \tag{3.1.3a}$$

$$A^{(3)} \sim \delta(r-\ell) + \Theta(r-\ell)\,, \tag{3.1.3b}$$

$$B^{(3)} \sim \Theta(r-\ell)\,, \tag{3.1.3c}$$

$$A'' \sim \Theta(r-\ell)\,. \tag{3.1.3d}$$

Then A, A', B, B', B'' will be continuous at $r = \ell$, while A'' has a step of size

$$A''_{\text{out}}(\ell_+) - A''_{\text{in}}(\ell_-) = \frac{M}{8\pi\ell} A^3 \frac{\ell(\alpha-3\beta)B' - 2(\alpha+6\beta)B}{36\alpha\beta}\bigg|_{r=\ell}\,. \tag{3.1.4}$$

We describe the region interior to the shell with the $(0,0)_0$ family (2.2.2), which is the vacuum family as discussed in section 2.2.1.1. This has 2+1 free parameters. Alternatively, one could think of the condition to be vacuum at the origin as the three constraints $A(0) = 1$, $A'(0) = 0 = B'(0)$ coming from (2.2.4). We describe the solution in the region exterior to the shell using some as yet undetermined solution family. We take inspiration from the linearised theory and assume that the continuity and step conditions (3.1.3) and (3.1.4) form a system of six independent constraints. Again inspired by the linearised theory we assume that the asymptotic flatness requirement amounts to two constraints. We know from the static symmetry that requiring $g_{tt}(r \to \infty) = -1$ is one constraint. We can count the total number of constraints we are imposing on the space-time and work out the minimum number of free

parameters necessary for the coupling scheme to work. We have two constraints for flatness at infinity, one to fix the time coordinate ($g_{tt} \to -1$), and six constraints for the shell coupling, totalling nine. There are three free parameters available in the interior metric, so we need the exterior metric to be one of the vacuum solution families with six free parameters. We can see from section 2.2.4 that such solutions are in the $(2,2)_0$ family near the origin. One can imagine taking the shell size ℓ to zero and in that limit finding the field of a point mass. This stress-energy tensor would then have exterior metric in the $(2,2)_0$ family, a clear contrast to general relativity where the field of a point source is in the $(1,-1)_0$ family.

We can consider this argument in the light of the results of [33] where solutions were found that coupled a stress-energy tensor to the $(0,0)_0$ family. The situation there was different - the source was a density going as $\rho \sim e^{-r^2}$ so it was not considering vacuum solutions. One might still expect that those non-vacuum results still serve as a test of our claim that only the non-GR $(2,2)_0$ family couples to matter. In fact those results found that asymptotically flat solutions required a constraint on the pressure part of the stress-energy tensor, reflecting the gist of our argument that $(0,0)_0$ family descriptions are over-constrained. In contrast, our claim is that a generic stress-energy tensor should be described by exterior solutions in the $(2,2)_0$ family. We shall only explicitly consider the example of shell sources but the principle is expected to hold for other sources too, and this comparison to results for a $\rho \sim e^{-r^2}$ source is encouraging.

An important feature of our argument was the assumption that the coupling conditions were independent. This may not be true. It may be that given that the interior metric is in the $(0,0)_0$ family, and given also that the two asymptotic flatness conditions have been imposed, one or more of the six shell-coupling conditions might be automatically satisfied. For example if two of the constraints were redundant with the other constraints then it would be possible to place the $(1,-1)_0$ family as the exterior solution. Unfortunately, it is not possible to establish if the constraints are independent or not without a closed form for the solution. However we can discuss the feasibility of the proposed coupling of a shell to a $(2,2)_0$ exterior solution. The method is slightly involved so we first discuss general relativity.

3.1.2 Details of coupling the series solutions to matter

In the previous section we proposed that in the higher-derivative theory the field of a matter source is completely different in the higher-derivative theory and general relativity, having a $(2,2)_0$ form instead of $(1,-1)_0$. However, it is not clear if this is possible or feasible. In this section we discuss the method and its difficulties, but we first illustrate them with an general relativistic example.

3.1.2.1 Coupling in general relativity using the closed form

In the higher derivative theory we do not know the solutions for the metric, instead have only series solutions. Our coupling method will be discussed in terms of series solutions, accordingly, and we can do a general relativistic example. Firstly though, in this section we derive the exact general-relativistic solution for comparison.

It is convenient to define the length scale

$$L_M := 2GM = M(8\pi\gamma)^{-1} \,. \tag{3.1.5}$$

The equations of motion of general relativity are compatible with the source (3.1.1) if there is a step in the A function:

$$B_{\text{out}}(\ell_+) = B_{\text{in}}(\ell_-) \,, \qquad A_{\text{out}}(\ell_+) - A_{\text{in}}(\ell_-) = \frac{L_M A_{\text{in}}(\ell_-)^2}{\ell\, B(\ell) - L_M A_{\text{in}}(\ell_-)} \,. \tag{3.1.6}$$

In terms of L_M the space-time of a spherical shell has metric

$$A_{\text{in}} = 1 \,, \tag{3.1.7a}$$
$$B_{\text{in}} = b \,, \tag{3.1.7b}$$
$$A_{\text{out}} = \frac{1}{1 - \frac{L_M}{b\, r}} \,, \tag{3.1.7c}$$
$$B_{\text{out}} = \frac{b}{1 - \frac{L_M}{b\,\ell}} \left(1 - \frac{L_M}{b\, r}\right) \,. \tag{3.1.7d}$$

We want to write the exterior solution in the Schwarzschild form

$$A_{\text{out}} = \frac{1}{1 - \frac{r_s}{r}} \,, \tag{3.1.8a}$$
$$B_{\text{out}} = k^2 \left(1 - \frac{r_s}{r}\right) \,, \tag{3.1.8b}$$

so we find expressions for the metric parameters in terms of the Schwarzschild radius r_s and time-scaling k^2:

$$b = k^2 \left(1 - \frac{r_s}{\ell}\right) \,, \tag{3.1.9a}$$
$$L_M = k^2 \left(1 - \frac{r_s}{\ell}\right) r_s \,. \tag{3.1.9b}$$

The signature of this space-time should be commented on, although it is not the key part of this discussion. When the source is larger than the Schwarzschild radius, $0 < r_s < \ell$, then the interior solution is $A = 1, B = b > 0$, i.e. normal flat space-time. The signature is $-+++$ for all r. When the source is smaller than the Schwarzschild radius, $0 < \ell < r_s$, there is a horizon s.t. the signature is $-+++$ for $r_s < r$, and then $+-++$ for $\ell < r < r_s$. However, then at $r = \ell$, as

stated already B is continuous (and non-zero) but A has a step. This step will actually change the sign of A to its positive interior value of 1. We see from (3.1.9a) that $B_{\text{in}} = b < 0$ and from (3.1.9b) that $L_M < 0$. So we find that inside the source, for $0 < r < \ell < r_s$, that the signature is $++++$. This is not so strange in the context of the static symmetry. The source is inside the horizon, so t is a space-like coordinate, but the source is static so it is in fact tachyonic, hence the strange interior metric signature and the negative mass L_M. The higher derivative theory will avoid this peculiarity because A and B are continuous across the shell radius, and so we expect a $-+++$ signature for all r.

The key part of this discussion is that the interior free parameter b blows up as ℓ^{-1} as the source is shrunk toward the origin. When one is using series solutions, expanded around the $r = 0$, we shall have to deal with the limit $\ell \to 0$, and we shall have to allow interior free parameters to behave in this way.

3.1.2.2 Coupling in general relativity using a series solution

We repeat the coupling calculation for GR, this time using series solutions instead of the closed-form solutions, to mimic the circumstances of the higher-derivative theory.

If one solved the equations of motion of general relativity using a Frobenius ansatz one would find two solution families. The first is a vacuum solution, suitable for putting inside the spherical shell, of the $(0,0)_0$ form:

$$A_{(0,0)_0} = 1 + \dots \tag{3.1.10a}$$

$$B_{(0,0)_0} = b + \dots \ . \tag{3.1.10b}$$

The second is a non-vacuum solution of the $(1,-1)_0$ form, corresponding to the Schwarzschild solution.

$$A_{(1,-1)_0} = xr - x^2r^2 + x^3r^3 - x^4r^4 + O(r^5) \tag{3.1.11a}$$

$$B_{(1,-1)_0} = \frac{y}{r} + xy + \dots \ . \tag{3.1.11b}$$

We shall place this solution outside the spherical shell source and solve the matching conditions (3.1.6). We shall find we need to allow the free parameters to depend on the shell size ℓ, $(x(\ell), y(\ell), b(\ell))$. The exterior free parameters will simply be Taylor series in ℓ so that as we shrink the source they remain finite and preserve the $(1,-1)_0$ form.

$$x(\ell) = x(0) + \ell x'(0) + \frac{1}{2}\ell^2 x''(0) + \dots \tag{3.1.12a}$$

$$y(\ell) = y(0) + \ell y'(0) + \frac{1}{2}\ell^2 y''(0) + \dots \ , \tag{3.1.12b}$$

whereas we take inspiration from the analytic solution of the previous section and allow b and L_M to be Laurent series in ℓ.

$$b = \ell^a \left(b_0 + b_1\ell + b_2\ell^2 + b_3\ell^3 + \dots\right) \tag{3.1.13a}$$

$$L_M = \ell^d \left(L_0 + \ell L_1 + \ell^2 L_2 + \ell^3 L_3 + \dots\right) \ , \tag{3.1.13b}$$

and we shall find that the poles should be $a = -1,\ d = -1$ for the coupling to work. Coupling the series solutions to the shell via (3.1.6) we find the solution:

$$\begin{aligned} y(\ell) =& -L_M(\ell)\left(\ell x(\ell) - \ell^2 x(\ell)^2 + O\left(\ell^3\right)\right) \\ =& -L_0 x(0) + \ell\left(L_0\left(x(0)^2 - x'(0)\right) - L_1 x(0)\right) + O\left(\ell^2\right) \end{aligned} \tag{3.1.14a}$$

$$\begin{aligned} b(\ell) =& -L_M(\ell)x(\ell) + O\left(\ell^3\right) \\ =& -\frac{L_0 x(0)}{\ell} + \left(-L_0 x'(0) - L_1 x(0)\right) + \frac{1}{2}\ell\left(-L_0 x''(0) - 2L_1 x'(0) - 2L_2 x(0)\right) + O\left(\ell^2\right) \ . \end{aligned} \tag{3.1.14b}$$

We see that we are solving for combinations of L_n and $x^{(m)}(0)$, so there is some extra freedom beyond what is needed for the matching. To understand this recall that for the purposes of understanding the situation in the higher-derivative theory, we are pretending that we do not know the exact forms of the interior and exterior solutions of the metric. The coupling conditions (3.1.6) do not make reference to the Schwarzschild radius. Holding r_s constant for all ℓ will completely specify $L_M(\ell)$ and $x(\ell)$. If we compare (3.1.14) to the closed-form solution (3.1.9a), (3.1.9b) and (3.1.8), where we held r_s fixed for all ℓ, we find they are of the same form, and we find agreement in the leading order for $x(0) = -\frac{1}{r_s}$ and $L_0 = -k^2 r_s^2$. Going to higher and higher orders in ℓ will gradually reveal the closed-form solution for all ℓ with the values $x(\ell) = -\frac{1}{r_s}$ and $L_M(\ell) = k^2\left(1 - \frac{r_s}{\ell}\right) r_s$.

3.1.2.3 Coupling in the higher-derivative theory

We now consider coupling a thin shell source described by (3.1.1). We describe the region interior to the shell with the $(0,0)_0$ family (2.2.2), which is the vacuum family as discussed in section 2.2.1.1. As argued in section 3.1.1 we want to see if it is possible to place the $(2,2)_0$ family outside the shell. In order to avoid confusion with re-use of a_n, b_m notation we shall write the exterior solution with w_n, v_m as

$$A = r^2 w_2 + \frac{r^3 v_3 w_2}{v_2} - \frac{r^4\left(w_2\left(2v_2\left(v_2 w_2 - 4v_4\right) + v_3^2\right)\right)}{6v_2^2} + r^5 w_5 + O(r^6)\,, \tag{3.1.15a}$$

$$B = r^2 v_2 + r^3 v_3 + r^4 v_4 + r^5 v_5 + O(r^6)\ . \tag{3.1.15b}$$

We presented the coupling scheme we intend to use in equations (3.1.3) and (3.1.4). The key problem we shall encounter is exemplified by the continuity of A at $r = \ell$. For a very small shell the interior solution is described by $(0,0)_0$ and therefore $A \sim 1$, whereas just outside in the $(2,2)_0$ family $A(\ell_+) \sim \ell^2 \sim 0$. There are similar problems in the other continuity conditions but we shall focus on this example. The resolution is in the same spirit as in the general relativistic example, where we saw in (3.1.9a) that the free parameters of the interior metric can be diverging functions of ℓ.

To proceed we will need a formula to understand the progression of terms in the $(0,0)_0$ series. Inspecting the full form of the series up to 14 orders one finds that the metric is of the form

$$A = 1 + a_2 r^2 + \sum_{n,p,q,m} X_{n,p,m,q}\ r^n \left(\frac{\gamma}{\beta}\right)^{\frac{n}{2}-p} a_2^m b_2^{p-m} \left(\frac{\beta}{\alpha}\right)^q \tag{3.1.16a}$$

$$\frac{B}{b_0} = 1 + b_2 r^2 + \sum_{n,p,q,m} Y_{n,p,m,q}\ r^n \left(\frac{\gamma}{\beta}\right)^{\frac{n}{2}-p} a_2^m b_2^{p-m} \left(\frac{\beta}{\alpha}\right)^q , \tag{3.1.16b}$$

where the $X_{n,p,m,q}$ and $Y_{n,p,m,q}$ are rational numbers and the n,p,q,m sums are taken over $n = 4,6,8,\ldots$; $1 \le p \le \frac{n}{2}$; $0 \le q \le \frac{n}{2} - 1$ and $0 \le m \le p$. Using this it can be shown that the free parameters should be written as functions of ℓ with the following scheme:

$$\begin{aligned} b_0 &= \ell^2 H_0(\ell)\,, & w_2 &= w_2(\ell)\,,\\ a_2 &= \ell^{-2} G_2(\ell)\,, & v_2 &= v_2(\ell)\,,\\ b_2 &= \ell^{-2} F_2(\ell)\,, & v_3 &= v_3(\ell)\,,\\ & & v_4 &= v_4(\ell)\,,\\ & & w_5 &= w_5(\ell)\,,\\ M &= \ell^d \mu(\ell)\,, & v_5 &= v_5(\ell)\,, \end{aligned}$$

where the functions of ℓ are all understood to be Taylor series, i.e. the poles have been made explicit. Specifically a_2 and b_2 should diverge as ℓ^{-2}. The ℓ-power of the leading order of M has not been determined.

For continuity of A, i.e. $A_{\text{in}}(\ell_-) = A_{\text{out}}(\ell_+)$, we need to evaluate the series (3.1.16) at $r = \ell$:

$$A_{\text{in}}(\ell_-) = 1 + G_2(\ell) + \sum_{k,n,q,m} \ell^k \left(\frac{\gamma}{\beta}\right)^{\frac{1}{2}k} X_{n,\frac{n-k}{2},m,q}\, G_2(\ell)^m F_2(\ell)^{\frac{n-k}{2}-m} \left(\frac{\beta}{\alpha}\right)^q , \tag{3.1.17}$$

where the sum is taken over $k = 0,2,4,6,\ldots$; $k+2 \le n = 4,6,8,\ldots$; $0 \le q \le \frac{n}{2} - 1$ and $0 \le m \le \frac{n-k}{2}$. Thus $A_{\text{in}}(\ell_-)$ goes as $A_0 + O(\ell^1)$, whereas $A_{\text{out}}(\ell_+)$ goes as ℓ^2. Solving the equation for all ℓ requires that A_0, defined as the coefficient of the ℓ^0 term in $A_{\text{in}}(\ell_-)$, should

vanish:

$$A_0 = 1 + G_2(0) + \sum_{n,q,m} X_{n,\frac{n}{2},m,q}\, G_2(0)^m F_2(0)^{\frac{n}{2}-m} \left(\frac{\beta}{\alpha}\right)^q , \tag{3.1.18}$$

where the sum is taken for $n = 4, 6, 8, \ldots$; $0 \leq q \leq \frac{n}{2} - 1$ and $0 \leq m \leq \frac{n}{2}$. We need this sum to converge, so that the coupling could be done with a finite-length series solution, and it must in fact converge to zero. We have not comprehensively studied the convergence properties, but have considered the simpler limit $\beta << \alpha$. In this limit, the $q \geq 1$ terms are suppressed and we need only consider $X_{n,\frac{n}{2},m,0}$. Of the coefficients appearing in this series, the $X_{n,\frac{n}{2},\frac{n}{2},0}$ equal 1 for all n while the other coefficients $X_{n,\frac{n}{2},m\leq\frac{n}{2}-1,0}$ appear to grow at most linearly with n (for at least $n \leq 14$). Let us rename $t = \frac{1}{2}n$, $X_{n,\frac{n}{2},m,0} = X_{t,m}$ and $G_2(0) = \zeta F_2(0)$ and consider only the first T terms. We get

$$A_0 = 1 + \sum_{\substack{t=1,2,3,4,\ldots T \\ 0\leq m\leq t}} X_{t,m}\, \zeta^m F_2(0)^t . \tag{3.1.19}$$

Assuming that the $X_{t,m}$ grow with t at most linearly we can estimate the sum A_0 by writing $X_{t,m} = a + bt$. For the estimate $\tilde{A}_0$:

$$\tilde{A}_0 = 1 + \sum_{t=1,2,3,4,\ldots T} (a + bt)\, \frac{1 - \zeta^{t+1}}{1 - \zeta} F_2(0)^t , \tag{3.1.20}$$

which has a ratio of terms at large t

$$\frac{a + b + bt}{a + bt}\ \frac{F_2(0)^{t+1}}{F_2(0)^t}\ \frac{1 - \zeta^{t+2}}{1 - \zeta^{t+1}} \sim \begin{cases} F_2(0), & |\zeta| < 1 \\ \zeta F_2(0) = G_2(0), & |\zeta| > 1 \end{cases} . \tag{3.1.21}$$

Thus the series converges if $|G_2(0)| < 1$ and $|F_2(0)| < 1$. One would expect that the series converges outside the $\beta << \alpha$ limit too. So one needs to know many terms in the $(0,0)_0$ series and also needs to deal with the matching of $\ell^{N\geq 1}$ terms and the matching of $A'(\ell), B(\ell), B'(\ell), B''(\ell), A''(\ell)$. We are encouraged by the $\tilde{A}_0$ result and expect that this could succeed if the computational difficulty was overcome. This would end with a solution for the interior and exterior metric written in terms of $\alpha, \beta, \gamma, L_M(\ell)$ and three other free parameters $p_1(\ell), p_2(\ell), p_3(\ell)$.

3.2 Global structure of black hole solutions

Possibly the most important question about any modified theory of gravity is : how do the black holes change? In this section we consider the global properties of black hole solutions, meaning the properties of the solutions that cover all r. Let us recap some of what we already know from analyses already done and see how much we can deduce from them, and afterwards build on them with new analyses.

The defining feature of black holes is that they have a horizon. We have already seen the family of solutions around a horizon, the $(1,1)_{r_0}$ family, in section 2.4.1.2. By the theorem (2.1.6) we saw that asymptotically flat solutions in this family must have $R = 0 \Leftrightarrow \beta = 0$. We can count parameters and constraints in this family to learn a lot about the global properties of the black hole solutions. Compare the $(1,1)_{r_0}$ family in expansions around r_0 (2.4.10), to the $(1,-1)_0$ family around the origin (2.2.6), for the $\beta = 0$ theory. The $(1,1)_{r_0}$ family has 2+1 free parameters and certainly contains the 2-parameter Schwarzschild black hole solution. It has a horizon in half of its 3d parameter space (f_1 finite, $r_0 > 0$, $b_1 \neq 0$). The $(1,-1)_0$ family also has 2+1 free parameters and also certainly contains the (1+1)-parameter Schwarzschild solution. The Schwarzschild family has a horizon for all values of the free parameter describing time-scaling and all positive values of the horizon radius r_0. Therefore in the $(1,-1)_0$ family there is a half-plane of parameter space, $r_0 > 0$, where the solution has a horizon. Considering the third free parameter, we consider it reasonable that the horizon exists not only in this half-plane but in an open 3-dimensional volume of the parameter space. If that is true then both $(1,-1)_0$ and $(1,1)_{r_0}$ have horizons in open 3d regions of their parameter spaces, both of which contain the half-plane of the Schwarzschild solution. Therefore we suppose further that these two asymptotic solution families are different descriptions of the same true solution family. This argument connects the $(1,1)_{r_0}$ family with the origin.

We can make some connection between the $(1,1)_{r_0}$ family and infinity $r \to \infty$. Consider the $(1,1)_{r_0}$ family for $\beta \neq 0$, (2.4.8) and define a reparameterisation:

$$\begin{aligned} \Delta f_2 &:= f_2 - \tilde{f}_2 \\ \tilde{f}_2 &:= \frac{3\gamma}{8\alpha} - \frac{3\gamma}{8\alpha f_1 r_0} - \frac{2f_1}{r_0} + \frac{1}{r_0^2} \,. \end{aligned}$$

We established in section 2.4.1.2 that asymptotic flatness implies that $\Delta f_2 = 0$ and $R = 0$, so it is clear that Δf_2 corresponds to the asymptotic non-flatness parameter C_{0+} from the linearised theory (2.3.5). We see that the $(1,-1)_0 \Leftrightarrow (1,1)_{r_0}$ family loses, one, not two, free parameters when going from the $\beta \neq 0$ theory to the $\beta = 0$ theory, so we conclude that it has no separate parameter analogous to C_{0-} from the linearised theory (2.3.5). In the $\beta = 0$ theory the $(1,-1)_0 \Leftrightarrow (1,1)_{r_0}$ family has 2+1 free parameters, one more than the Schwarzschild solution.

We make the difference from Schwarzschild explicit by writing the reparameterisation

$$\Delta f_1 := f_1 - \tilde{f}_1$$
$$\tilde{f}_1 := \frac{1}{r_0}$$

where $\Delta f_1 = 0$ corresponds to the Schwarzschild solution (2.4.10). If we now make a comparison to the linearised theory again, note that in the $\beta = 0$ theory there are four free parameters $C, C_{2,0}, C_{2-}, C_{2+}$. In the $(1,1)_{r_0}$ family the free parameter b_1 is certainly analogous to C, since these describe time-scaling symmetry, and r_0 is analogous to $C_{2,0}$, since for Schwarzschild this is $r_0 \sim GM$, the mass of the solution. This suggests that the higher-derivative corrections C_{2-}, C_{2+} manifest as the single parameter Δf_1. We are particularly interested in how $\Delta f_1 \neq 0$ affects the asymptotic behaviour of the family. We certainly would imagine that $\Delta f_1 \neq 0$ will produce asymptotically non-flat solutions, but this is not necessarily the case and more analysis is needed. The key question about the global structure of the $(1,-1)_0 \Leftrightarrow (1,1)_{r_0}$ family is then: what asymptotically flat black hole solutions are there? In the remainder of this section we shall answer this question with a perturbative analysis and a numerical analysis. We shall find that when Δf_1 is small, it does control asymptotic non-flatness, but that a finite value of it can restore asymptotic flatness, i.e. that there are two asymptotically flat black hole solutions. They both have $R = 0 \Leftrightarrow \beta = 0$, and one has $\Delta f_1 = 0$, r_0 free, b_1 free, and the other has $\Delta f_1 = \Delta f_1(r_0)$, r_0 free, b_1 free.

3.2.1 Asymptotically flat perturbations from the Schwarzschild solution

We have established that in the higher derivative theory the family of black hole solutions is two parameters larger than the Schwarzschild family in GR. We wish to consider asymptotically flat solutions, so we set one of the parameters (Δf_2) to zero, or equivalently restrict consideration to the $\beta = 0$ theory. We are left with a solution space one parameter wider than the Schwarzschild solution. We wish to understand this solution space, and learn about the asymptotically flat solutions. We first study perturbations of the Schwarzschild solution.

Write the metric perturbations around the Schwarzschild solution as

$$f(r) = 1 - \frac{r_0}{r\left(1 + \epsilon Z_A(r)\right)} \tag{3.2.1a}$$
$$\frac{B(r)}{b_t} = 1 - \frac{r_0}{r\left(1 + \epsilon Z_B(r)\right)}\,, \tag{3.2.1b}$$

and we expand the equations of motion to first order in ϵ, giving us two coupled linear second-order ODEs in $Z_A(r)$ and $Z_B(r)$. These equations will have four solutions modes. We expect two solution modes to exist within the Schwarzschild solution, and two perturbations away from Schwarzschild. The two solution modes within Schwarzschild are shifts of r_0 and

changes of the time-scaling parameter. Solutions that shift r_0 look like

$$1 - \frac{r_0 + \delta r_0}{r} = 1 - \frac{r_0}{r\,(1 + \epsilon Z_A(r))} \tag{3.2.2a}$$

$$1 - \frac{r_0 + \delta r_0}{r} = 1 - \frac{r_0}{r\,(1 + \epsilon Z_B(r))} \tag{3.2.2b}$$

$$\therefore \epsilon Z_A(r) = \epsilon Z_B(r) = -\frac{\delta r_0}{r_0} = \text{constant}\,. \tag{3.2.2c}$$

Solutions that shift the time-scaling parameter look like

$$B = (b_t + \delta b_t)\left(1 - \frac{r_0}{r}\right) = b_t\left(1 - \frac{r_0}{r\,(1 + \epsilon Z_B(r))}\right) \tag{3.2.3a}$$

$$\therefore \epsilon Z_B = \frac{r - r_0}{r_0}\,\frac{\delta b_t}{b_t}$$

$$Z_B \propto (r - r_0) \qquad , \qquad Z_A = 0\,. \tag{3.2.3b}$$

The two remaining modes are away from Schwarzschild, but recall that the $(1,1)_{r_0}$ family has fewer free parameters than generic solutions to the $\beta = 0$ theory. The $(1,1)_{r_0}$ family only has 2+1 free parameters, 1+1 of which are Schwarzschild and one of which describes solutions different from Schwarzschild. So in effect, the condition that there be a horizon somewhere in the space is a one-parameter constraint on the generic solution. Therefore we expect that in the perturbations about Schwarzschild, described by two coupled linear second-order ODEs in $Z_A(r)$ and $Z_B(r)$, one of the solution modes must remove the horizon. From the table 2.2 (assuming it does in fact have a complete list of all solution families) we see that solution families with 4 (rather than 3) free parameters have $B(r \to r_0) \to$ const.. Looking for functions Z_B that have $B(r \to r_0) \to$ const., but discarding the mode (3.2.2), we find that the mode that removes the horizon has Z_B divergent for small $(r - r_0)$. Thus we already know a lot about what we will find in the solution space. There will be a mode where Z_B diverges at r_0, which we will discard, a mode like (3.2.2), which we will discard, and a mode like (3.2.3) which we will discard, and one remaining mode that we wish to study. Since we wish to discard the mode (3.2.3) it is convenient to take a superposition of the two coupled linear second-order ODEs that eliminates Z_B and leaves a linear ODE in Z_A alone.

By taking a suitable superposition of our two linear ODEs we can eliminate Z_B in this combination:

$$Z_B(r) - (r - r_0)Z_B'(r) = Z_A(r) + \frac{\alpha\left(-8r^2 + 16rr_0 - 9r_0^2\right)(r - r_0)Z_A'(r)}{2\gamma r^4 - 2\gamma r^3 r_0 - 4\alpha r r_0 + 5\alpha r_0^2} + \frac{2\alpha r(2r - 3r_0)(r - r_0)^2 Z_A''(r)}{2\gamma r^4 - 2\gamma r^3 r_0 - 4\alpha r r_0 + 5\alpha r_0^2}\,,$$

leaving us with an equation of motion that is a linear ODE in $Z_A'(r), Z_A''(r)$ and $Z_A'''(r)$. One of the solutions to this equation is obviously Z_A is constant, $Z_A = k$, which corresponds to

functions $Z_B = k + \text{const.}(r - r_0)$, which are our two Schwarzschild modes (3.2.2) and (3.2.3) which we want to discard. Thus the two Schwarzschild modes appear as the trivial solution to the linear ODE in $Z'_A(r), Z''_A(r), Z'''_A(r)$ and are easily dropped from consideration by looking for the non-trivial solutions. Define a function $Y(r)$ with

$$Z_A = \int^r \frac{Y(r')}{\omega(r')}\,\mathrm{d}r' \,, \tag{3.2.4}$$

where $\omega(r)$ is a function that we shall fix, to change the form of the ODE for Y to convenient forms. We now have a second-order linear ODE in $Y(r)$ whose two solutions describe the two perturbations away from Schwarzschild.

To write down the differential equation define a shorthand

$$\xi := \frac{\alpha}{\gamma r_0^2} = \frac{1}{2m_2^2 r_0^2} \,. \tag{3.2.5}$$

The differential equation we are studying is then

$$0 = h_0(r)Y(r) + h_1(r)Y'(r) + h_2(r)Y''(r) \,, \tag{3.2.6a}$$

where

$$\begin{aligned}
h_0 = {} & \omega(r)^2\left(2r^7 - r_0\left(2r^6 + \xi r_0\left(8r^5 + r_0\left(r_0\left(5r^3 + 4\xi r_0\left(8r^2 - 11r_0 r + 5r_0^2\right)\right) - 16r^4\right)\right)\right)\right) \\
& - \omega'(r)^2 4\xi r^2\left(r - r_0\right) r_0^2\left(2r^4 - 2r_0 r^3 - 4\xi r_0^3 r + 5\xi r_0^4\right) \\
& - \omega(r)\omega'(r) 4\xi r^2\left(2r - 3r_0\right) r_0^2\left(r^3 - r_0 r^2 + \xi r_0^3\right) \\
& + \omega(r)\omega''(r) 2\xi r^2\left(r - r_0\right) r_0^2\left(2r^4 - 2r_0 r^3 - 4\xi r_0^3 r + 5\xi r_0^4\right)
\end{aligned} \tag{3.2.6b}$$

$$\begin{aligned}
h_1 = {} & \omega(r)^2 4\xi r^2\left(2r - 3r_0\right) r_0^2\left(r^3 - r_0 r^2 + \xi r_0^3\right) \\
& + \omega(r)\omega'(r) 4\xi r^2\left(r - r_0\right) r_0^2\left(2r^4 - 2r_0 r^3 - 4\xi r_0^3 r + 5\xi r_0^4\right)
\end{aligned} \tag{3.2.6c}$$

$$h_2 = -\omega(r)^2 2\xi r^2\left(r - r_0\right) r_0^2\left(2r^4 - 2r_0 r^3 - 4\xi r_0^3 r + 5\xi r_0^4\right) \,. \tag{3.2.6d}$$

We shall solve this equation in two approximations, the large-r limit and the near-horizon limit, and to make it easier we choose $\omega(r) = 1$:

$$0 = h_0(r)Y(r) + h_1(r)Y'(r) + h_2(r)Y''(r) \tag{3.2.7a}$$

$$h_0 = 2r^7 - 2r_0 r^6 - 8\xi r_0^2 r^5 + 16\xi r_0^3 r^4 - 5\xi r_0^4 r^3 - 32\xi^2 r_0^5 r^2 + 44\xi^2 r_0^6 r - 20\xi^2 r_0^7 \tag{3.2.7b}$$

$$h_1 = 4\xi r^2\left(2r - 3r_0\right) r_0^2\left(r^3 - r_0 r^2 + \xi r_0^3\right) \tag{3.2.7c}$$

$$h_2 = -2\xi r^2\left(r - r_0\right) r_0^2\left(2r^4 - 2r_0 r^3 - 4\xi r_0^3 r + 5\xi r_0^4\right) \,. \tag{3.2.7d}$$

Let us solve this near the horizon, using Frobenius's method. Write $Y(r) = (r-r_0)^s \sum y_n (r-r_0)^n$. The leading order term is

$$-\frac{2\,\xi^2\, r_0^8\, s\,(s+1)\, y_0}{r-r_0} + O((r-r_0)^0)\ , \tag{3.2.8}$$

so we see that there are two roots, $s=0$ and $s=-1$. These roots differ by an integer so the solution is of the form (1.2.26). The larger root is $s=0$ so name the solution for the larger root Y_0:

$$Y_0(r) = \sum_{n=0} y_n (r-r_0)^n\ , \tag{3.2.9}$$

so that the full solution is

$$Y(r) = c_1 Y_0(r) + c_2 \left(Y_0(r)\ln(r-r_0) + \frac{1}{r-r_0}\sum_n y'_n (r-r_0)^n \right)\ , \tag{3.2.10}$$

where y'_n are some coefficients to be determined. We see that the second solution, controlled by c_2, is divergent, and it is clear that it corresponds to $Z_A \sim \ln(r-r_0)$ and $Z_B \sim (r-r_0)^{-2}$ both divergent, and thus corresponds to removing the horizon from the solution. Therefore we have found a two-parameter family of solutions, which is reduced to a one-parameter family after requiring the horizon to exist, which is as we predicted. Thus we have now established that we can eliminate all three modes that we wish to disregard, leaving only the fourth mode still to study.

Next we consider what behaviours exist at large r. In fact we already have the answer - in the large r limit the Schwarzschild solution that we are perturbing around becomes Minkowski, and we have already written down the large-r solutions of perturbations around Minkowski in equation (2.3.5). We write the $\beta = 0$ version of this solution here:

$$\begin{aligned} B = 1+V =& (1+C) + \frac{C_{2,0}}{r} + C_{2-}\frac{e^{-m_2 r}}{r} + C_{2+}\frac{e^{m_2 r}}{r} + O(\epsilon^2) \\ A = 1+W =& 1 - \frac{C_{2,0}}{r} - \frac{1}{2}C_{2-}\frac{e^{-m_2 r}}{r}(1+m_2 r) - \frac{1}{2}C_{2+}\frac{e^{m_2 r}}{r}(1-m_2 r) + O(\epsilon^2)\ , \end{aligned}$$

so we can find the large-r behaviour of Z_A and Z_B in terms of W and V:

$$\begin{aligned} A = \frac{1}{1-\frac{r_0}{r(1+\epsilon Z_A)}} &\approx \frac{r}{r-r_0}\left(1-\frac{r_0}{r-r_0}\epsilon Z_A\right) \\ \therefore \epsilon Z_A &\approx -\frac{r}{r_0}W(r) \\ Y = Z_A'(r) = &-\frac{1}{2}C_{2-}\frac{e^{-m_2 r}}{r_0}m_2^2 r - \frac{1}{2}C_{2+}\frac{e^{m_2 r}}{r_0}m_2^2 r \\ \frac{B}{b_t} = 1-\frac{r_0}{r(1+\epsilon Z_B)} &\approx 1-\frac{r_0}{r}+\frac{r_0}{r}\epsilon Z_B \\ \therefore \epsilon Z_B &\approx 1+\frac{r}{r_0}\,V|_{C=0} \\ &\approx \left(1+\frac{C_{2,0}}{r_0}\right)+C_{2-}\frac{e^{-m_2 r}}{r_0}+C_{2+}\frac{e^{+m_2 r}}{r_0}\,. \end{aligned} \tag{3.2.11}$$

Alternatively one can take the large-r behaviour only of h_0, h_1 and h_2 (3.2.7) and solve the simple resulting ODE to get

$$Y = \frac{\text{const.}}{m_2^{3/2}}\,e^{m_2 r}(1-m_2 r)+\frac{\text{const.}}{m_2^{3/2}}\,e^{-m_2 r}(1+m_2 r)\,, \tag{3.2.12}$$

which clearly agrees, for large-r, with the $Y = Z_A'$ expression obtained in (3.2.11). We see two behaviours: the $e^{-m_2 r}$ term describes asymptotically flat perturbations and the the $e^{m_2 r}$ term describes non-asymptotically flat perturbations. Generically, then, we expect that admissible perturbations would not be asymptotically flat, but it is possible that by excluding the three modes we've said that we are disregarding, we may have implicitly excluded the non-asymptotically flat perturbation. That is, it seems likely that the perturbations around the Schwarzschild solution are not asymptotically flat, but we have not yet proved it one way or the other. It was shown in [2] that if α satisfies an inequality we can write such a proof, a "no-hair" theorem that proves that the perturbations from Schwarzschild are not asymptotically flat, and we turn to that next.

Take the ODE equation (3.2.6) (for a general function $\omega(r)$ once more) and multiply it by $u(r)Y(r)$, and integrate it over r:

$$\begin{aligned} 0 &= \int_{r_0}^{\infty}\Big(h_0(r)Y(r)+h_1(r)Y'(r)+h_2(r)Y''(r)\Big)u(r)Y(r)\,\mathrm{dr} \\ &= \int_{r_0}^{\infty} uh_0Y^2-uh_2(Y')^2+(uh_2Y'Y)'+Y'Y(uh_1-u'h_2-uh_2')\;\mathrm{dr}\,. \end{aligned}$$

We choose a function $u(r)$ such that $(uh_1-u'h_2-uh_2')=0$ for convenience:

$$u(r) = \frac{\text{const.}\,(r-r_0)}{\left(2\,(r-r_0)\,r^4+\xi r_0^3\,(5r_0-4r)\,r\right)^2\omega(r)^4}\,, \tag{3.2.13}$$

which has no sign changes in $r_0 < r < \infty$ for any $\omega(r)$. Let us assume WLOG that $u(r)$ is positive. Recalling our assumption that Y is finite near r_0, we have that $uh_2Y'Y \sim \frac{(r-r_0)^2}{\omega(r)^2} \to 0$ so the boundary term does not contribute at the inner boundary. At large r it goes as $uh_2Y'Y \sim \frac{1}{m_2^2\, r^2\, \omega(r)^2} Y'Y$, and for asymptotically flat perturbations $Y'(r \to \infty) \to 0$ vanishes, so the boundary term does not contribute at the outer boundary either. So we establish, for functions $\omega(r)$ with suitable limits, that asymptotically flat perturbations about a horizon must satisfy the following equation:

$$0 = \int_{r_0}^{\infty} uh_0 Y^2 - uh_2 (Y')^2 \ \mathrm{dr} \ . \tag{3.2.14}$$

We have already said that $u(r)$ is positive, so if h_0 and h_2 have opposite signs then the integrand is positive-definite or negative-definite, so using this and the fact that the integral vanishes we could then prove that $Y(r) = 0 = Y'(r)$ throughout the integration region $r_0 < r < \infty$.

We want h_0 and h_2 to have no sign changes in the integration region. It is clear from (3.2.6d) that h_2 cannot be positive throughout the region $r > r_0$, but on the other hand if can be negative throughout all that region if

$$0 < \xi < \frac{27}{8} = 3.375 \ . \tag{3.2.15}$$

Therefore we consider the condition for h_0 to be positive. Positivity of (3.2.6b) is rather harder to prove than negativity of h_2. Transform the problem to new variables

$$r = r_0(1+x) \ , \qquad\qquad \xi = \frac{\xi_{\text{max}}}{1+y} \ ,$$

and require positivity of h_0 throughout the quadrant $x > 0, y > 0$, and find the largest value of ξ_{max} that our proof permits. With this substitution h_0 is

$$h_0 = \frac{\sum_{n=0}^{N} \sum_{m=0}^{M} C_{n,m}(r_0, \xi_{\text{max}})\, x^n y^m}{(1+y)^2} \ . \tag{3.2.16}$$

A sufficient condition for h_0 to be positive is then that $C_{n,m} \geq 0$ for all n, m. Let us initially consider the simple case $\omega(r) = 1$, where h_0 is given by (3.2.7b). In this case $C_{n,m} \geq 0$ reduces to $\xi_{\text{max}} < \frac{3}{8}$, and one can also show that this is not only a sufficient condition but also the necessary condition. We take the largest value $\xi_{\text{max}} = \frac{3}{8}$ and therefore write the bound on ξ to be:

$$0 < \xi < \frac{3}{8} \ . \tag{3.2.17}$$

At this point the function $\omega(r)$ becomes useful. By trying different functions in $\omega(r)$ in (3.2.4) and repeating the steps we can arrive at an equation of the same form but with different $C_{n,m}$, and the transformed condition $C_{n,m} \geq 0$, which is sufficient but not necessary, may allow greater values of ξ_{max}. In [2] the best function that was found is

$$\omega(r) = (c\, r_0^3 + r^3)^{1/3} \ , \tag{3.2.18}$$

where c can be varied to find an optimal value. This choice of ω allows a maximum value of ξ_{max} of

$$\begin{aligned}\xi_{\text{max}} &= \left[\text{the largest root of the equation:} \quad 0 = 28160x^4 + 12176x^3 - 43374x^2 + 19179x - 2322\right] \\ &\approx 0.626 \\ c &= \frac{3 - 4\xi_{\text{max}}}{8\xi_{\text{max}} - 3} \approx 0.246 \ .\end{aligned}$$

Numerical study could reduce this bound by considering the necessary condition rather than a sufficient one, and it may also be possible to increase the upper bound on ξ using other functions $\omega(r)$, all of which must be subject to the limit from considering h_2 (3.2.15).

The result we have established is that there are no asymptotically flat perturbations away from Schwarzschild if the horizon radius satisfies the inequality

$$\frac{\alpha}{\gamma r_0^2} \lesssim 0.626 \qquad \text{or equivalently} \qquad m_2\, r_0 \gtrsim 0.894 \ . \tag{3.2.19}$$

This immediately suggests three questions. One is: what happens when the r_0 saturates this inequality? The Schwarzschild solution might not be isolated around that point. The second is: what happens for small r_0 violating this inequality? We have tried but have not been able to prove anything about that region, which may be because the situation is different there. The third is: what about solutions with horizons that are *finitely* different from Schwarzschild? To answer this last question we must now turn to a numerical analysis, and in doing so we shall answer the other two questions as well.

3.2.2 Numerical study of solutions with horizons

To learn about solutions finitely different from the Schwarzschild solution we shall have to resort to a numerical analysis. We remain in the $\beta = 0$ theory and fix the numerical values of some of the free parameters in this description:

$$\gamma = 1 \tag{3.2.20a}$$
$$\alpha = \frac{1}{2} \tag{3.2.20b}$$
$$(\therefore\, m_2 = 1) \tag{3.2.20c}$$
$$b_1 = 1 \tag{3.2.20d}$$
$$f_1 = \frac{1+\phi}{r_0} \tag{3.2.20e}$$
$$r_0, \phi \text{ left free} \ .$$

We shall study different values of r_0, and for each one vary ϕ such that when we numerically shoot outwards from the horizon we reach an asymptotically flat solution. We shall shoot from $r_0 \times 1.01$, using values for A, A', B, B' given by (2.4.10) to 9 orders, and shoot outwards to $r \approx 30$ or $r \approx 20$.

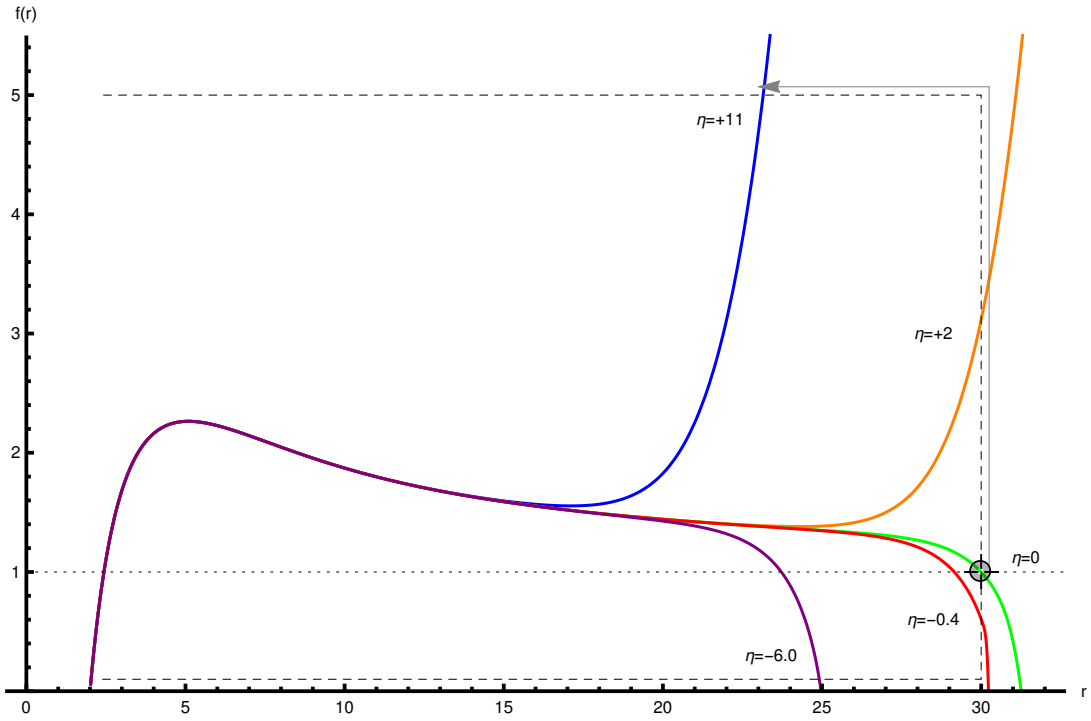

FIGURE 3.1: Illustration of how a score η is assigned to a solution $f(r)$. Five example curves are shown, for $r_0 = 2$, with ϕ in the range $5.0844594 < \phi < 5.0844617$, each labelled with their score $\eta[f(r)]$. Curves that grow too large or small before reaching the right-hand boundary are given a score that is the distance around the edge of the box to the intersection with the curve, illustrated for the $\eta = 11$ curve with an arrow.

To find the asymptotically flat solutions we shall assign each solution a flatness score $\eta[f(r)]$. Working with a numerical solution covering the region $r_0 < r < r_{\text{max}}$, we analyse the region $1.2r_0 < r < r_{\text{max}}$, and there are two cases. The first case is that f doesn't get very large or very small, $0.1 < f(r) < 5$, and the score is simply $f(r_{\text{max}}) - 1$. The second case is that f becomes too large or too small at some radius r_1, in which case the score is $\pm(r_{\text{max}} - r_1) + \text{const.}$ where the $\pm$ is such that too-large curves have positive score and too-small curves have negative score, and the constant is chosen so that $\eta[f(r)]$ is smooth. A diagram showing some example solutions annotated with these requirements is shown in fig 3.1. For each radius r_0 of black hole we can vary ϕ and observe how the score, η, changes. We expect that for every r_0 there will be some values of ϕ that cause the score to vanish. We know to expect that $\phi \approx 0$ will be asymptotically flat, with zero score, because it will be the Schwarzschild solution. In fact we shall find there is another asymptotically flat solution. Let us call the two values of ϕ that correspond to asymptotically flat solutions ϕ_0, where this should be Schwarzschild $\phi_0(r_0) \approx 0$,

and $\phi_1(r_0)$, where this is another solution, $|\phi_1| > |\phi_0|$. Then $\eta(\phi_0(r_0)) = 0$ and $\eta(\phi_1(r_0)) = 0$. In practice, since this will be done numerically, we shall not obtain exact zeroes of the score, nor shall we find that $\phi_0 = 0$ exactly.

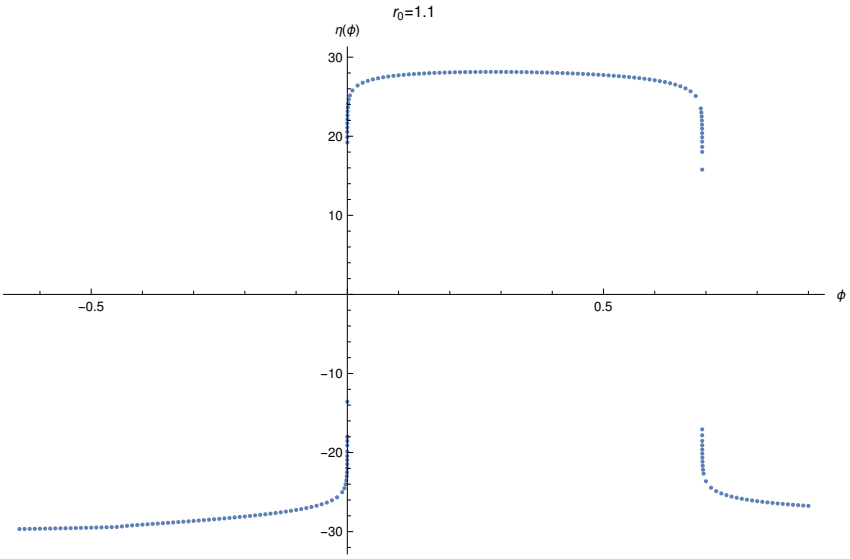

FIGURE 3.2: The asymptotic-flatness score η as a function of ϕ for $r_0 = 1.1$, clearly showing two zeroes and indicating a second type of black hole for positive ϕ.

Let us understand the system and the score using two examples. We shoot outwards from a black hole of radius 1.1, varying the parameter ϕ, and obtaining the score for each space-time, and plot the results in figure 3.2. The plot shows negative score for $\phi \lesssim 0$, positive score for $0 \lesssim \phi \lesssim 0.7$, and negative score again for $\phi \gtrsim 0.7$, clearly showing that there are *two* zeroes, i.e. two asymptotically flat black hole solutions. The scores $\eta(\phi)$ are typically large in magnitude, indicating that $f(r)$ becomes large or small very close to the horizon. Around the two zeroes of $\eta(\phi)$ the gradient is very steep, indicating that ϕ has to be extremely finely tuned to find the asymptotically flat solutions, and this was troublesome throughout the numerical work. Next, we shoot outwards from a horizon of a smaller radius, $r_0 = 0.7$, and plot the scores $\eta(\phi)$ in figure 3.3. The plot shows similar characteristics, except that the second zero now occurs for negative $\phi \approx -0.4$. We shall see later that for some range of r_0 the function $\eta(\phi)$ passes so steeply through a zero that we can only put a bound on the ϕ value of that zero, but cannot find the solution itself. When discussing the properties of the asymptotically flat solutions we are forced to restrict consideration to r_0 outside that range.

The graphs of $\eta(\phi)$ for these two radii are typical of those of other radii as well. All have a rough top-hat shape of varying width, with two zeroes. We expect there to be a degenerate top-hat shape, where the width vanishes and the two zeroes coincide. We used an automatic routine to search for $\phi_1(r_0)$ and $\phi_0(r_0)$, and obtain approximations to them (note that we do not require perfect flatness, but admit space-times with $-6 < \eta(\phi_1) < 11$ for ϕ_1 and $-3 < \eta(\phi_0) < 3$

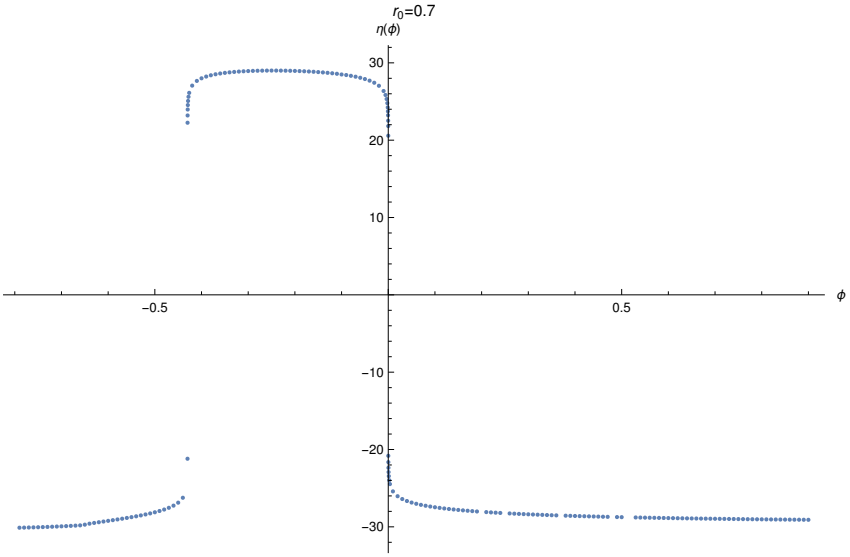

FIGURE 3.3: The asymptotic-flatness score η as a function of ϕ for $r_0 = 0.7$, clearly showing two zeroes and indicating a second type of black hole for negative ϕ.

for ϕ_0). We plot the so-obtained values of ϕ_0 and ϕ_1 as a function of r_0 in figure 3.4. The ϕ_0 values are not exactly zero but are of order 10^{-5} and 10^{-6}, reflecting the small inaccuracies inherent in numerical work, and seemingly have a random distribution in r_0, as can be seen from a plot of them on an expanded scale in figure 3.5. It was not possible to obtain values of ϕ_1 for horizon radii $r_0 \lesssim 0.58$ because the solutions become extremely sensitive to the value of ϕ, being extremely non-flat for tiny deviations from ϕ_0 or ϕ_1, and do not yield easily to analysis, not even to assigning a score. The minimum value of ϕ_1 that we found is ≈ -0.66, and we note from equation (3.2.20e) that as $\phi \to -1$ then $f_1 \to 0$, but since we know from our indicial treatment that $f_1 = 0$ is not a solution, then perhaps it is not surprising that there are problems probing this regime numerically.

The key result is that there are two asymptotically flat black hole solutions, at all values of $0.6 \lesssim r_0 \lesssim 2$ except one. Polynomial fits of $\phi_1(r_0)$ can find the point where it vanishes, and at this point $\phi_1 \approx \phi_0$ and there is only a single asymptotically flat solution. This coincidence point is at

$$r_0 \approx 0.876\,. \tag{3.2.21}$$

The next thing to do is to look at the properties of the new black holes, and to match their large-radius behaviour to the linearised theory. This is most conveniently done for $B(r)$, since it includes all four parameters, and for Schwarzschild solutions the linearised solution for B is also the exact solution. We write the linearised theory solution for B as

$$B \approx C_t \left(1 + \frac{C_{2,0}}{r} + C_{2-}\frac{e^{-m_2 r}}{r} + C_{2+}\frac{e^{m_2 r}}{r}\right)\,, \tag{3.2.22}$$

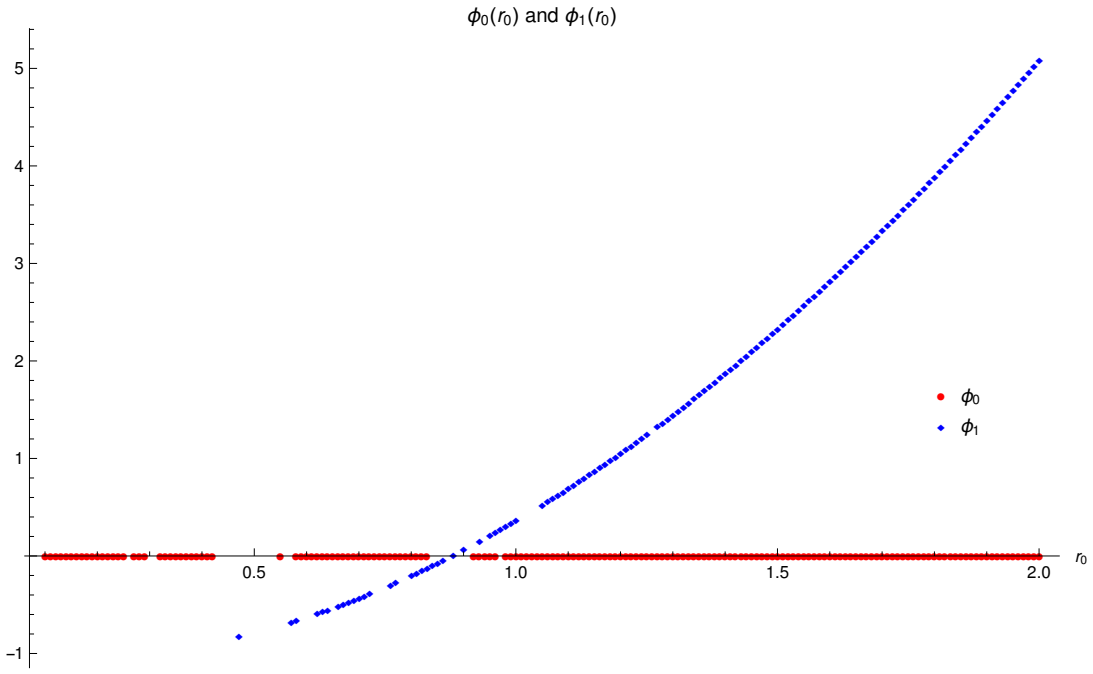

FIGURE 3.4: The values of ϕ that produce asymptotically flat solutions as a function of horizon radius r_0, showing two values: the $\phi_0(r) \approx 0$ Schwarzschild solution and a second curve $\phi_1(r)$ that intersects at $r_0 \approx 0.876$.

where the time-scaling has been made exact using C_t (instead of using the perturbative treatment with C as in (2.3.5)) By correspondence with GR, in these units ($\beta = 0, \alpha = \frac{1}{2}, \gamma = 1$),

$$GM = -\frac{1}{2}C_{2,0} \, . \tag{3.2.23}$$

Let us first discuss what we expect to find. Since we are considering approximately asymptotically flat solutions, we hope to find small values for C_{2+}. For Schwarzschild black holes this linearised expression has $C_{2-} = 0 = C_{2+}$ and is exact for all radii. The new black holes are distinct from Schwarzschild, and the only parameter available to describe this distinction is C_{2-}, so we expect that they will have non-zero values of C_{2-}. Now let us turn to our numerical results and see if they agree. We numerically find the new black holes for $r_0 < r < 30$ and the Schwarzschild black holes for $r_0 < r < 20$, where these ranges have been chosen to be as large as possible while keeping the maximum gradient of $\eta(\phi)$ small enough to allow its roots to be found. We fit the $B(r)$ from the approximately asymptotically-flat numerical solutions to the $B(r)$ from the linearised theory, and obtain values for C_t, C_{2-}, C_{2+} and GM. The values of C_t, C_{2-}, C_{2+} for the Schwarzschild branch and the new black hole branch are plotted in figure 3.6 . The values of C_{2+} are tiny, as intended, and are not clearly grouped, reflecting that we intend to use only results with $C_{2+} = 0$, but numerical issues cause random variations around 0. The values of C_{2-} for the Schwarzschild black holes are also small, of order 10^{-2} or 10^{-1}, as they should be, while for the new black holes the C_{2-} are of order 10^3, in line with what was expected. The values of C_{2-} do not form a neat line because the fitting procedure

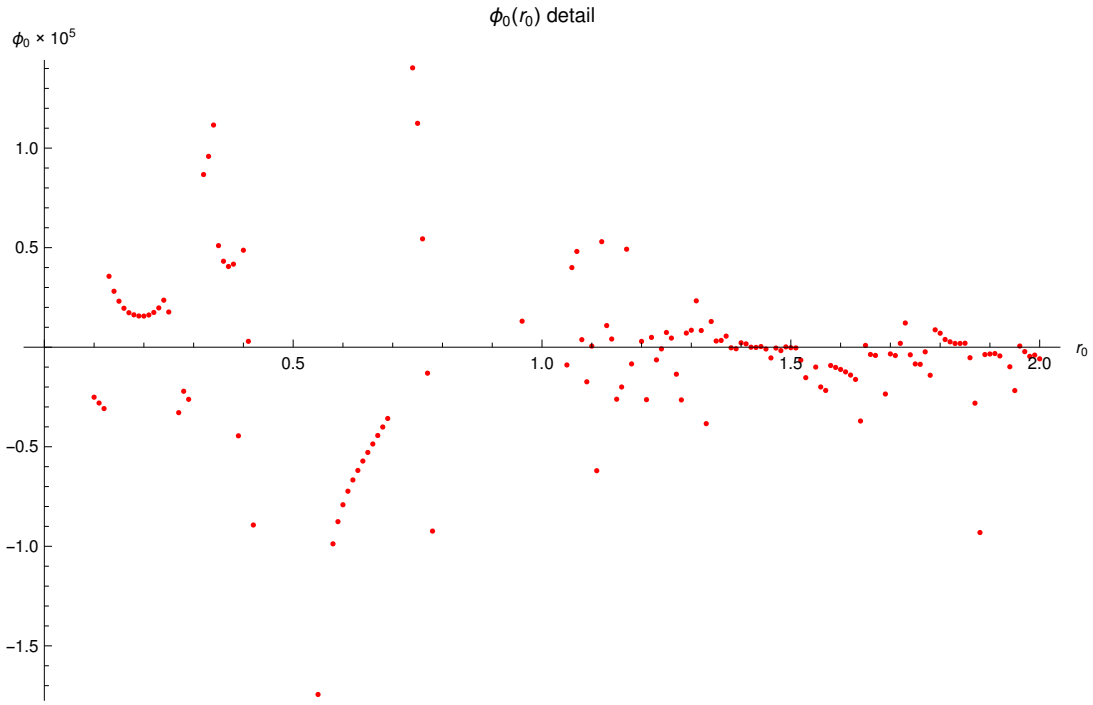

FIGURE 3.5: Detail of the values $\phi_0(r)$ of the Schwarzschild solutions. If the method was perfect these values would all be exactly zero, so their non-zero values of order 10^{-5} give us an indication of the method's accuracy. The intermittent patterns that are visible are assumed to be artefacts of the algorithms used.

is not well sensitive to this parameter, because the term it controls ($\frac{e^{-r}}{r}$) is small in the large-r region where the fitting takes place. The masses GM of the two branches are plotted together in figure 3.7, along with a line showing the ideal Schwarzschild relation $r_0 = 2GM$. The found values $GM(r_0)$ on the Schwarzschild branch deviate from the ideal line by an amount of order 10^{-5}, showing good agreement. This deviation of the numerical Schwarzschild black holes from the ideal results is assumed to be purely due to inaccuracies of the method (and not to be a physical result) and gives us a rough estimate of those inaccuracies.

The horizon radius $r_0 \approx 0.876$ at which the Schwarzschild black hole and new black hole coincide compares well with the best bound (3.2.19) we obtained from the perturbative treatment (recall we used $m_2^2 = 1$ for the numerics), which is close and slightly larger. It seems that the bound we obtained is no accident, that in fact it is reflecting the existence of the coincidence point. By optimising the choice of function ω in (3.2.4) we could presumably improve the bound (3.2.19) slightly to eventually obtain

$$m_2\, r_0 \gtrsim 0.876\ . \tag{3.2.24}$$

When this bound is saturated there is a crossing point where the Schwarzschild black hole is not isolated from the new black hole. When r_0 violates this bound we see that the Schwarzschild

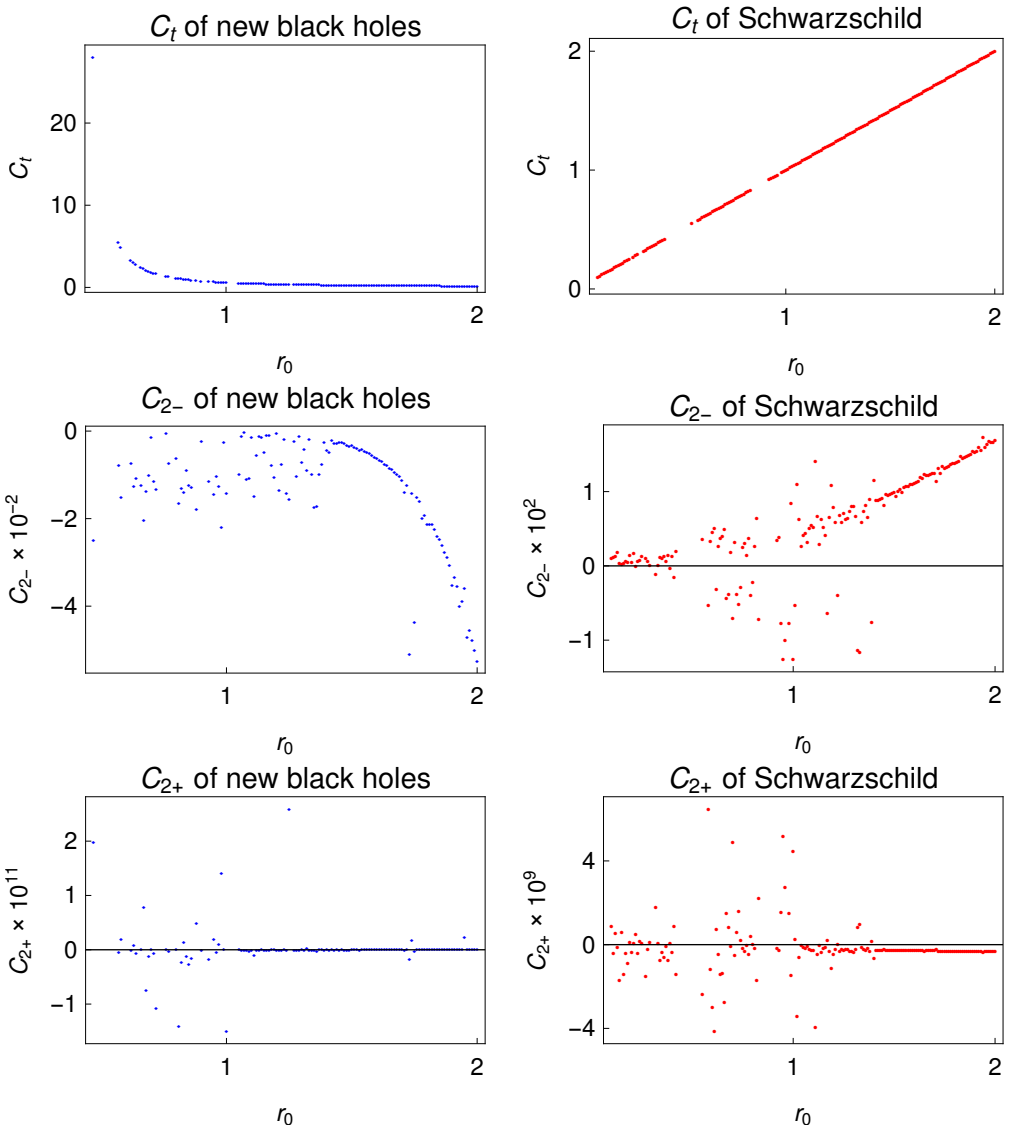

FIGURE 3.6: The values of the C_{2-}, C_{2+} and C_t found when fitting the two types of numerical black hole to the linearised theory as written in equation (3.2.22).

solution becomes isolated again, and the new black hole becomes distinct again. The most notable feature of the new black holes is that as well as existing with a positive mass, they also exist with a negative mass. Negative-mass new black holes appear in the approximate range $r_0 \gtrsim 1.141$, and restoring the dimensions we write the negative mass range as:

$$m_2\, r_0 \gtrsim 1.141$$
$$\phi_1 \gtrsim 0.837\ .$$

We can comment on how realistic these solutions are by considering the curvature scalar $R_{\mu\nu}R^{\mu\nu}$. The numerical solutions of the new black hole show that the curvature reduces to ≈ 0 at large r as expected. The value of the curvature at the horizon may not be the maximum

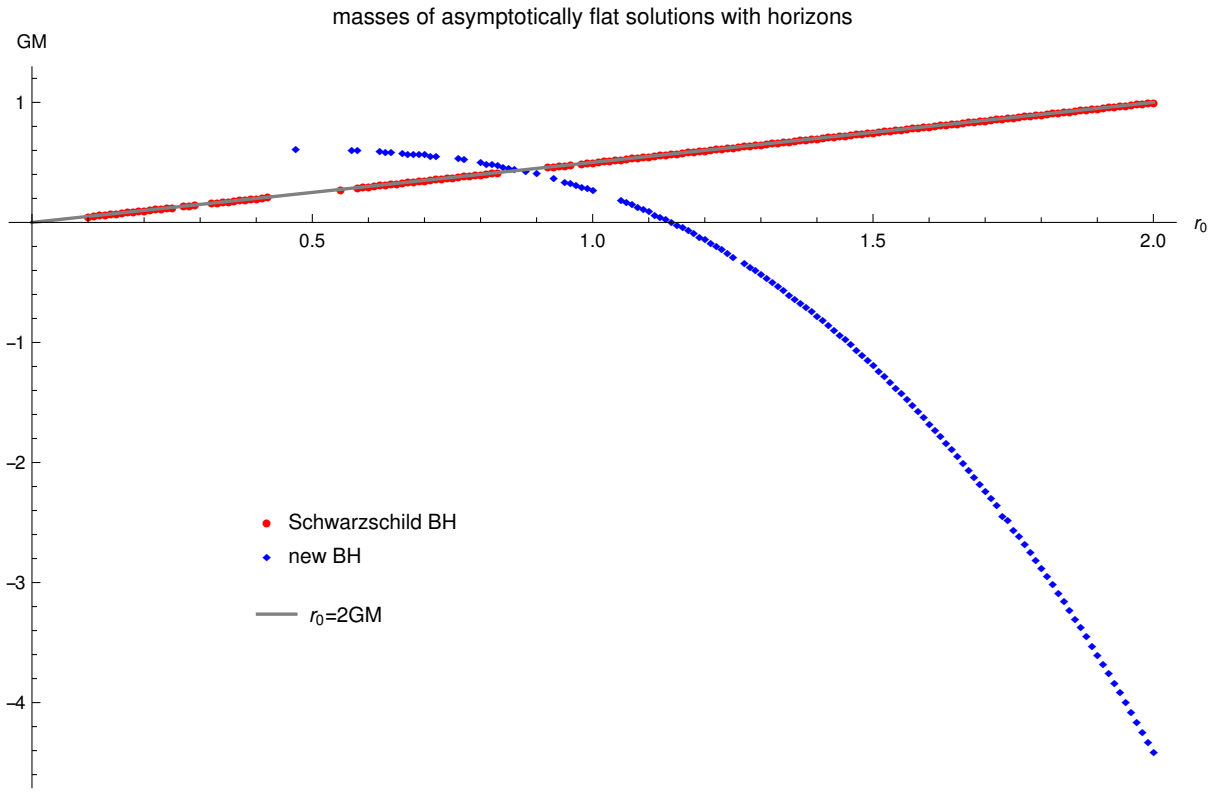

FIGURE 3.7: The values of the mass found when fitting the two types of numerical black hole to the linearised theory as written in equation (3.2.22). The curves intersect at $r_0 \approx 0.876$ and negative masses appear for $r_0 \gtrsim 1.141$.

curvature of the space-time, but gives us some indication and is easy to evaluate. Using the series expansion (2.4.10), we find that the value of the curvature near the horizon is given by

$$\frac{1}{\gamma^2} R_{\mu\nu} R^{\mu\nu} = \frac{4\phi^2}{\gamma^2 r_0^4} + O(r - r_0) \tag{3.2.25}$$

(for general values of the couplings). This indicates that if the parameter of the asymptotically flat solution $\phi_1(r_0, m_2)$ is of order $\frac{1}{2}\gamma r_0^2 = \alpha m_2^2 r_0^2$ then the curvature is large and higher-curvature terms might significantly affect the solutions. In our numerical results, the value of $\frac{4\phi_1^2}{r_0^4}$ takes its minimum, of zero, at the intersection point of the non-Schwarzschild and Schwarzschild black holes (as expected) and monotonically increases as one moves away from that point in either direction along the non-Schwarzschild black hole branch. Around the appearance of negative-mass solutions we have $\frac{4\phi_1^2}{r_0^4} \approx 1.6$, so if one considered corrections from even-higher derivative terms in the Lagrangian, it is likely that the negative-mass non-Schwarzschild black holes will change considerably or not appear, which chimes well with their arguably unphysical nature.

To give the reader some physical intuition about the new solutions we plot ones with positive, negative and zero mass in figure 3.8.

The thermodynamic properties of the new black holes were studied in [1] where it was

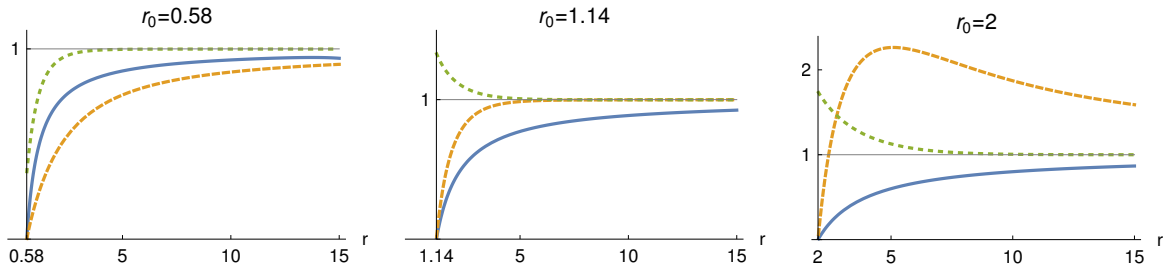

FIGURE 3.8: Comparison of the Schwarzschild black hole and the new black hole for three different radii. The solid blue line shows $f(r)$ of the Schwarzschild solution. The dashed orange line shows $f(r)$ of the new black hole solution. The dotted green line shows the ratio $\frac{B(r)}{f(r)}$ for the new black hole solution, scaled so that it approaches 1 at large radius. The $r_0 = 0.58$, $r_0 = 1.14$ and $r_0 = 2$ plots are for positive, $\approx$ zero and negative mass new black holes, respectively.

found that for a given mass the temperature of the non-Schwarzschild black holes is lower than the temperature of the Schwarzschild black hole, and conversely that for a given temperature the mass of the non-Schwarzschild black hole is lower than the mass of the Schwarzschild black hole. For a fixed mass below the coincidence mass ($GM_c \approx 0.44$) the non-Schwarzschild black hole has lower entropy than the Schwarzschild black hole, and for a fixed mass above the coincidence mass the non-Schwarzschild black hole has a greater entropy than the Schwarzschild black hole. An approximate relation for the masses and temperatures in terms of the Wald entropy, for small entropy, was found and the non-Schwarzschild black holes were seen to approximately obey the first law $\mathrm{dM} = \mathrm{TdS}$. The thermodynamical properties of the two types of black hole will be revisited in [54].

We note that the existence of a second branch of asymptotically flat black hole solutions was predicted earlier by Brian Whitt in [55]. He considered the equations of motion of fourth-order gravity in four dimensions, and studied perturbations around solutions to the Einstein equation $R_{\mu\nu} = 0$, with a view to determining their dynamic stability. We now know that static asymptotically flat solutions with horizons must have $R = 0$ and similarly that static asymptotically flat perturbation must also have $\delta R = 0$, so we consider only the Einstein-Weyl theory. Whitt did not know about this restriction and considered the general 4-dimensional theory and a governing equation that features both perturbations $\delta R_{\mu\nu}$ and perturbations δR. Fortunately, however, Whitt decided to study the part governing $\delta R_{\mu\nu}$ in isolation, as this is sufficient for the time-dependent discussion, which makes his analysis equivalent to ours. The governing equation of the perturbations is then found to be

$$\left((\Delta_{\mathrm{L}})_{\mu\alpha\nu\beta} + \frac{1}{\beta_{\mathrm{Whitt}}} g_{\mu\alpha} g_{\nu\beta} \right) \delta \bar{R}_{\mu\nu} = 0 \,, \tag{3.2.26}$$

where $\delta\bar{R}_{\mu\nu}$ is the traceless part s.t. $g^{\mu\nu}\delta\bar{R}_{\mu\nu} = 0$, and where his couplings are related to ours by

$$\alpha_{\text{Whitt}} = -\frac{3\beta + 2\alpha}{3\gamma} , \qquad \beta_{\text{Whitt}} = \frac{2\alpha}{\gamma} = \frac{1}{m_2^2} ,$$
$$\alpha = \frac{\gamma}{2}\beta_{\text{Whitt}} , \qquad \beta = -\frac{\gamma}{3}\left(\beta_{\text{Whitt}} + 3\alpha_{\text{Whitt}}\right) .$$

As a side note on the way to studying the dynamical stability, he noted that on the Schwarzschild background there exists a single normalizable static spherically symmetric perturbation. This was noted to indicate the existence of a second branch of spherically symmetric black hole solutions that intersects the Schwarzschild branch. The perturbation exists at $\frac{1}{\beta_{\text{Whitt}}} \approx \frac{0.19}{(GM)^2}$, which we translate to be in terms of horizon radius and our couplings to get

$$m_2 r_0 \approx 2\sqrt{0.19} \approx 0.87 , \tag{3.2.27}$$

and we see that this is in good agreement with our numerical result (3.2.21). While our numerical results are limited in what they can say, the calculation by Whitt provides an algebraic proof of the existence of the second branch. A detailed treatment of this bifurcation of black hole solutions, the dynamical stability of the two types of black holes, their thermodynamics and the relation between thermodynamics and stability will appear in [54].

3.3 Asymptotically flat numerical solutions

3.3.1 Method

Our goal has been to learn about the asymptotically flat solutions to higher derivative gravity. Our investigations so far have found that asymptotically flat solutions must have $R = 0$ if there is a horizon or if the behaviour near the origin is either vacuum ($(0, 0)_0$) or Schwarzschild-like ($(1, -1)_0$). The $R = 0$ case is thus seen to be important, but certain classes of asymptotically flat space-times, notably those with wormholes and those that have $(2, 2)_0$ behaviour near the origin, allow non-vanishing R. Our analyses using free parameter counts in the non-linear and linearised theories have indicated that solutions minimally coupled to matter are of the latter type, and need not have $R = 0$. The major missing component has been the relationships between behaviours near the origin, or near r_0, and behaviours near infinity. In particular we want to find an explicit example of a solution that is asymptotically flat, but has $(2, 2)_0$ behaviour near the origin, as a critical piece of evidence in our argument that matter-coupled solutions have those properties. In this section we use numerical shooting techniques to investigate the relationships between behaviours at large r and behaviours at smaller r. We shall find some agreement with results already obtained, albeit with significant difficulties with the accuracy of the numerical method, and some areas of disagreement. Ultimately we will conclude that the method is promising but more study is needed, and in particular it must address the accuracy issues.

We use numerical solutions to connect the origin and infinity, working in the $\beta = 0$ theory for simplicity. We fix the large-r behaviour to be asymptotically flat, using the solutions to the linearised theory at NLO as described in section 2.3.6, and fixing $C = 0$ and $C_{2+} = 0$. This leaves us with two free parameters, $C_{2,0}$ and C_{2-}. We can shoot towards the origin for many different values of these, and for each solution we find we can categorise it as one of the known behaviours (from tables 2.1 and 2.2).

Let us discuss what we expect to see. We look at the free parameter counts for each family. The stated parameter counts always include the trivial time-scaling parameter, which we have fixed in our shooting s.t. $B(r \to \infty) \to 1$, so this should be discounted. The stated parameter counts may or may not include a parameter that corresponds to C_{2+}, which we have fixed in our shooting to vanish $C_{2+} = 0$. We generally assume that they do include such a parameter. So if we consider shooting inwards, varying $C_{2,0}$ and C_{2-}, and picture the $C_{2,0}$, C_{2-} plane, then the asymptotic solution families will appear as areas, lines or points. Table 3.1 shows how we expect the families to appear. Consider one such example: from the results of section 3.2.2, especially the graphs 3.6, we expect that the $(1, 1)_{r_0}$ family will appear as two lines, one along $C_{2,0} < 0, C_{2-} \approx 0$ corresponding to Schwarzschild and another corresponding to the new black hole.

Family	No. of free parameters	Expected appearance in $C_{2,0}$, C_{2+} plane
$(0,0)_0$	1+1	point
$(1,-1)_0$	2+1	line
$(2,2)_0$	3+1	area
$(1,1)_{r_0}$	2+1	line
$(1,0)_{r_0}$	1+1	point
$(1,0)_{1/2}$	3+1	area

TABLE 3.1: The way we expect small/finite r solution families to appear in the $C_{2,0}$, C_{2-} plane when shooting inwards from large-r, $C = 0 = C_{2+}$. We have fixed both the trivial parameter and asymptotic flatness, which we usually expect to constrain 1+1 free parameters.

We may not be able to resolve points or lines where certain solution families appear, and we will have an issue where we need to know behaviours very close to the origin but the origin is a singular point of the differential equations that is therefore likely to be fraught with numerical issues. We also will have difficulty determining which (s,t) solution family we have found. This may sound easy, but there are transitions between different near-origin families, that are realised continuously, while s and t change discretely. For values of $C_{2,0}$, C_{2-} near a (s,t) transition (e.g. where there is a line of different family) it can be difficult to determine the (s,t) of a solution. To help understand the difficulty of resolving lines and determining (s,t), we consider the solutions to general relativity.

An easy way to determine the (s,t) values of a solution is to plot the functions

$$P_A(r) := r\,\partial_r\,\ln(A(r)) = \frac{rA'(r)}{A(r)} \tag{3.3.1a}$$

$$P_B(r) := r\,\partial_r\,\ln(B(r)) = \frac{rB'(r)}{B(r)}\,. \tag{3.3.1b}$$

The advantage of these is that if $A(r)$ and $B(r)$ are Frobenius series, of the form $r^s a_s + r^{s+1}a_{s+1} + r^{s+2}a_{s+2} + r^{s+3}a_{s+3} + \ldots$, then P_A and P_B are of the form

$$P_A = s + r\frac{a_{s+1}}{a_s} - r^2\frac{\left(a_{s+1}^2 - 2a_s a_{s+2}\right)}{a_s^2} + \ldots\,, \tag{3.3.2}$$

i.e. they are Taylor series and s and t can be determined as the intercept of P_A and P_B, which can easily be extrapolated from data that doesn't quite reach the origin. The extrapolated value of the intercept can be rounded to one of the few known values that s can take. This should work very well away from transitions of s, but near a transition how does a discrete change of

s manifest with a continuous change of the function? Consider the Schwarzschild solution:

$$A(r) = \frac{1}{1 - \frac{r_s}{r}} \tag{3.3.3a}$$

$$= -\frac{r}{r_s} - \frac{r^2}{r_s^2} + \dots \qquad (r_s \neq 0) \tag{3.3.3b}$$

$$P_A = 1 + \frac{r}{r_s} + \frac{r^2}{r_s^2} + \dots \qquad (r_s \neq 0)\ . \tag{3.3.3c}$$

For non-zero r_s the function P_A has intercept 1 and we would easily deduce that $A \sim r^1$. We plot P_A for different values of r_s in figure 3.9. For non-small negative r_s it is easy to interpret the graphs and to find the s value of the solution from the intercept of P_A. For small negative r_s we see that $P_A \approx 0$ near the origin, except at very small r, where it suddenly steeply rises in order to satisfy $P_A(r \to 0) \to 1$. For positive r_s there is a horizon, and numerical integration cannot see the behaviour near the origin. However, for very small positive r_s the solution appears to have $P_A \approx 0$ near the origin, and the steep slope corresponding to the horizon only appears at very small radius. So if the numerical solution stops before $r = 0$, at some $r = \epsilon$, then we would not see these steep slopes and we would wrongly believe that $A \sim r^0$ for some values of r_s s.t. $-\epsilon' < r_s < \epsilon''$. The complete picture we would draw in r_s space would be

$$\begin{cases} \text{horizon}, & \epsilon'' < r_s \\ A \sim r^0 + \dots, & -\epsilon' < r_s < \epsilon'' \\ A \sim r^1 + \dots, & r_s < \epsilon' \end{cases} \tag{3.3.4}$$

i.e. the single point in the variable r_s where $A \sim r^0$ becomes smeared into a finite range of r_s due to difficulties in numerically probing very small radius.

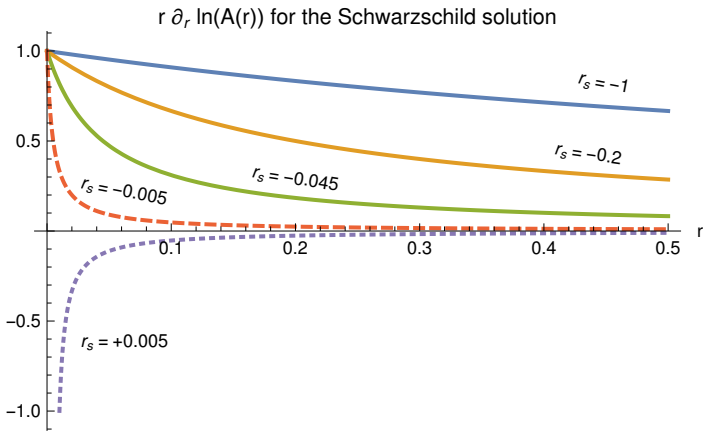

FIGURE 3.9: Illustration of how data very near the origin may be needed in order to correctly identify the s index of a solution

This Schwarzschild example illustrates a second important point. Note that the analytic

form of $A(r)$ (3.3.3a) can be seen to have r^1 behaviour at small r for $r_s \neq 0$, but in the limit $r_s \to 0$ to have r^0 behaviour at small r. However, if one did not know the analytic form of $A(r)$ (3.3.3a) but only knew part of the series form (3.3.3b) then taking the limit $r_s \to 0$ would take the apparent radius of covergence of the series to zero, and so the r^0 behaviour cannot be discovered. In the asymptotic series we found in sections 2.2 and 2.4 to the higher derivative theory, the various solution families found must be continuous deformations of each other (in e.g. the variables of the linearised solution C, $C_{2,0}$, C_{2-} and C_{2+}) but in practice this is difficult or impossible to demonstrate from the series approach. This illustrates another reason to do a shooting-inwards analysis of the system: this is the only way to gain an understanding of how solution families deform into each other.

We shall employ this method of using P_A and P_B as defined in (3.3.1) to estimate the (s,t) values of numerical solutions in the higher derivative theory as well. As we move around the $C_{2,0}$ - C_{2-} plane we generally expect that things are similar to the Schwarzschild example above, i.e. points and lines become blurred out to have a small width, and appear as small circles or lines with finite width, respectively. This over-identification of constrained solutions is fortunate in a way, because it will enable us to detect solutions that exist as lines or points.

Let us summarise the method. We use the same numerical values for the couplings as in section 3.2.2

$$\gamma = 1 \tag{3.3.5a}$$

$$\alpha = \frac{1}{2} \tag{3.3.5b}$$

$$(\therefore m_2 = 1)\ , \tag{3.3.5c}$$

and we shoot inwards from large radius $r_{\text{max}} = 10$ towards small radius. The differential equations we shall use are (1.3.19). We fix initial conditions $A(r_{\text{max}}), A'(r_{\text{max}}), B(r_{\text{max}})$, and $B'(r_{\text{max}})$ using the solutions to the linearised theory at LO and NLO as described in section 2.3.6. We fix $C = 0$ and $C_{2+} = 0$ and vary $C_{2,0}$ and C_{2-}, so see what ranges of $C_{2,0}$ and C_{2-} connect to which small-r families. We stop numerical integration if either function $A(r)$ or $B(r)$ become zero since such points are singular points of the differential equations. The ranges of $C_{2,0}$ and C_{2-} will be chosen so that the perturbative solution (that is used as initial value) is valid. The $C_{2,0}\frac{1}{r}$ term at $r = r_{\text{max}}$ has size $0.1 \times C_{2,0}$ and should be much less than 1, so $|C_{2,0}| \lesssim O(1)$ is appropriate. The $C_{2-}\frac{e^{-m_2 r}}{r}$ term $r = r_{\text{max}}$ has size $C_{2-} \times 5 \times 10^{-6}$ so $|C_{2-}| \lesssim O(10^5)$ may be appropriate. In fact the term controlled by C_{2-} grows so fast as we shoot towards small r that we find it better to limit C_{2-} to smaller values than that. It will turn out that presenting results for larger values of $|C_{2,0}| \lesssim 5$ make the results clearer. We will present results for $|C_{2,0}| \lesssim 8$ and $|C_{2-}| \lesssim 10^3$.

Our choice of r_{max} is chosen so that the exponential growth of the e^{-mr}/r terms is manageable, but it may strike the reader as modestly small. Later on we shall briefly discuss how the

choice of $r_{\max}$ can significantly affect the accuracy of the findings and the numerical problems one encounters.

3.3.2 Results

The $C_{2,0}$-C_{2-} plane is plotted to scale in figure 3.10. Some features are not visible in that diagram though, so a diagram with exaggerated dimensions is presented in figure 3.11. Let us consider each of the features we see in turn and comment on whether they conform to our expectations or not.

The most apparent feature visible in the $C_{2,0}$-C_{2-} plane is that open 2-dimensional ranges of ($C_{2,0}$-C_{2-}) values correspond to wormhole solutions. This conforms to our expectations since we saw in table 3.1 that since wormhole solutions have the maximum number of free parameters, they appear generically. Wormholes appear in three quadrants of the diagram and we show an example wormhole solution from each quadrant in figure 3.12. They show diverging gradients of $B(r)$ as the surface of the wormhole is approached, indicating that they are members of the $(1,0)_{1/2}$ family rather than the $(1,0)_{r_0}$ family, as expected since the $(1,0)_{r_0}$ has fewer free parameters (we did not do a thorough check to find where the single asymptotically flat $(1,0)_{r_0}$ solution (fig 2.1) appears). Note that the curvature scalar $R_{\mu\nu}R^{\mu\nu}$ is smaller than $O(1)$ for the whole space outside the wormhole $r_0 < r$, so we speculate that they might also appear in theories with even higher curvature terms.

The second most apparent feature is that open 2-dimensional ranges of the $C_{2,0}$-C_{2-} plane are $(1,-1)_0$ solutions. This does not conform to our expectations. We saw in table 3.1 that the $(1,-1)_0$ family in the $\beta = 0$ theory was expected to have one fewer free parameter than generic solutions, and thus to appear as a line in the $C_{2,0}$-C_{2-} plane. There are several possible explanations. This may indicate that the asymptotic analysis around the origin was not done to enough orders, and an additional free parameter was not seen. Alternatively, it may indicate that the count of free parameters is correct, but all solutions in the $(1,-1)_0$ family are naturally asymptotically flat, but this possibility is discounted very quickly after numerical shooting outwards from the origin using (2.2.6) because non-asymptotically-flat solutions appear at once. Another possibility is that it indicates a non-Frobenius family of solutions that also shares the leading-order characteristics of the $(1,-1)_0$ family but has terms of other forms at sub-leading order (e.g. logarithms or fractional powers) but that escaped our investigations. The final possibility is that there are issues with the numerical method in the specific context of the equations (1.3.19). It doesn't seem likely that numerical issues could cause such a striking distortion of the features that a one-dimensional line wrongly appears as a two-dimensional area covering around half the parameter space, though, but a more precise argument should be made and a more careful study done before we can reach any conclusion with confidence. We show the reader some plots from the $(1,-1)_0$ region as a basis to let them judge the evidence for themselves. Plots of P_A and P_B from the top-right and bottom-left $(1,-1)_0$ regions are shown

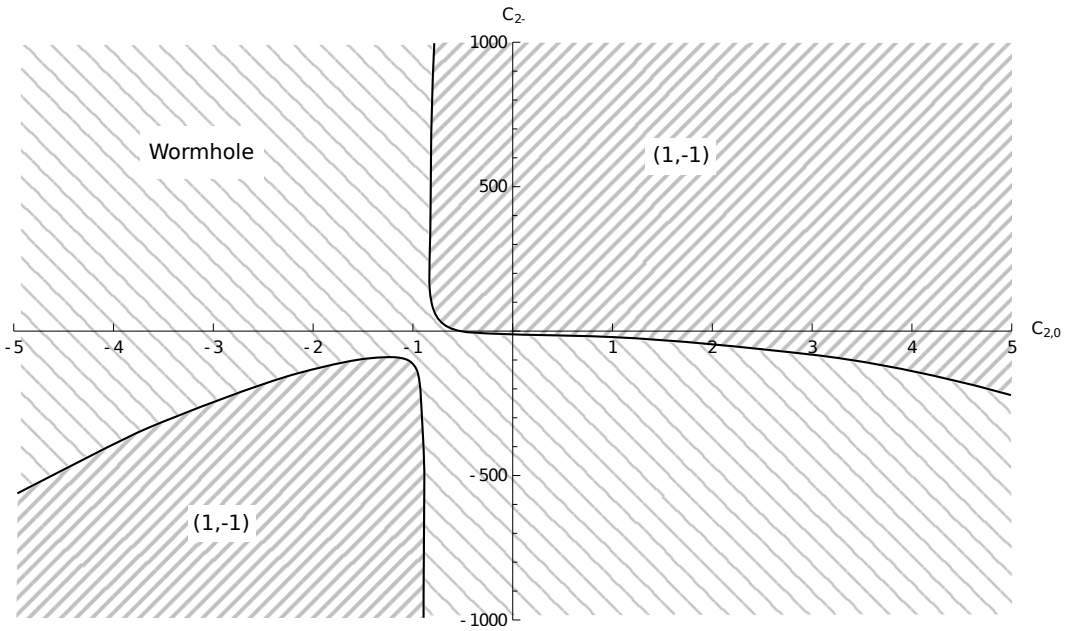

FIGURE 3.10: The solution families encountered when shooting inwards from large radius, varying $C_{2,0}$ and C_{2-}. The diagram is to scale. Between the wormhole behaviour and the $(1,-1)_0$ behaviour are horizon and $(2,2)_0$ and behaviours, but they are not visible on this scale. They are visible on a diagram with exaggerated sizes in figure 3.11

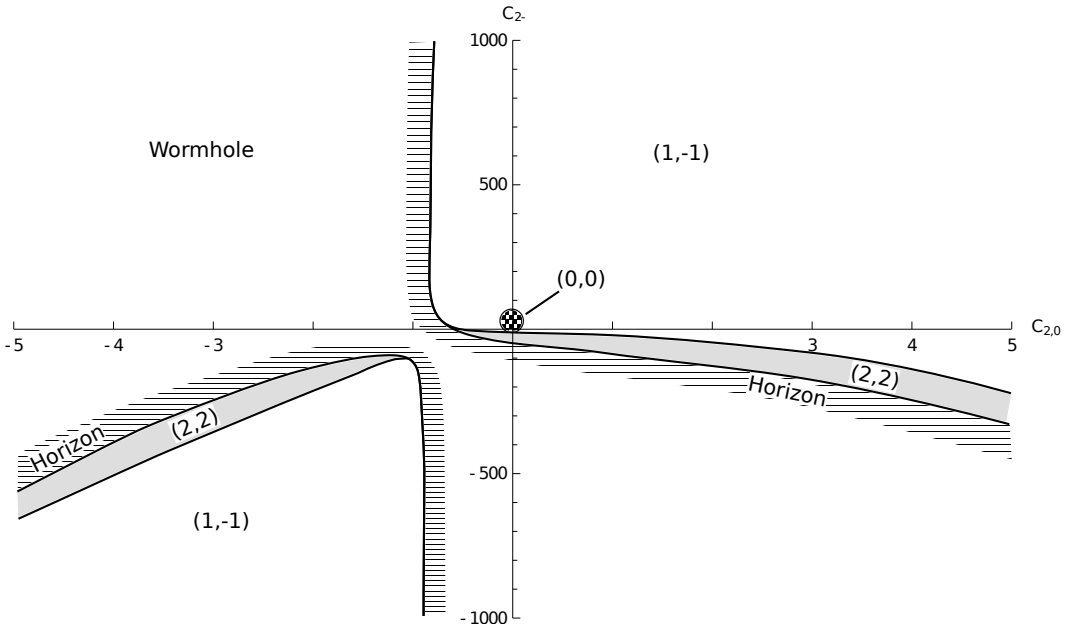

FIGURE 3.11: The solutions families encountered when shooting inwards from large radius, varying $C_{2,0}$ and C_{2-}, with dimensions exaggerated so that the areas of $(2,2)_0$ solutions and the lines of horizon solutions are visible. The horizon solutions appear at the boundary of the wormhole region, and in a rough cross shape, with the upper and right arms separated from the lower and left arms by the region of wormhole solutions.

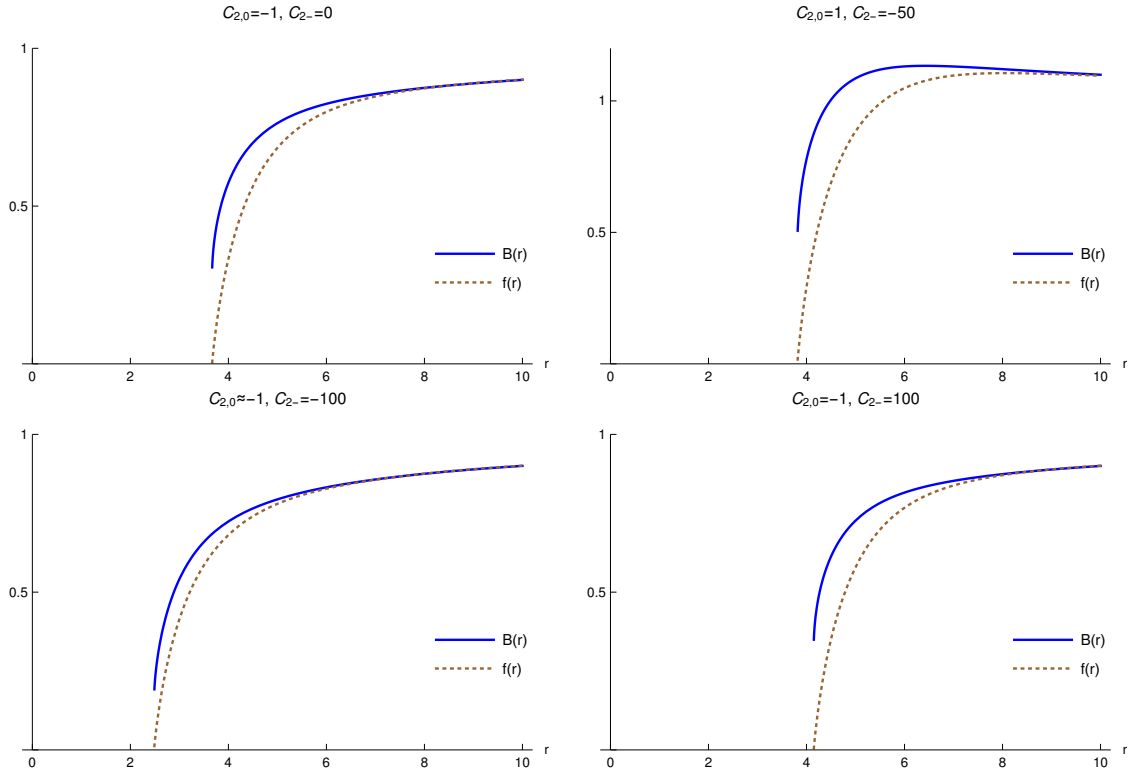

FIGURE 3.12: Examples of wormhole solutions from all three quadrants and the quadrant boundary where they appear. Both positive and negative masses $2GM = -C_{2,0}$ are exhibited. The diverging gradient of the function $B(r)$ indicates that they are members of the $(1,0)_{1/2}$ family rather than the $(1,0)_{r_0}$ family.

in figures 3.14 and 3.15 respectively. Note that the intercepts of the graphs are usually not exactly 1 and -1, but nearby values. Due the issue illustrated in figure 3.9 we expect that near the boundaries of the $(1,-1)_0$ regions there are continuous changes of our estimates of (s,t), even though the true (s,t) would change discretely. So we are expecting estimates of (s,t) that are neither $(1,-1)_0$ nor $(2,2)_0$ for certain regions of the $C_{2,0}-C_{2-}$ plane. But what about the bulk of the $(1,-1)_0$ regions? Define the bulk of the top-right $(1,-1)_0$ region as $-0.5 < C_{2,0}$, $10 < C_{2-}$, and the bulk of the bottom-left $(1,-1)_0$ region as $C_{2,0} < -1.1$, $C_{2-} < 121.622\,C_{2,0} + 8.10811$, i.e. the excluding the regions near the boundaries. Then the (s,t) values in that top-right region have $1.129 < s < 1.180$, $-1.32 < t < -1.42$, and in the bottom-left region have $1.133 < s < 1.147$, $-1.359 < t < -1.328$. These are plotted in figure 3.16. It is clear that there is a spread of values, following a clear trend, and that the values are distinct from their expected values of $(1,-1)_0$. The larger values of s in the graphs are taken from nearer the point in figure 3.10 that is mid-way between the two $(1,-1)_0$ regions, roughly $(C_{2,0}, C_{2-}) \approx (-0.9, 0)$. The smaller values of s are taken from farther from the centre. The fact that the (s,t) estimates differ from $(1,-1)_0$ slightly could be simply put down to various numerical inaccuracies, or it could be due to the effect illustrated in figure 3.9. The latter would suggest that the size of the $(1,-1)_0$ region is being exaggerated. It would be quite wishful thinking to speculate that the

$(1,-1)_0$ region is actually a line that has been smeared out into a very large area by this effect and thus be consistent with our understanding of free parameter counts. Note finally that the only place where $0.99 < s < 1.01$ and $-1.01 < t < -0.99$ simultaneously is at the border of the top-right region of $(1,-1)_0$ with the right-hand $(2,2)_0$ region (see figure 3.11).

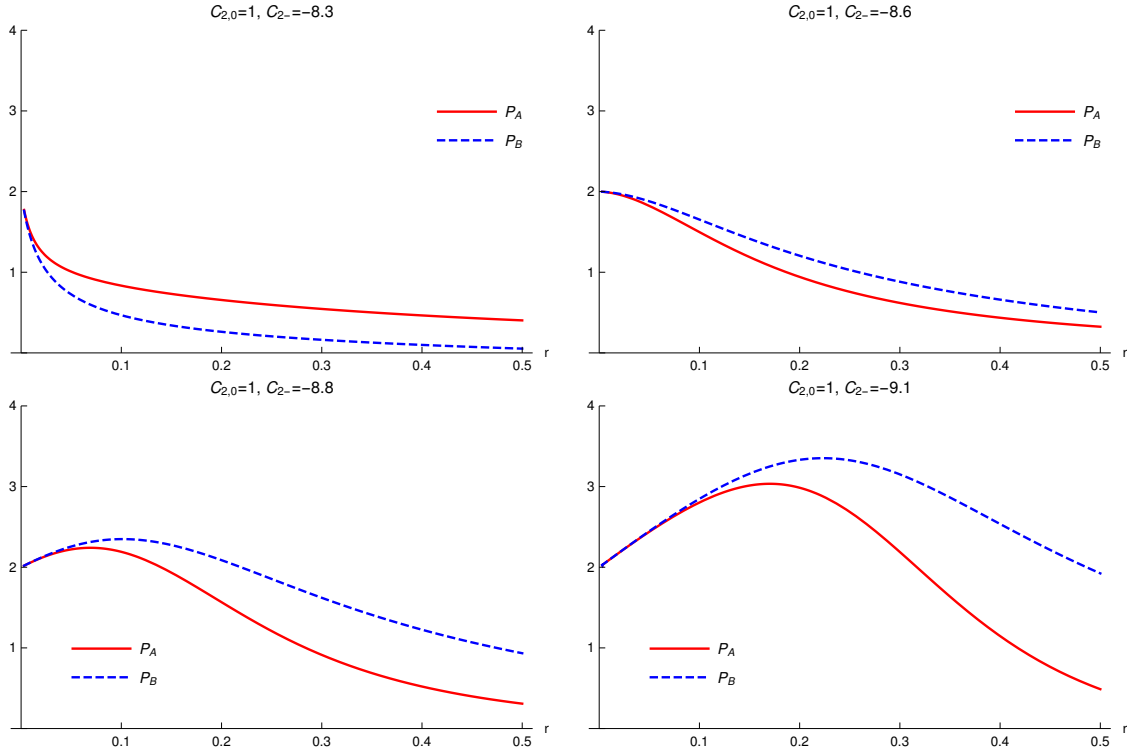

FIGURE 3.13: Plots of P_A and P_B for a finite range of C_{2-}, showing that $(2,2)_0$ behaviour has finite width in C_{2-}, and thus a 2-dimensional area.

Another unexpected feature of the $C_{2,0}$-C_{2-} plane is the way the $(2,2)_0$ solutions appear. This solution family has the maximum number of free parameters, so we expect it to appear as an area in the plane. Its area of appearance is so narrow, though, that it is only visible as a line in figure 3.10. We said above that lines may appear as narrow areas and gave an example in equation (3.3.4). We can show that the width of the $(2,2)_0$ region appears to be different; it appears to reflect a genuine width. We show plots of P_A and P_B for $C_{2,0} = 1$ for a selection of values of C_{2-} in the range $-9.1 < C_{2-} < -8.3$ in figure 3.13. It is apparent that for a finite deformation of the curves the intercepts remain constant at 2, so the $(2,2)_0$ solution clearly appears to occupy an area rather than a line. To be more precise, in the part of the $(2,2)_0$ region away from the boundary the (s,t) estimates satisfy $1.94 < s < 2.06$ and $1.96 < t < 2.03$ (c.f. the $(1,-1)_0$ region which actually had $(s,t) \approx (1.14,-1.35)$). The centres of the two branches

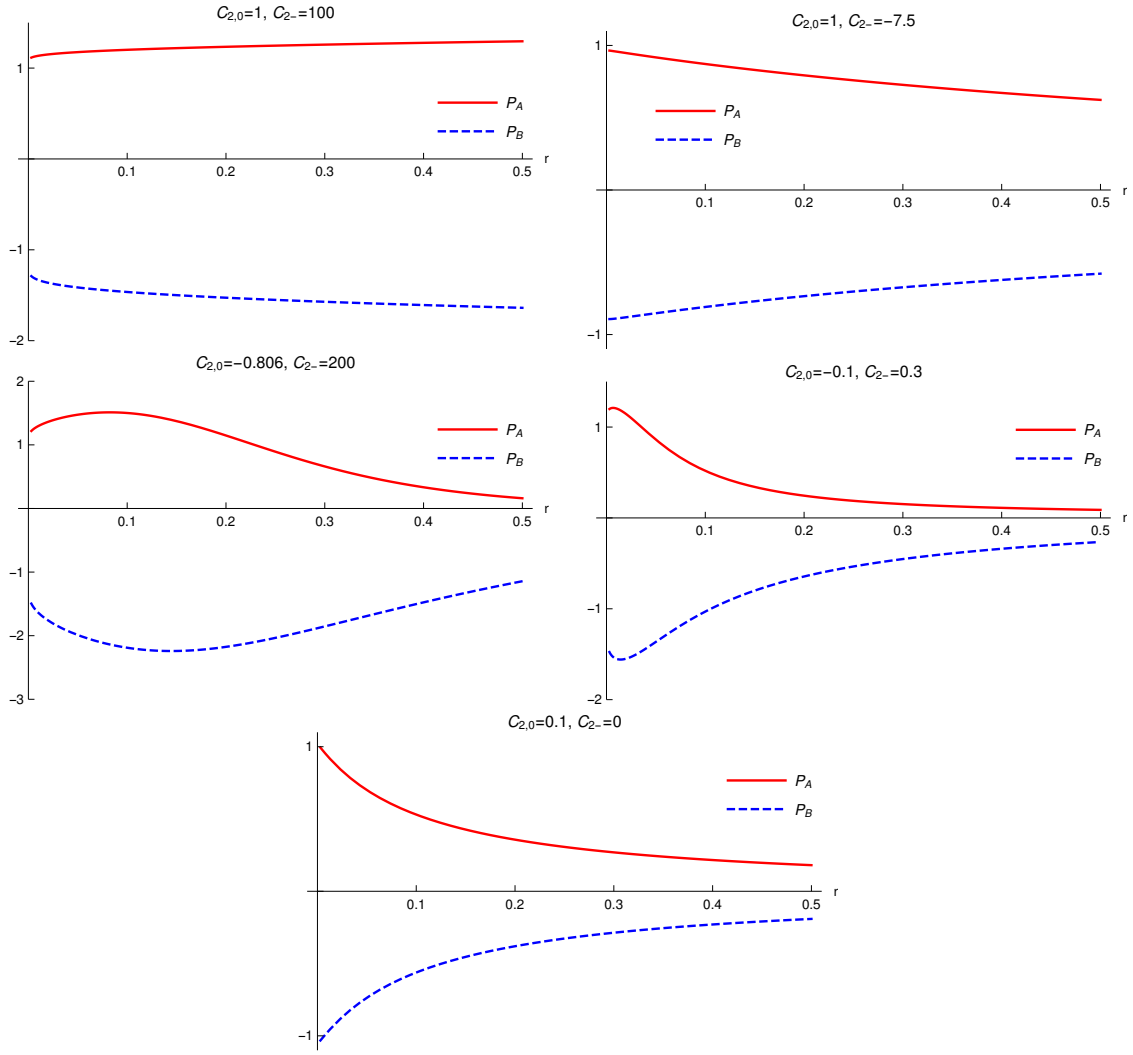

FIGURE 3.14: An illustrative selection of plots of P_A and P_B from solutions in the top-right region of $(1,-1)_0$ solutions, from both near to and far from the region's boundary.

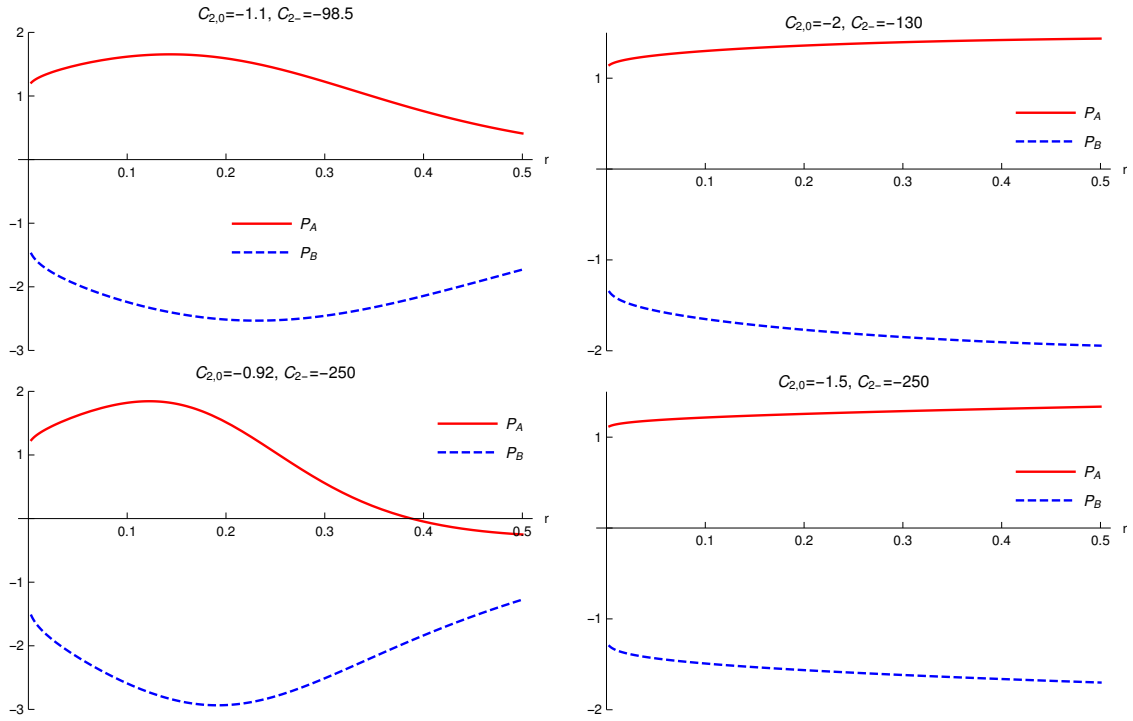

FIGURE 3.15: An illustrative selection of plots of P_A and P_B from solutions in the bottom-left area of $(1,-1)_0$ solutions, from both near to and far from the region's boundary.

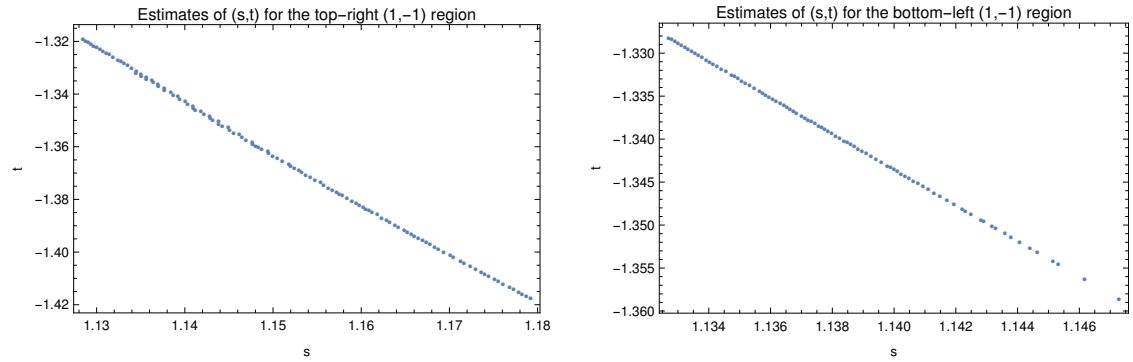

FIGURE 3.16: The estimates of (s,t) for the top-right and bottom-left regions of $(1,-1)_0$ solutions. In each graph the region with larger s is taken from nearer the mid-point $(C_{2,0}, C_{2-}) \approx (-0.9, 0)$ and the region with smaller s is taken from farther the mid point.

of the $(2,2)_0$ solution can be approximately fitted to polynomials:

$$\begin{aligned} C_{2-}^{(\text{left } 2,2)} \approx & -1267.7 - 3861.87\,(C_{2,0}) - 5574.46\,(C_{2,0})^2 - 4770.1\,(C_{2,0})^3 - 2696.\,(C_{2,0})^4 \\ & - 1043.18\,(C_{2,0})^5 - 279.186\,(C_{2,0})^6 - 50.9575\,(C_{2,0})^7 \\ & - 6.06474\,(C_{2,0})^8 - 0.424736\,(C_{2,0})^9 - 0.0132866\,(C_{2,0})^{10} \end{aligned} \tag{3.3.6a}$$

$$\begin{aligned} C_{2-}^{(\text{right } 2,2)} \approx & -0.866796 + 2.88585\,(C_{2,0}) - 11.4821\,(C_{2,0})^2 \\ & + 0.238216\,(C_{2,0})^3 + 0.309514\,(C_{2,0})^4 - 0.0525535\,(C_{2,0})^5\,, \end{aligned} \tag{3.3.6b}$$

so we define coordinates measuring deviations from these lines

$$C_{2-}^{(\text{right } 2,2 \text{ residual})} := C_{2-} - C_{2-}^{(\text{right } 2,2)} \tag{3.3.7a}$$

$$C_{2-}^{(\text{left } 2,2 \text{ residual})} := C_{2-} - C_{2-}^{(\text{right } 2,2)}\,. \tag{3.3.7b}$$

We plot the width profiles of the left branch and right branch in fig 3.17. The widths are only approximately 0.01 (left) and 2 (right), which is extremely small on the scale of the range of C_{2-} we consider, but appears to be finite. This is in line with what we expected from our other analyses, but it is a little surprising that the $(2,2)_0$ area is quite so narrow.

Representative plots of A and B and the scalar curvature for various $(2,2)_0$ solutions are shown in figure 3.18. Plots for other points in the $(2,2)_0$ region are similar in character. In each solution it is apparent that curvature is small at large radii but then increases greatly towards small radii. Let us define the strong curvature region as the region where $R_{\mu\nu}R^{\mu\nu} > 1 \Leftrightarrow \ln(R_{\mu\nu}R^{\mu\nu}) > 0$, and its outer radius as r_{strong}.

$$\ln(R_{\mu\nu}R^{\mu\nu}) \sim \begin{cases} > 0\,, & r < r_{\text{strong}} \\ < 0\,, & r_{\text{strong}} < r \end{cases}\,. \tag{3.3.8}$$

These plots are in accord with Holdom's similar result in [33], where he found a horizonless asymptotically-flat $(2,2)_0$ solution and observed that it had a region of strong curvature near to the would-be horizon. Our results show this again for a different choice of couplings (we use $\beta = 0, \alpha = \frac{1}{2}$ and he used $\alpha = 3\beta = \frac{1}{32\pi}$) and for a large number of solutions (of which only a selection are shown in fig 3.18). In the positive-mass $\Leftrightarrow$ negative $C_{2,0}$ $(2,2)_0$ plots we presented one can clearly see the function A become large and B become small, reminiscent of the Schwarzschild solution where as $r_s \sim -C_{2,0}$ is approached $A \to +\infty$ and $B \to 0$, but unlike the Schwarzschild solution the curvature gets strong and the metric functions curve away again to avoid forming a horizon. The size of the region of strong curvature, r_{strong}, for $(2,2)_0$ solutions at the centre of each of the region, is plotted as a function of $C_{2,0}$ in figure 3.19. It shows that for positive ADM mass $2GM := -C_{2,0}$ there is a rough relation $r_{\text{strong}} \sim -C_{2,0} = 2GM = r_{\text{Schwarzschild}}$, i.e. that the strong curvature region is always roughly

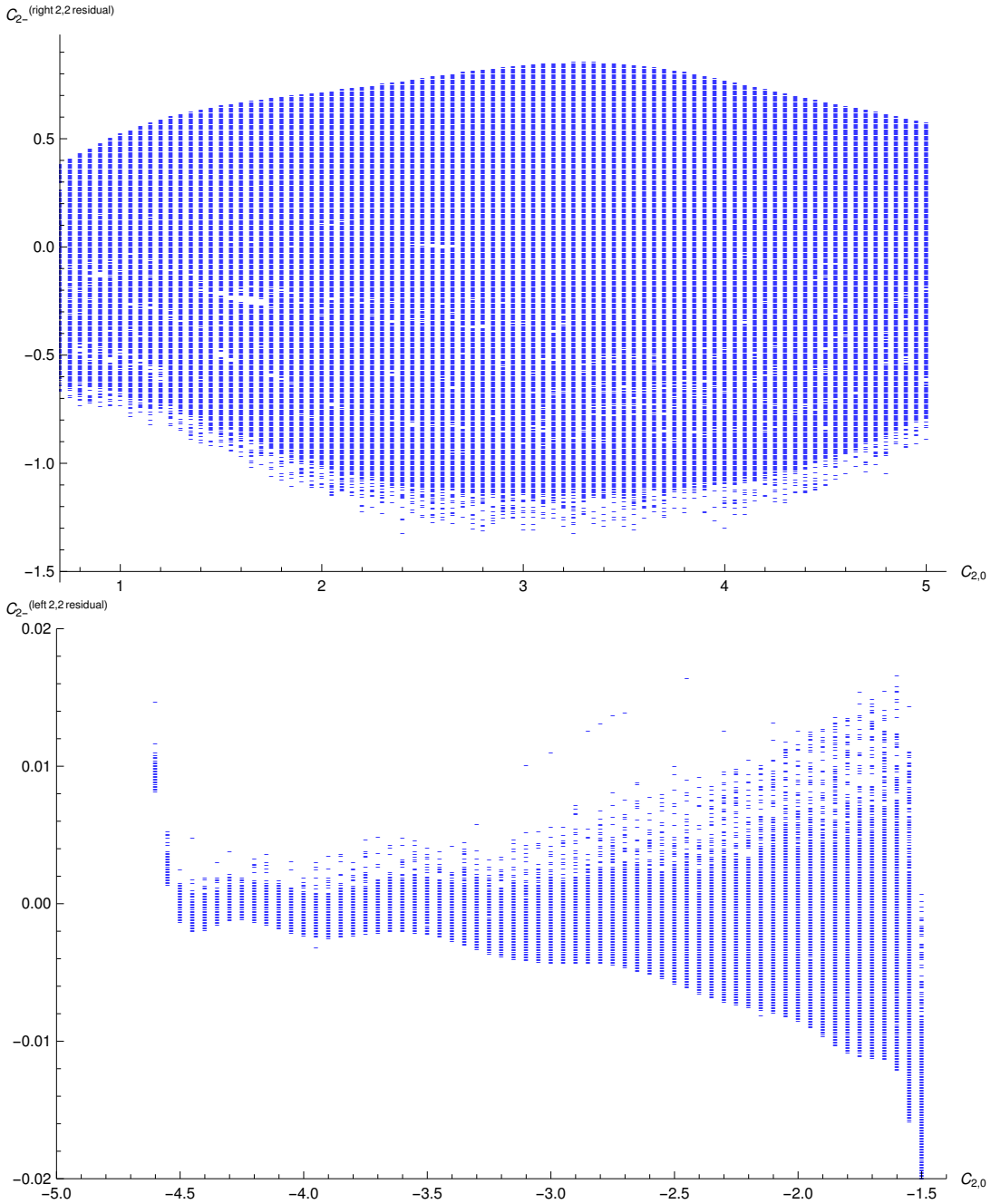

FIGURE 3.17: Width profiles of most of the left ($C_{2,0} < 0$) and right ($C_{2,0} > 0$) areas of $(2,2)_0$ solution. The coordinates on the vertical axes are defined in 3.3.6. It is a scatter plot of ($C_{2,0}$, $C_{2-}^{\text{right/left 2,2 residuals}}$) points whose space-time is in the $(2,2)_0$ family. Details of the numerics, and of the automatic algorithm for determining if a space-time is a member of the $(2,2)_0$ family, have resulted in ragged edges of the borders with the wormhole region (the region below the right-hand $(2,2)_0$ region and above the left-hand $(2,2)_0$ region). Manual examinations of the space-times near the $(2,2)_0$-wormhole border can sharpen the edge but proved too time-consuming.

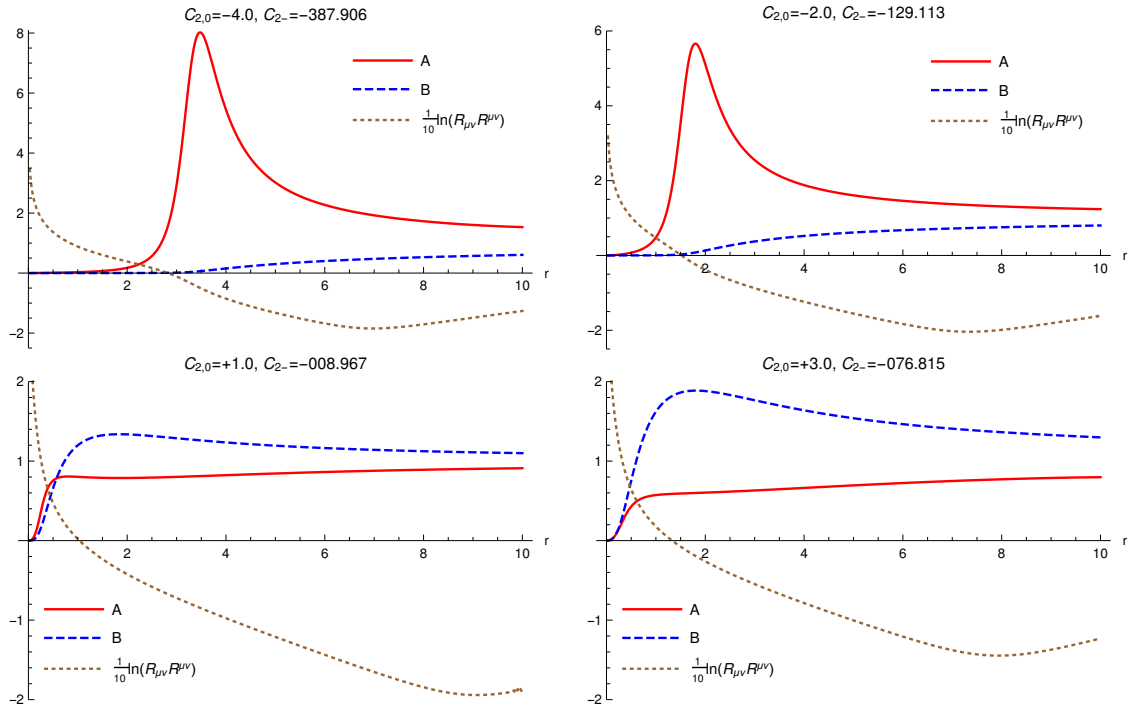

FIGURE 3.18: Example $(2,2)_0$ solutions from both the right-hand ($C_{2,0} > 0$, negative mass) and left-hand ($C_{2,0} < 0$, positive mass) regions.

of the necessary size to interfere with the formation of a horizon. Holdom's similar result led him to speculate that other theories with even higher curvature terms will also lack horizons. The presence of higher curvature terms would likely mean that the "interior" regions are significantly different from the ones in this theory, however. Holdom found that only the $(0,0)_0$ family is present in generic theory with even higher derivatives, so he speculated that the effect of many even-higher-curvature terms would be to deform the "interior" into this family, to make it non-singular. Our discussion of coupling in section 3.1 emphasised parameter counting of solution families, and in our discussion of the non-singular $(0,0)_0$ family in sections 2.2.1.1 and 2.3.6 we concluded that what few free parameters this family does have are all fixed by the requirement of asymptotic flatness. This makes it difficult to see how higher-curvature corrections to the example $(2,2)_0$ solutions could deform them into $(0,0)_0$ solutions, but on the other hand we have already described how Holdom's considerations of higher-curvature theories seem to suggest that they must. We consider this question unresolved. For comparison, in the wormhole solutions the curvature does not become strong outside of the wormhole, and in the $(1,-1)_0$ solutions (recall that these do not have horizons) r_{strong} is generally larger than in nearby $(2,2)_0$ solutions. In the $(1,-1)_0$ regions r_{strong} gets larger as one moves away from the centre of the diagram 3.10 and as one moves away from the boundary of the $(1,-1)_0$ region (the places where there are horizons) into the interior.

Horizons are apparent in the $C_{2,0}$-C_{2-} plane, in an approximate cross shape. They appear

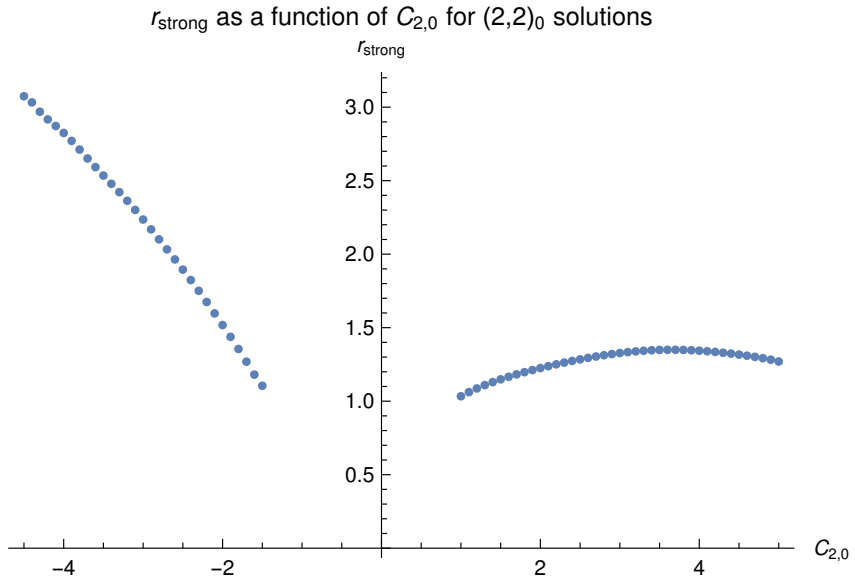

FIGURE 3.19: The outer radius r_{strong} of the region of strong curvature (defined as $R_{\mu\nu}R^{\mu\nu} > 1$) in $(2,2)_0$ solutions near the centre of the $(2,2)_0$ strip in the $C_{2,0}$-C_{2-} plane, as a function of $C_{2,0}$.

at the edges of the wormhole region as a limit of a wormhole solution. Recall that both wormholes and horizons have a zero of $f(r) = \frac{1}{g_{rr}(r)}$ at $r = r_0$, but that wormholes have $B(r_0) \neq 0$ and horizons have $B(r_0) = 0$. The values of $B(r_0)$ are largest away from the edges of the wormhole region, and tend to zero towards the edges, becoming zero at the boundary, thus forming horizons. The solutions with horizons on the upper, lower and left-hand branches are exactly the Schwarzschild solution, to good accuracy [1] , with masses $2GM = r_0 = -C_{2,0}$ matching the $C_{2,0}$ value at which they appear and not depending on their supposed value of C_{2-} (we do not plot these solutions since the reader is so familiar with the Schwarzschild solution). This cannot be correct and must represent numerical issues, but we postpone discussion until we have finished the description of the horizon solutions. The remaining solutions with horizons, on the right-hand branch, are the non-Schwarzschild, or "new", black holes, and we show examples with positive and negative mass in 3.20.

We can compare the non-Schwarzschild black holes we have found when shooting inwards from large-r to the non-Schwarzschild black holes we found when shooting outwards from a horizon in section 3.2.2. The relation between the horizon radius r_0 and the mass $GM = -\frac{1}{2}C_{2,0}$ is shown in figure 3.22 for both these two classes of numerical non-Schwarzschild black holes. There is good agreement for $GM \gtrsim -2$ or equivalently $C_{2,0} \lesssim 4$. The numerical results from shooting inwards use perturbative solutions as initial conditions, so inaccuracies at larger values of $C_{2,0}$ are to be expected.

Now we must comment on how this compares to what we expected to find. We know

[1] This can be checked by examining e.g. $rA'(r) + A(r)(A(r) - 1)$ and $rB'(r) + B(r) - 1$ for these solutions, which will be zero for all $r > r_0$ IFF Schwarzschild, for any r_s

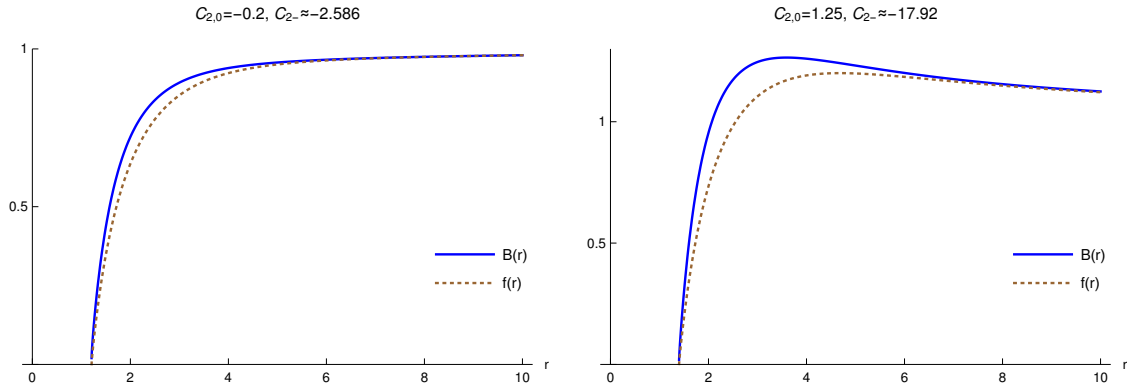

FIGURE 3.20: Non-Schwarzschild solutions with horizons, for both positive and negative mass, found by shooting inwards from asymptotic flatness. See also figure 3.8

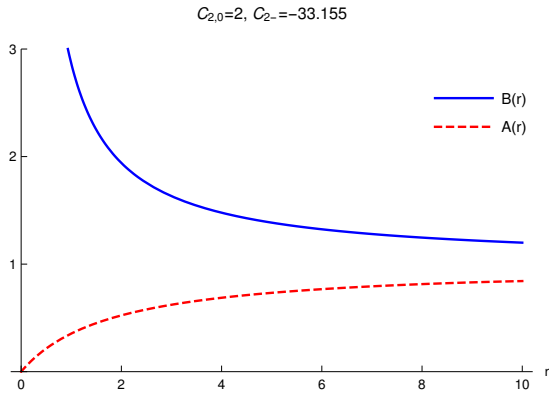

FIGURE 3.21: A negative-mass Schwarzschild solution found with a small non-zero value of C_{2-} rather than the expected location of $C_{2-} = 0$.

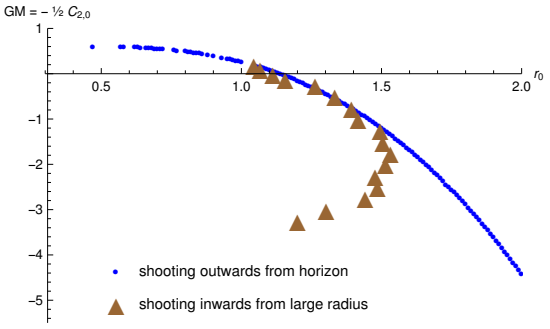

FIGURE 3.22: A comparison of the mass-radius relation for Non-Schwarzschild black holes, for the solutions obtained by shooting outwards from a horizon and for the solutions obtained by shooting inwards from asymptotic flatness. See also figure 3.7

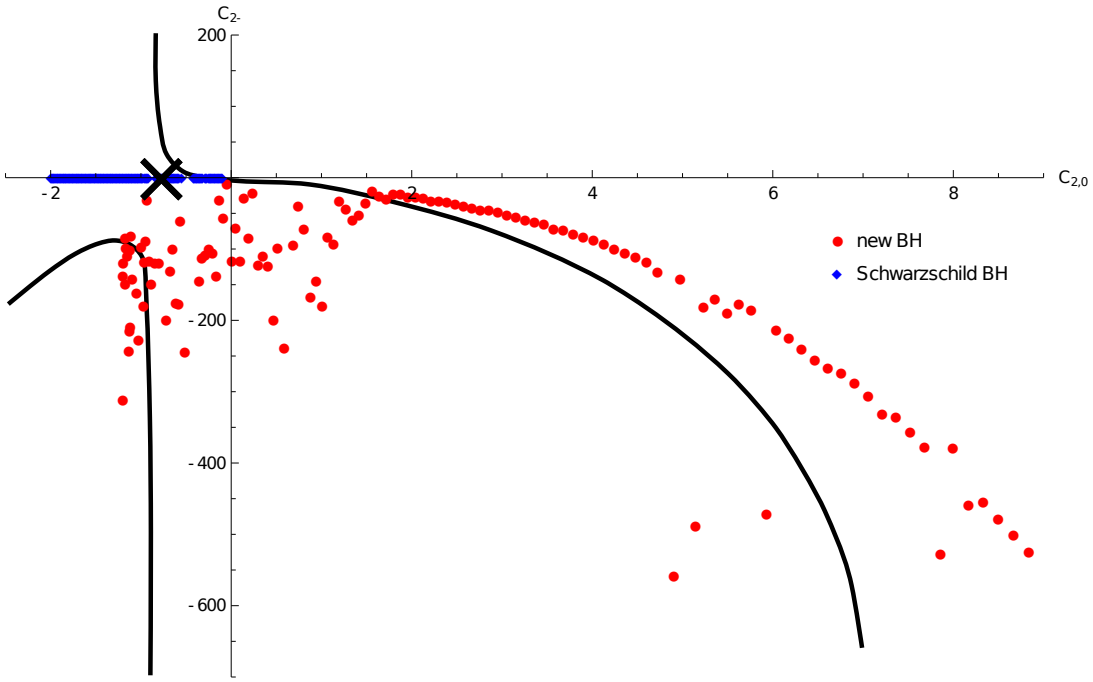

FIGURE 3.23: A scatter plot of the $C_{2,0}$ and C_{2-} values found for the asymptotically flat horizon solutions in section 3.2.2 found by shooting outwards from horizons. A large X marks the point $(C_{2,0}, C_{2-}) \approx (-0.9, 0)$ of the solution where the Schwarzschild and non-Schwarzschild black holes coincide. This scatter plot is overlaid on a close-up of the lower-right quadrant of the diagram figure 3.10 of shooting-inwards results, i.e. the black lines mark the location of horizon solutions between $(1,-1)_0$ and wormhole regions. The non-Schwarzschild black hole scatter data can be seen to qualitatively agree with the shooting-inwards data for $C_{2,0} > 1.5$ (though with some numerical differences), and the Schwarzschild black hole scatter data to agree with the shooting-inwards data for $-0.5 \lesssim C_{2,0} \lesssim 0$, but the remainder of the scatter data requires discussion and analysis.

that Schwarzschild black holes have $C_{2-} = 0$ and $C_{2,0} = -2GM < 0$, so we expect to find Schwarzschild horizons of radii $r_0 = -C_{2,0}$ along the negative $C_{2,0}$ axis. In fact we find Schwarzschild horizons of those radii a little below the negative $C_{2,0}$ axis, which we write off as numerical inaccuracies on the effect of $C_{2-} \neq 0$ without worrying too much. Similarly, we would expect $(1,-1)_0$ negative-mass Schwarzschild solutions along the positive $C_{2,0}$ axis. Again, the expected Schwarzschild solutions are to be found slightly off the axis and we show an example from position $C_{2,0} = 2, C_{2-} \approx -33.155$ in figure 3.21. We also found Schwarzschild black hole solutions along the upper and lower arms, for $C_{2,0} \approx -0.8$, all having roughly the same radius $r_0 = -C_{2,0} \approx 0.8$, even for large values of C_{2-}. We know that Schwarzschild solutions should only appear for $C_{2-} = 0$ so this represents very significant numerical issues, but we shall make another observation before commenting on numerical accuracy.

We have said where we expected to find the Schwarzschild solutions, but we have yet to say where we expected to find the non-Schwarzschild black holes and whether our results match. The non-Schwarzschild black holes found by shooting outwards from a horizon in

section 3.2.2 had values of $C_{2,0}$ and C_{2-} fitted to them (plotted in figures 3.6 and 3.7). In figure 3.23 we compare those values to the $C_{2,0}$ and C_{2-} values where we found the non-Schwarzschild black holes in this section. There was some difficulty in fitting values of C_{2-} to non-Schwarzschild black hole solutions with small mass, so the corresponding points have poor precision, but it is still visible that the non-Schwarzschild black holes lie approximately where they were expected to lie, in a seeming endorsement of the numerical accuracy of the method. The Schwarzschild black holes to the right of the vertical arms, i.e. $C_{2,0} \gtrsim -0.9$, show good agreement as well. However, for $C_{2,0} \lesssim -0.9$ the agreement becomes very poor. We have said already that we consider the left arm of 3.11 to be the continuation of the Schwarzschild family of solutions for larger positive masses, but figure 3.23 shows that the left arm of the shooting-inwards data starts at $(C_{2,0}, C_{2-}) \approx (-1.5, -100)$ but the scatter data from shooting outwards clearly has $C_{2-} \approx 0$. Worse, there are upper and lower arms of horizons in the shooting-inwards data for this value of $C_{2,0}$. We can no longer avoid commenting on these upper and lower branches of horizon solutions, which we have said must be incorrect both because they have non-zero values of C_{2-} and because they do not even vary with C_{2-}. This may indicate that $C_{2,0} \approx -0.9$ is some sort of critical value where not only do the non-Schwarzschild and Schwarzschild black holes coincide in a shooting-outwards analysis, but also the numerical shooting becomes insensitive to C_{2-} in a shooting-inwards analysis.

It is not clear why there should be a critical value of $C_{2,0}$ where significant numerical issues appear, nor is it clear what exactly these issues are. The presence of the upper and lower arms of Schwarzschild horizon solutions seems like it must be wrong, but it is closely linked to the overall, broad shapes of the $C_{2,0}$,C_{2-} plane. At the moment, the upper and lower arms of horizon solutions form a separation between large areas of $(1, -1)_0$ solutions and $(1, 0)_{1/2}$ wormhole solutions. It is hard to cast doubt on the presence of these areas themselves, because they show up for very large ranges of values. There must therefore be boundaries where other solutions appear, as $C_{2,0}$ and C_{2-} are varied continuously but solution properties change discretely. The numerical solutions close to these boundaries are, not surprisingly, hard to interpret, but it generally seems reasonable that a line of another family might appear at the boundary. It seems natural that the extreme limit of a wormhole solution is a horizon, since both have $f(r_0) = 0$, while the wormhole has $B(r_0) > 0$ and the horizon has $B(r_0) = 0$. On the other hand, in section 3.2 we tried to find all solutions with horizons. The non-Schwarzschild black holes we found were determined to have $C_{2,0}$,C_{2-} values of another region of the plane, far away from the upper and lower branches of horizons. There were some numerical limits on that work, however, so it is possible that there are other branches of non-Schwarzschild black hole solutions. Optimistically, such a hypothetical additional branch of non-Schwarzschild black holes might have $C_{2,0}$,C_{2-} values of roughly this part of the plane and might look extremely similar to Schwarzschild, but this is speculation. The other possibility is that some undiscovered solution family is responsible for the seeming appearance of the upper and lower branches of

horizon solutions, but there are no obvious candidates from among the families listed in table 3.1.

We can imagine that with some effort the numerical accuracy could be improved and the reason for the upper and lower branches of black holes and for $C_{2,0}$ having a critical value could be unravelled, and these current problems could be overcome. Perhaps something far more radical could happen that simultaneously addresses the issues of the critical value of $C_{2,0}$, the upper and lower horizon branches, and the issue that the $(1,-1)_0$ region is an area instead of the line that was expected, and we would be left with results that simply confirm our beliefs from the other analyses. However, this doesn't seem at all likely. We must conclude that this shooting-inwards analysis has revealed unexpected new information to us, but it is not clear what. It does not seem entirely safe even to say that the $(1,-1)_0$ family is an area, and thus has more free parameters than we realised from the asymptotic analyses, because there is a contradiction in its boundary with the wormhole solutions. More analysis is needed.

Perhaps the most important way to improve the quality of the results would be to increase the radius r_{max} from which the shooting starts. We had numerical issues with larger values, but with more precision these could be overcome. Let us explain the nature of the problem. The initial values for the shooting are calculated from evaluating the linearised solutions at r_{max}, and the effect of this is that the initial values do not exactly correspond to asymptotically flat solutions (though by the number of free parameters they will always correspond to *some* solution). This is likely responsible for a lot of problems with the results. The difficulty overcoming it is that the value of the falling Yukawa term e^{-mr}/r is so small at large radii that rounding errors at large r have huge effects at small r. Our way around this problem was to use only a modest value of r_{max} and to assume the shooting's initial conditions were accurate enough, but perhaps an approach using large r_{max} could be complementary to ours, even though it swaps our issues for others.

As a final comment, we note that varying the value of α does not seem to change any of the main features of the $C_{2,0}$,C_{2-} plane but does shift the boundaries around. In a similar fashion to figure 3.10, we assume that the only features visible on the $C_{2,0}$,C_{2-} plane are a large region of wormhole solutions, covering most of the top-left and bottom-right quadrants, and two regions of $(1,-1)_0$ solutions in the top-right and bottom-left. Assuming that, to draw the $C_{2,0}$,C_{2-} plane one only needs to draw the lines indicating the boundaries between these regions. In figure 3.24 we show the $C_{2,0}$,C_{2-} plane with such lines drawn, overlaying three sets of such lines for three different values of α. We note that as α varies, the coincidence point of the Schwarzschild and non-Schwarzschild black holes is given by (3.2.27) to be

$$m_2\, r_0^{(\text{coincidence})} \approx 0.87$$
$$\therefore \quad -2\,G\,M^{(\text{coincidence})} = C_{2,0}^{(\text{coincidence})} \approx -\sqrt{\frac{2}{\gamma}}\,\sqrt{\alpha}\,0.87\,,$$

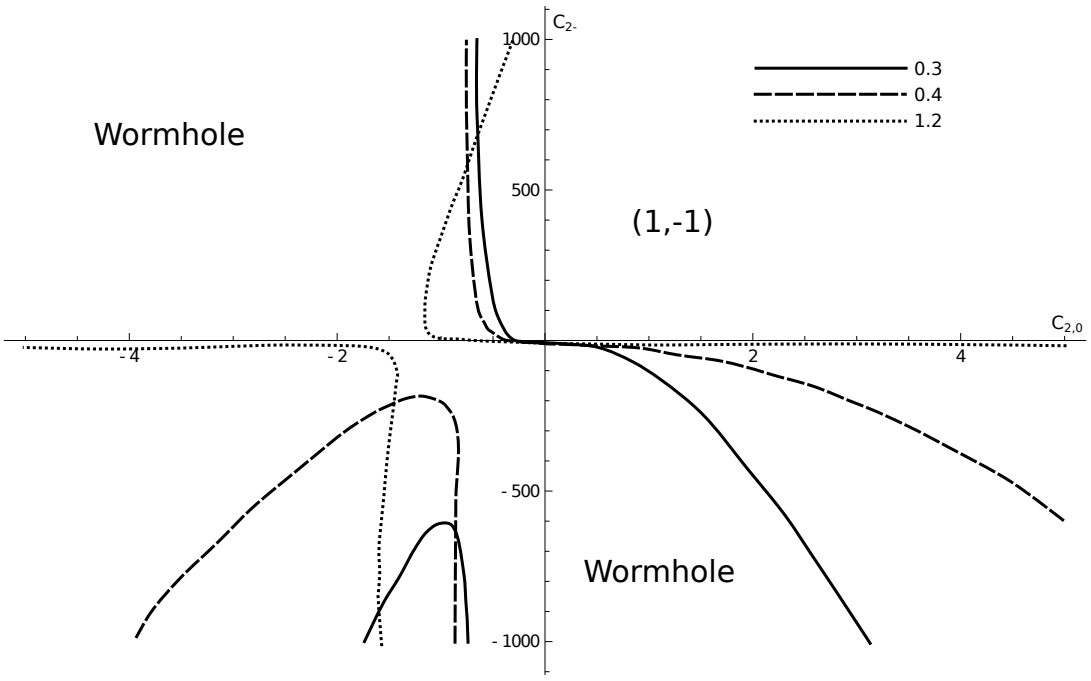

FIGURE 3.24: The outlines of the $(1,-1)_0$ regions of the $C_{2,0}$,C_{2-} plane, for three different values of alpha: 0.3, 0.4 and 1.2. In each case the area to the top-right of the top-right line is $(1,-1)_0$, the area to the bottom-left of the bottom-left line is also $(1,-1)_0$, and the area in-between, extending from the top-left through the centre to the bottom-right, is wormholes. The plot shows that for increasing values of α the bottom-left $(1,-1)_0$ region grows and reaches towards the left axis. For increasing value of α the bottom-right boundary of the $(1,-1)_0$ region retreats out of the bottom-right quadrant towards the right axis.

so that $C_{2,0}$ becomes more negative with increasing α. The $C_{2,0}$ value of the mid-point between the upper and lower lines of boundary moves to more negative values as α is increased. The analysis is too rough to dignify with a quantitative treatment, but we note that our results are consistent with the supposition that the coincidence point of the Schwarzschild and non-Schwarzschild black holes is always directly between the upper and lower boundary lines.

Chapter 4

Conclusion

In this thesis we considered the classical solutions to four-dimensional higher derivative gravity truncated at four derivatives and without a cosmological term. We considered the static spherically symmetric problem, in particular building on the work in [6], [33] and [34], and reached an improved understanding of the solution space, especially the properties of solutions coupled to matter, solutions that have horizons and solutions that are asymptotically flat.

In the first part we attempted to document all the solution families that exist in the theory, using both a Frobenius ansatz and other ansatzes. We reproduced the families around the origin originally found in [6], the $(0,0)_0$, $(1,-1)_0$ and $(2,2)_0$ families, and confirmed the count of free parameters for $(0,0)_0$ and $(2,2)_0$ given in [33], and counted the free parameters of the $(1,-1)_0$ family, which can include logarithmic terms. We also found series solutions around $r = r_0 \neq 0$, which come in five families: $(0,0)_{r_0}$, $(1,1)_{r_0}$, $(1,0)_{r_0}$, $(1,0)_{1/2}$ and $(\frac{3}{2},\frac{1}{2})_{1/2}$. We reproduced the solutions to the linearised theory originally found in [6] and expanded upon their discussion of linearised coupling to matter sources. Comparison of families from all three of these methods allowed us to infer a lot about true solutions. This was bolstered considerably by the spherically symmetric application of a theorem generalised from [34] which relates local properties of a solution (an ideal application of the series expansions) to the property $R = 0$ that must hold for an open range of r. A key application was allowing us to identify which combination of the free parameters of the $R \neq 0$ part of a solution family corresponded to non-flatness at infinity (for certain families). For example, it was possible to show that the $(\frac{3}{2},\frac{1}{2})_{1/2}$ family has no asymptotically flat members. Most importantly though it proved that static asymptotically flat black hole solutions are fully described by the special Lagrangian $\gamma R - \alpha C^2$, which is very significant because the spherically symmetric solutions of that theory have two fewer free parameters than the general theory.

All of the knowledge of vacuum solution families of the full theory, and vacuum and non-vacuum solutions of the linearised theory, was brought together to make several arguments that the Schwarzschild solution does not describe minimal coupling to positive matter. Many arguments were made that solutions with minimal coupling to matter do not have horizons. In fact, based primarily on knowledge of free parameter counting, it was argued that matter-coupled solutions belong to the $(2,2)_0$ family, which has no analogue in general relativity. This is interesting if one looks to theories with even higher derivatives, since the curvature of $(2,2)_0$ solutions is large for radii out to around the Schwarzschild radius, so disruption to the would-be horizon may be taken seriously even if "interior" properties may not be. Holdom pointed out in [33] that the $(2,2)_0$ solution family is generically not present in theories with higher derivatives, however, so the matter coupling of such theories still needs investigation.

The Schwarzschild black hole is still a vacuum solution to the higher-derivative theory, but a second branch of black hole solutions was found, that coincide with the Schwarzschild solution for $m_2\, r_0 = m_2\, 2GM \approx 0.876$. The existence of a second branch was analytically

proved by Whitt in [55]. For Schwarzschild black holes larger than at the branch point it was shown that there are no asymptotically flat deformations. The non-Schwarzschild black holes also appear with negative ADM mass, but these solutions have strong curvature at the horizon and it is possible that they would not appear if higher derivative corrections were considered (if, indeed, the non-Schwarzschild black holes would still appear at all).

The space of asymptotically flat solutions was explored using numerical shooting. It was found that the generic asymptotically flat solutions are wormholes $(1,0)_{1/2}$ and horizonless $(1,-1)_0$ solutions. At the boundaries of the wormhole region the solutions limited to horizons of the $(1,1)_{r_0}$ family, including the non-Schwarzschild black holes, which appeared where expected and with the radii predicted by the numerical shooting outwards from horizons towards infinity. Between the wormhole region and the $(1,-1)_0$ regions there were very narrow areas of $(2,2)_0$ solutions. There were several reasons to question the accuracy of these results, however. It was mildly surprising that the $(2,2)_0$ family, which was expected to be the generic solution, appeared only in a small area. On the other hand, the $(1,-1)_0$ family was expected, based on its count of free parameters from the series analysis, to appear as a line rather than a region. As it is, around half of the asymptotically flat solutions were found to be $(1,-1)_0$, but there was some reason to doubt the numerical accuracy of this, especially that the solutions consistently deviated from (r^1, r^{-1}) behaviour and instead had $\approx (r^{1.14}, r^{-1.35})$ behaviour. The strangest result was that there seems to be a critical value of $C_{2,0} = -2GM$ corresponding to the mass at which the Schwarzschild and non-Schwarzschild black holes intersect. The point $(C_{2,0}, C_{2-}) = (C_{2,0}^{(\text{coincidence})}, 0)$ lies approximately right between the two $(1,-1)_0$ regions (even for other values of α). The two $(1,-1)_0$ regions both have a boundary with the wormhole region on part of the line $C_{2,0} = C_{2,0}^{(\text{coincidence})}$. As you approach this boundary from the wormhole side the wormhole solutions limit to horizons, but these horizon solutions appear to be identical to a single Schwarzschild solution, even though they have a large range of non-zero values of C_{2-} which corresponds to higher-derivative effects. The findings are certainly interesting but unfortunately they must be repeated with more numerical accuracy before the physical message becomes clear. The most important factor may be to repeat the study using a different starting radius r_{max} for the numerical shooting, though this trades our problems for others.

One of the most important areas for future research is the dynamical stability of these static solutions in the presence of time-dependent perturbations. We have often restricted consideration to asymptotically flat solutions, which are assumed to be more physically realistic, but our static analysis tells us nothing about whether the solutions are dynamically stable, which would be key to any claim of astrophysical relevance. The only non-trivial solution that is known analytically is the Schwarzschild solution. The dynamical stability of Schwarzschild in the four-derivative theory was studied by Whitt in [55], who concluded that it was stable, but revisited by Myung in [56] who drew a comparison to a black string to find an unstable mode that Whitt hadn't considered. This will be followed up in [54] where the instability of small

Schwarzschild black holes will be discussed and the thermodynamics of both types of black hole presented in detail.

Our attempt to discover all solution families should be seen in the context of the solution families of stationary space-times. It may be that some families are not physically realistic because they are not limits of stationary solutions. There is also the question of theories with even higher derivatives. Holdom [33] found that only the $(0,0)_0$ family exists as a vacuum solution to generic theories with more derivatives, which is interesting because we have found that black holes and matter-coupled solutions belong to other families, and we argued that the $(0,0)_0$ family has flat space as its only asymptotically flat member. The issue of matter coupling has been discussed thoroughly for the four-derivative theory, and it has been argued that the $(2,2)_0$ family provides the correct description. Since this family doesn't exist in theories with more derivatives, the issue of matter coupling in those theories is unresolved. The classical, static, spherically symmetric solutions to four-derivative theory with a cosmological constant will be different from the ones considered in this work, but it may be possible to find them without too much difficulty using this work as a guide. Such theories are of particular interest because of the possibilities raised in [31] and [32] that they offer solutions to the higher-derivative theory's problems with unitarity.

Finally, we recall that there are very few uniqueness theorems for higher-derivative gravity, so it may be that the most astrophysically realistic black hole solutions are of an even more difficult character, for example without spherical symmetry, or without axisymmetry, or even black holes with non-spherical topology.

Appendix A

Constraining the Ricci scalar in the presence of a cosmological constant

In [2] the expressions of section 2.1 were generalised to the case with a cosmological constant. The Lagrangian is

$$I = \int d^4x\sqrt{-g}\left(\gamma(R-2\Lambda) - \alpha C_{\mu\nu\rho\sigma}C^{\mu\nu\rho\sigma} + \beta R^2\right) . \tag{A.0.1}$$

The equations of motion implied by this action are the same as (1.3.1) and (1.3.4) except for an additional cosmological constant term.

$$H_{\mu\nu}(\Lambda) = H_{\mu\nu}(\Lambda=0) + \gamma\Lambda g_{\mu\nu} \tag{A.0.2}$$
$$H_{\mu}^{\ \mu}(\Lambda) = H_{\mu}^{\ \mu}(\Lambda=0) + 4\gamma\Lambda . \tag{A.0.3}$$

The proof that the Ricci scalar vanishes no longer holds - but instead one can show that the Ricci scalar is constant. Start with the trace of the equations of motion:

$$H_{\mu}^{\ \mu}(\Lambda) = 6\beta\Box R - \gamma\left(R-4\Lambda\right) \tag{A.0.4}$$
$$= 6\beta\left(\Box R - m_0^{\,2}(R-4\Lambda)\right) \tag{A.0.5}$$
$$= 6\beta\left(\Box S - m_0^{\,2}S\right) , \tag{A.0.6}$$

where the quantity S is defined as a shift of the Ricci scalar

$$S := R - 4\Lambda . \tag{A.0.7}$$

The equation (2.1.13h) is used to obtain an equation similar to the $\Lambda = 0$ calculation of equation (2.1.6):

$$0 = \int_{\mathcal{S}} \sqrt{h}\,\mathrm{d}^3x \frac{H_{\mu}^{\ \mu}(\Lambda)}{6\,\beta}\lambda S = \int_{\mathcal{S}} \sqrt{h}\,\mathrm{d}^3x\left[D^a\left(\lambda\, S\, D_aS\right) - \lambda\,\left(D^aS\right)\left(D_aS\right) - m_0^{\,2}\,\lambda\, S^2\right] . \tag{A.0.8}$$

Now the requirement that the contribution from the boundary term vanishes is actually unchanged: we need the vanishing of $D_aS = D_aR$ at infinity. The consequence is that the bulk terms must vanish throughout the integration region:

$$S = 0 \quad \Leftrightarrow \quad R = 4\Lambda . \tag{A.0.9}$$

Note that while in section 2.1 we assumed asymptotic flatness, which was sufficient for D_aR to vanish on the boundary, in the case with a cosmological constant we will be considering a space-time satisfying $R = 4\Lambda$, which is not asymptotically flat.

To discuss the trace-free part of the equations of motion we define shifts of other quantities too:

$$S_{\mu\nu} := R_{\mu\nu} - g_{\mu\nu}\Lambda \tag{A.0.10}$$

$$\bar{S} = \bar{R} - 2\Lambda \tag{A.0.11}$$

$$m_2(\Lambda)^2 = m_2^2 + \Lambda\,\frac{8}{6}\,\frac{3\beta-\alpha}{\alpha}\,. \tag{A.0.12}$$

The trace-free part of the equations of motion is then given by

$$0 = \left.\frac{H_{\mu\nu}(\Lambda)}{-2\alpha}\right|_{S=0} = \Box S_{\mu\nu} - m_2(\Lambda)^2 S_{\mu\nu} + 2S^{\rho}_{\mu}S_{\nu\rho} - 2\nabla_\rho\nabla_\mu S^\rho_\nu - \frac{1}{2}g_{\mu\nu}S^{\rho\sigma}S_{\rho\sigma}\,, \tag{A.0.13}$$

where we have used the identity

$$R^{\rho\sigma}R_{\mu\rho\nu\sigma} = R_{\mu\rho}R^\rho_\nu - \nabla_\rho\nabla_\mu R^\rho_\nu + \frac{1}{2}\nabla_\mu\nabla_\nu R \tag{A.0.14}$$

$$= S_{\mu\rho}S^\rho_\nu - \nabla_\rho\nabla_\mu S^\rho_\nu + \frac{1}{2}\nabla_\mu\nabla_\nu S + 2\Lambda S_{\mu\nu} + g_{\mu\nu}\Lambda^2\,. \tag{A.0.15}$$

Note also that the $S = 0$ equations of motion are not equivalent to Einstein-Weyl gravity (the $\beta = 0$ case), but it is still true that they depend on the two couplings only through one parameter, $m_2(\Lambda)$ [1].

The dimensional reduction of the trace-free part of the equations of motion (A.0.13) proceeds exactly as in section 2.1.3 where the identities (2.1.13) and (2.1.14) can all still be used if one reads every R, $R_{\mu\nu}$ and $\bar{R}$ as S, $S_{\mu\nu}$ and $\bar{S}$ respectively. The final result is

$$\begin{aligned}
0 &= \int_{\mathcal{S}} \sqrt{h}\,\mathrm{d}^3x \left[\lambda\, S^{\mu\nu}\left.\frac{H_{\mu\nu}}{-2\alpha}\right|_{S=0}\right] \\
&= \int_{\mathcal{S}} \sqrt{h}\,\mathrm{d}^3x \Bigg[D_i\left(\frac{\lambda}{4}\bar{S}D^i\bar{S} + \lambda\, S^{\cdot\cdot}D^i S_{\cdot\cdot} - 2\lambda\, S_{\cdot\cdot}D^{\cdot}S^{\cdot i} - \lambda\,\bar{S}D_j S^{ji}\right) \\
&\quad - \frac{\lambda}{4}\,D^i\bar{S}\,D_i\bar{S} + 2\lambda\, D^i\bar{S}D^j S_{ji} - \lambda\, D^i S^{jk}\left[D_i S_{jk} - 2D_j S_{ki}\right] \\
&\quad - \lambda\,\frac{\bar{S}^2}{4}\left(m_2(\Lambda)^2 + \bar{S}\right) - \lambda\, S^{ij}S_{ij}\left(m_2(\Lambda)^2 - 2\mathcal{S}\right)\Bigg]\,,
\end{aligned}$$

where $\mathcal{S}$ is defined as

$$\mathcal{S} := \frac{S^i_j S^j_k S^k_i}{S^{mn}S_{mn}}\,. \tag{A.0.16}$$

Unfortunately this suffers from the same problem as the $\Lambda = 0$ case and we cannot conclude anything about $S_{\mu\nu}$.

[1] if one had parameterised the Lagrangian as $\gamma(R-2\Lambda) - \frac{3(8\beta'\Lambda+\gamma)}{8\Lambda+6m_2(\Lambda)^2}C^2 + \beta' R^2$ then the statement is that there is no dependence on β'.

We can try using a slightly more general integrand,

$$
\begin{aligned}
0 = \lambda \ \left(aS^{00} + bS^{ij}\right)^{\mu\nu} \left.\frac{H_{\mu\nu}}{-2\alpha}\right|_{S=0} \\
=& D^i \left(\frac{a\lambda}{4} \bar{S} D_i \bar{S} + b\lambda \ S^{\cdot\cdot} D_i S_{\cdot\cdot} - 2b\lambda \ S^{\cdot\cdot} D_{\cdot} S_{\cdot i} - a\lambda \ \bar{S} D^j S_{ji} \right) \\
& - a\lambda \ \frac{D^i \bar{S}}{2} \frac{D_i \bar{S}}{2} + a\lambda \ 2 D^i \bar{S} D^j S j i - b\lambda \ D^i S^{jk} \left[D_i S_{jk} - 2 D_j S_{ki} \right] \\
& + \frac{a-b}{2\lambda} D^i \bar{S} S_{ij} D^j \lambda \\
& - \lambda \ \frac{\bar{S}^2}{4} \left(a \, m_2(\Lambda)^2 + \frac{3a+b}{4} \bar{S} \right) - S^{ij} S_{ij} \lambda \ \left(b \, m_2(\Lambda)^2 - 2b\mathcal{S} + \frac{b-a}{4} \bar{S} \right) \ ,
\end{aligned}
$$

but we still cannot see any way to prove constraints on the curvature.

Bibliography

[1] H. Lu et al. "Black Holes in Higher-Derivative Gravity". *Phys. Rev. Lett.* 114.17 (2015), p. 171601. DOI: 10.1103/PhysRevLett.114.171601. arXiv: 1502.01028 [hep-th].

[2] H. Lu et al. "Spherically symmetric solutions in higher-derivative gravity". *Phys. Rev. D* 92 (12 2015), p. 124019. DOI: 10.1103/PhysRevD.92.124019. arXiv: 1508.00010. URL: http://link.aps.org/doi/10.1103/PhysRevD.92.124019.

[3] Astrid Eichhorn. "Lecture notes on Asymptotic Safety" (2015). (internal).

[4] Gerard 't Hooft and M. J. G. Veltman. "One loop divergencies in the theory of gravitation". *Annales Poincare Phys. Theor.* A20 (1974), pp. 69–94.

[5] Marc H. Goroff and Augusto Sagnotti. "Quantum Gravity At Two Loops". *Phys. Lett.* B160 (1985), pp. 81–86. DOI: 10.1016/0370-2693(85)91470-4.

[6] K. S. Stelle. "Classical Gravity with Higher Derivatives". *Gen. Rel. Grav.* 9 (1978), pp. 353–371. DOI: 10.1007/BF00760427.

[7] K. S. Stelle. "Renormalization of Higher Derivative Quantum Gravity". *Phys. Rev.* D16 (1977), pp. 953–969. DOI: 10.1103/PhysRevD.16.953.

[8] Mikhail Valilevich Ostrogradskii. *Memoire sur les equations differentielles relatives au probleme des isoperimetres. Lu le 17 (29) novembre 1848*. l Academie imperiale des sciences, 1850.

[9] Jonathan Z. Simon. "Higher Derivative Lagrangians, Nonlocality, Problems and Solutions". *Phys. Rev.* D41 (1990), p. 3720. DOI: 10.1103/PhysRevD.41.3720.

[10] Andrei V. Smilga. "Benign versus malicious ghosts in higher-derivative theories". *Nucl. Phys.* B706 (2005), pp. 598–614. DOI: 10.1016/j.nuclphysb.2004.10.037. arXiv: hep-th/0407231 [hep-th].

[11] S. W. Hawking and Thomas Hertog. "Living with ghosts". *Phys. Rev.* D65 (2002), p. 103515. DOI: 10.1103/PhysRevD.65.103515. arXiv: hep-th/0107088 [hep-th].

[12] Alberto Salvio and Alessandro Strumia. "Quantum mechanics of 4-derivative theories" (2015). arXiv: 1512.01237 [hep-th].

[13] D. Lovelock. "The Einstein tensor and its generalizations". *J. Math. Phys.* 12 (1971), pp. 498–501. DOI: 10.1063/1.1665613.

[14] Xing-Hui Feng and H. Lu. "Higher-Derivative Gravity with Non-minimally Coupled Maxwell Field" (2015). arXiv: 1512.09153 [hep-th].

[15] Barton Zwiebach. "Curvature Squared Terms and String Theories". *Phys. Lett.* B156 (1985), p. 315. DOI: 10.1016/0370-2693(85)91616-8.

[16] David G. Boulware and Stanley Deser. "String Generated Gravity Models". *Phys. Rev. Lett.* 55 (1985), p. 2656. DOI: 10.1103/PhysRevLett.55.2656.

[17] Brian Whitt. "Fourth Order Gravity as General Relativity Plus Matter". *Phys. Lett.* B145 (1984), p. 176. DOI: 10.1016/0370-2693(84)90332-0.

[18] Alexei A. Starobinsky. "A New Type of Isotropic Cosmological Models Without Singularity". *Phys. Lett.* B91 (1980), pp. 99–102. DOI: 10.1016/0370-2693(80)90670-X.

[19] Salvatore Mignemi and David L. Wiltshire. "Black holes in higher derivative gravity theories". *Phys. Rev.* D46 (1992), pp. 1475–1506. DOI: 10.1103/PhysRevD.46.1475. arXiv: hep-th/9202031 [hep-th].

[20] E. Pechlaner and R. Sexl. "On quadratic Lagrangians in general relativity". *Comm. Math. Phys.* 2.3 (1966), pp. 165–175. URL: http://projecteuclid.org/euclid.cmp/1103815047.

[21] F. C. Michel. "Gravitational collapse and higher-order gravitational lagrangians". *Annals Phys.* 76 (1973), pp. 281–298. DOI: 10.1016/0003-4916(73)90451-X.

[22] Antonio De Felice and Shinji Tsujikawa. "f(R) theories". *Living Rev. Rel.* 13 (2010), p. 3. arXiv: 1002.4928 [gr-qc].

[23] David G. Boulware, Stanley Deser, and K. S. Stelle. "Properties of Energy in Higher Derivative Gravity Theories" (1985).

[24] David G. Boulware, Stanley Deser, and K. S. Stelle. "Energy and Supercharge in Higher Derivative Gravity". *Phys. Lett.* B168 (1986), p. 336. DOI: 10.1016/0370-2693(86)91640-0.

[25] David G. Boulware, Gary T. Horowitz, and Andrew Strominger. "Zero Energy Theorem for Scale Invariant Gravity". *Phys. Rev. Lett.* 50 (1983), p. 1726. DOI: 10.1103/PhysRevLett.50.1726.

[26] Stanley Deser and Bayram Tekin. "Gravitational energy in quadratic curvature gravities". *Phys. Rev. Lett.* 89 (2002), p. 101101. DOI: 10.1103/PhysRevLett.89.101101. arXiv: hep-th/0205318 [hep-th].

[27] Stanley Deser and Bayram Tekin. "Energy in generic higher curvature gravity theories". *Phys. Rev.* D67 (2003), p. 084009. DOI: 10.1103/PhysRevD.67.084009. arXiv: hep-th/0212292 [hep-th].

[28] Ronald J. Riegert. "Birkhoff's Theorem in Conformal Gravity". *Phys. Rev. Lett.* 53 (1984), pp. 315–318. DOI: 10.1103/PhysRevLett.53.315.

[29] Alex Kehagias et al. "Black hole solutions in R^2 gravity". *JHEP* 05 (2015), p. 143. DOI: 10.1007/JHEP05(2015)143. arXiv: 1502.04192 [hep-th].

[30] Francis Duplessis and Damien A. Easson. "Traversable wormholes and non-singular black holes from the vacuum of quadratic gravity". *Phys. Rev.* D92.4 (2015), p. 043516. DOI: 10.1103/PhysRevD.92.043516. arXiv: 1506.00988 [gr-qc].

[31] H. Lu and C. N. Pope. "Critical Gravity in Four Dimensions". *Phys. Rev. Lett.* 106 (2011), p. 181302. DOI: 10.1103/PhysRevLett.106.181302. arXiv: 1101.1971 [hep-th].

[32] H. Lu, Yi Pang, and C. N. Pope. "Conformal Gravity and Extensions of Critical Gravity". *Phys. Rev.* D84 (2011), p. 064001. DOI: 10.1103/PhysRevD.84.064001. arXiv: 1106.4657 [hep-th].

[33] Bob Holdom. "On the fate of singularities and horizons in higher derivative gravity". *Phys. Rev.* D66 (2002), p. 084010. DOI: 10.1103/PhysRevD.66.084010. arXiv: hep-th/0206219 [hep-th].

[34] William Nelson. "Static Solutions for 4th order gravity". *Phys. Rev.* D82 (2010), p. 104026. DOI: 10.1103/PhysRevD.82.104026. arXiv: 1010.3986 [gr-qc].

[35] W. Israel. "Singular hypersurfaces and thin shells in general relativity". *Nuovo Cim.* B44S10 (1966). [Nuovo Cim.B44,1(1966)], p. 1. DOI: 10.1007/BF02710419;10.1007/BF02712210.

[36] E. Poisson. *A Relativist's Toolkit: The Mathematics of Black-Hole Mechanics*. Cambridge University Press, 2004. ISBN: 9781139451994. URL: https://books.google.co.uk/books?id=bk2XEgz_ML4C.

[37] Robert P. Geroch and Jennie H. Traschen. "Strings and Other Distributional Sources in General Relativity". *Phys. Rev.* D36 (1987). [Conf. Proc.C861214,138(1986)], p. 1017. DOI: 10.1103/PhysRevD.36.1017.

[38] Werner Israel. "Event horizons in static vacuum space-times". *Phys. Rev.* 164 (1967), pp. 1776–1779. DOI: 10.1103/PhysRev.164.1776.

[39] Werner Israel. "Event horizons in static electrovac space-times". *Commun. Math. Phys.* 8 (1968), pp. 245–260. DOI: 10.1007/BF01645859.

[40] S. W. Hawking. "Black holes in general relativity". *Commun. Math. Phys.* 25 (1972), pp. 152–166. DOI: 10.1007/BF01877517.

[41] H. Müller Zum Hagen, David C. Robinson, and H. J. Seifert. "Black holes in static vacuum space-times". *General Relativity and Gravitation* 4.1 (1973), pp. 53–78. ISSN: 1572-9532. DOI: 10.1007/BF00769760. URL: http://dx.doi.org/10.1007/BF00769760.

[42] H. Muller zum Hagen, David C. Robinson, and H. J. Seifert. *General Relativity and Gravitation* (). ISSN: 1572-9532. DOI: 10.1007/BF00758075.

[43] D. C. Robinson. "A simple proof of the generalization of Israel's theorem". *General Relativity and Gravitation* 8.8 (1977), pp. 695–698. ISSN: 1572-9532. DOI: 10.1007/BF00756322. URL: http://dx.doi.org/10.1007/BF00756322.

[44] B. Carter. "Axisymmetric Black Hole Has Only Two Degrees of Freedom". *Phys. Rev. Lett.* 26 (1971), pp. 331–333. DOI: 10.1103/PhysRevLett.26.331.

[45] D. C. Robinson. "Uniqueness of the Kerr black hole". *Phys. Rev. Lett.* 34 (1975), pp. 905–906. DOI: 10.1103/PhysRevLett.34.905.

[46] D. C. Robinson. "Classification of black holes with electromagnetic fields". *Phys. Rev.* D10 (1974), pp. 458–460. DOI: 10.1103/PhysRevD.10.458.

[47] P. O. Mazur. "Proof of uniqueness of the Kerr-Newman black hole solution". *J. Phys.* A15 (1982), pp. 3173–3180. DOI: 10.1088/0305-4470/15/10/021.

[48] Saul A. Teukolsky. "The Kerr Metric". *Class. Quant. Grav.* 32.12 (2015), p. 124006. DOI: 10.1088/0264-9381/32/12/124006. arXiv: 1410.2130 [gr-qc].

[49] B. Carter. "Has the black hole equilibrium problem been solved?" *Recent developments in theoretical and experimental general relativity, gravitation, and relativistic field theories. Proceedings, 8th Marcel Grossmann meeting, MG8, Jerusalem, Israel, June 22-27, 1997. Pts. A, B.* 1997, pp. 136–155. arXiv: gr-qc/9712038 [gr-qc]. URL: http://alice.cern.ch/format/showfull?sysnb=0264110.

[50] R.M. Wald. *General Relativity*. University of Chicago Press, 2010. ISBN: 9780226870373. URL: https://books.google.co.uk/books?id=9S-hzg6-moYC.

[51] S.W. Hawking and W. Israel. *General Relativity; an Einstein Centenary Survey*. Cambridge University Press, 1979. ISBN: 9780521222853. URL: https://books.google.co.uk/books?id=pxA4AAAAIAAJ.

[52] K.F. Riley, M.P. Hobson, and S.J. Bence. *Mathematical Methods for Physics and Engineering: A Comprehensive Guide*. Cambridge University Press, 2006. ISBN: 9781139450997. URL: https://books.google.co.uk/books?id=Mq1nlEKhNcsC.

[53] H. T. H. Piaggio. *Differential Equations*. Read Books, 2008. ISBN: 9781409724346. URL: https://books.google.com/books?id=7LbEyy37GYsC.

[54] H. Lu et al. "Lichnerowicz Eigenmodes and Black Holes in Ricci Quadratic Gravity" (2016). To appear.

[55] Brian Whitt. "The Stability of Schwarzschild Black Holes in Fourth Order Gravity". *Phys. Rev.* D32 (1985), p. 379. DOI: 10.1103/PhysRevD.32.379.

[56] Yun Soo Myung. "Stability of Schwarzschild black holes in fourth-order gravity revisited". *Phys. Rev.* D88.2 (2013), p. 024039. DOI: 10.1103/PhysRevD.88.024039. arXiv: 1306.3725 [gr-qc].